COORDINATED ACTIVITIES OF CHROMATIN MODIFYING COMPLEXES IN DNA REGULATION IN *SACCHAROMYCES CEREVISIAE*

by

Ya Ting Phoebe Lu

B.SC., The University of British Columbia, 2008

A THESIS SUBMITTED IN PARTIAL FULFILLMENT OF

THE REQUIREMENTS FOR THE DEGREE OF

DOCTOR OF PHILOSOPHY

in

THE FACULTY OF GRADUATE AND POSTDOCTORAL STUDIES

(Genetics)

THE UNIVERSITY OF BRITISH COLUMBIA

(Vancouver)

March 2015

Abstract

As the sole carrier of genetic information, DNA does not exist as a naked template in the eukaryotic genome; instead DNA exists as a nucleoprotein complex. Wrapped around specialized histone proteins, DNA and histones are assembled into the organized chromatin structure. The chromatin structure is regulated by a wide assortment of factors to facilitate access to the genetic material while at the same time compacting the genome. Perhaps it is not surprising that the coordinated activities of multiple chromatin-modifying complexes are necessary to regulate the many biological process occurring on DNA. We are beginning to understand how chromatin-modifying mechanisms cooperate to regulate gene promoters and define unique chromatin neighbourhoods. In this dissertation, I explore the functional connections between chromatin remodeling complexes, histone chaperones and histone variants in various aspects of chromatin biology. Focusing on the synthetic genetic interaction between *ASF1* and *YAF9,* I uncovered the cooperative activities of histone chaperone and the SWR1-C H2A.Z exchange complex in maintaining heterochromatin boundaries. Furthermore, I also identified that H2A.Z occupancy at gene promoters is partially dependent on Asf1-mediated H3K56 acetylation. I specifically studied the functional relationship between H3K56 acetylation and H2A.Z occupancy. I determined that acetylation of H3K56 was required for maintaining H2A.Z levels at gene promoters. Furthermore, I discovered that H3K56 acetylation was also important in positioning H2A.Z containing nucleosomes at promoters. Lastly, I explored the specific features required for NuA4 structure and histone acetylation function. I uncovered a novel regulatory relationship between the Eaf1 scaffold protein and the Epl1 C-terminus that

anchors the catalytic module to the NuA4 complex. In addition, I demonstrated that the Epl1 C-terminus and the Eaf1 HSA domain are the two key domains regulating the cellular equilibrium of NuA4 and picNuA4. Collectively, the work presented in the dissertation adds to our understanding of the interface between chromatin remodeling complexes, histone chaperones and histone variants in the regulation of chromatin biology and highlights the important role chromatin structure plays in basic cellular processes.

Preface

Chapter 1 of this dissertation was published in part in the journal of Biochemistry and Cell Biology as a mini-review in 2009 (Lu PYT, Levesque N, and Kobor MS, 2009). As co-first author, I analyzed the large-scale genetic interaction and together with Nancy Levesque, we designed the outline of the review and wrote the manuscript.

Chapter 2 of this dissertation was published in whole in Genetics (Lu PYT and Kobor MS 2014). As first author, I generated the strains, designed and conducted all the experiments in this manuscript. I was responsible for making the figures and writing the paper.

Chapter 3 is based on experiments following up the work published in Chapter 2. I constructed the strains and conducted the biochemical and ChIP-on-chip experiments for this chapter. I analyzed the microarray data and wrote the algorithms used to examine the localization of promoter-associated H2A.Z peaks.

I currently lead the project described in Chapter 4, which includes contributions from Maria Aristizabal and Nancy Levesque. I provided primary contributions to the formation of research questions, research design, data collection and data analysis. Maria Aristizabal performed the E-MAP screen in collaboration with N. Krogan (UCSF) and F. Holstege laboratory (U of Utrecht) carried out the microarray expression experiments. I constructed the strains and performed the biochemical characterization of NuA4 for Figures 4.1, 4.4, 4.5, 4.6 and contributed to all figures.

In Chapter 2-4, I consistently use “we” to reflect the co-authors that contributed to the studies.

Table of Contents

List of Tables

List of Figures

List of Abbreviations

ATP	Adenosine triphosphate
ChIP	Chromatin immunoprecipitation
DDR	DNA damage response
DNA	Deoxyribose nucleic acid
DSB	Double stranded break
E-MAP	Epistatic miniarray profiling
HAT	Histone acetyltransferase
HDAC	Histone deacetylase
HSA	Helicase SANT associated
HU	Hydroxyurea
INO80	Inositol 80
MMS	Methyl methane sulfonate
MYST	MOZ, Ybf2/Sas3, Sas2, and Tip60
NFR	Nucleosome free region
NuA4	Nucleosome acetyltransferase of H4
ORF	Open reading frame
PCR	Polymerase chain reaction
picNuA4	piccolo NuA4
PTM	Post-translational modification
RNA	Ribonucleic acid

RSC	Remodel the structure of chromatin
SAGA	Spt-Ada-Gcn5-acetyltransferase
SANT	Swi3, Ada2, N-Cor and TFIIIB
SRCAP	Snf2-related CBP activator protein
SWR1-C	Swi2/Snf2-related ATPase 1 – complex
TAP	Tandem affinity purification
TIP60	Tat interacting protein (60kDa)
TSS	Transcriptional start site

Acknowledgements

I am grateful for the many people who have been a part of my life through this long and challenging journey.

Firstly, I would like to thank my supervisor, Dr. Michael Kobor for giving me the freedom to explore novel and interesting research questions as a mere undergraduate student more than eight years ago. For it was this first taste of scientific curiosity, the ability to question and test an idea that inspired me to pursue a career in scientific research. Thank you for your unwavering mentorship, guidance, and support.

I would also like to thank my supervisory committee, Dr. Carolyn Brown, Dr. Leann Howe and Dr. Stefan Taubert, for their time and guidance over the years. Thank you for always keeping me on track and for continuously challenging me. Thank you to Dr. Hugh Brock for teaching me the basics of genetics and for your continuous support in the Genetics Graduate Program. Furthermore, I am thankful for the funding that the Canadian Institute of Health Research has provided me to support my studies and for the incredible research conferences the travel grant has allowed me to attend.

Thank you to the many Kobor lab members (past, present and honorary) for keeping me sane through the long and seemingly never ending list of experiments, through the trials and tribulations of failed experiments, and the celebration of getting the perfect silver stain! Words

cannot express how grateful I am to have had the privilege of working alongside each and every one of you. I am truly thankful of all the lasting friendship I have made over the years and I look forward to celebrating all of your successes in the future.

Finally, I would like to thank my family for their constant love and support. My mom and dad for always making sure I had everything I need and their heartfelt efforts to understand what I was doing. Thank you to my amazing sisters, Jane and Daphne, for their, sometimes, unconventional ways of being supportive and loving. Lastly, thank you to Jaques, my personal editor, my cheerleading squad and my shoulder to lean on. Thank you for always being here with me.

This thesis is dedicated to my parents

for their love, endless support

and encouragement.

Chapter 1: Introduction

DNA is traditionally believed to be the sole carrier of genetic information that is passed down to the next generation. Confirmed more than half a century ago by groundbreaking experiments by Avery-MacLeod-McCarty and Hershey-Chase, the identification of DNA as the transforming principle was cemented. From that moment onward, an explosion of research on DNA commenced. Within ten years, the structure of the DNA double helix was solved, the genetic code was deciphered and the central dogma of molecular biology was conceived. In the eukaryotic nucleus, DNA does not exist as a naked template; instead, it is compacted into a dynamic structure known as chromatin. Specialized histones proteins facilitate the condensation and packaging of DNA into the chromatin structure, allowing vast amounts of DNA to fit within a cell nucleus only a few microns in diameter. Intense research in molecular biology over the last two decades has revealed that chromatin structure plays an immense role in controlling the accessibility of the genetic information stored within the DNA nucleotides. Furthermore, crosstalk between multiple chromatin-modifying complexes and their targets results in a dynamic chromatin landscape, which has profound influences on gene expression, DNA replication, DNA repair, and DNA recombination. Pioneering work in the field of chromatin biology recognized that the information contained in chromatin structure could also be inherited, much like DNA (Eissenberg and Reuter 2009; Girton and Johansen 2008; Ekwall *et al.* 1997). Thus, the field of research in epigenetics was initiated;

which is defined in this dissertation as the study of "the structural adaptation of chromosomal regions so as to register, signal, or perpetuate altered activity states" (Bird 2007).

1.1 Chromatin Structure

Chromatin, in its very initial conception by Walther Flemming in 1880, referred to the stainable thread-like material found in the cell nucleus (Flemming 1882). Today, we recognize chromatin as an organizational structure that packages billions of nucleotides of DNA into the eukaryotic nucleus. The dynamic capacity of chromatin to "open" up its structure is vital in accessing much of the information contained within the condensed structure, allowing cells to carry out basal cellular functions and respond to the changing environment.

The fundamental unit of chromatin is the nucleosome, consisting of 147 bp of DNA wrapped 1.7 superhelical turns around a histone octamer comprising two molecules each of H2A, H2B, H3, and H4 (Luger *et al.* 1997). The eight canonical histones in the nucleosome core particle are small and highly basic. Each core histone is composed of a globular protein domain and a flexible tail that protrudes from the core of the nucleosome (Figure 1.1). A combination of hydrogen bonds, salt linkages and non-polar interactions between the histone core and the negatively charged phosphate backbone of DNA contribute to the overall stability of the nucleosome (Luger *et al.* 1997; Li and Reinberg 2011). The histone tails, which make up 20% of the octamer mass, are largely unstructured and serve as a platform for a large number of post-translational covalent modifications in addition to mediating interactions with nearby nucleosomes. For example, the basic patch in the H4 N-terminal tail

interacts with an acidic patch on the H2A/H2B heterodimer of a neighbouring nucleosome for compaction of a nucleosome array (Dorigo *et al.* 2003; Fan *et al.* 2004; Gordon *et al.* 2005; Luger *et al.* 1997).

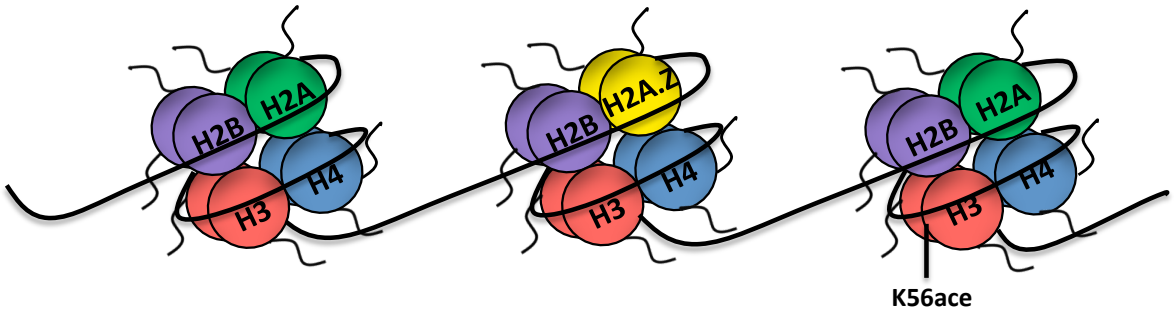

Figure 1.1 DNA wrapped around a core of eight histones
Schematic representation of DNA wrapped around two each of H2A, H2B, H3, and H4. The replacement of canonical histone H2A for the histone variant H2A.Z and K56acetylation on histone H3 are two major chromatin modifying mechanisms examined in this dissertation.

Nucleosome core particles are joined by sections of linker DNA, which form the iconic "beads on a string" structure (Figure 1.1) (Kornberg 1974; Olins and Olins 1974). Together, the nucleosome core particle and the linker DNA form repeating units of the chromatin polymer. The 11 nm "beads on a string" structure of chromatin is largely unfolded, and represents a transcriptionally active and accessible form of chromatin commonly referred to as euchromatin. Incorporation of the linker histone, H1, promotes condensation of the chromatin polymer into the 30 nm structure (Li and Reinberg 2011; Robinson *et al.* 2006; Robinson and Rhodes 2006). The precise mechanism of how the 30 nm structure is further compacted into a series of higher order structures resulting in the mitotic chromosome

remains an active area of research. It is clear, however, that inter-fiber interactions play a large role (Li and Reinberg 2011).

Compaction of DNA into these higher structures leads to formation of the transcriptionally silent heterochromatin structure (Li and Reinberg 2011). In an interphase nucleus, the chromatin polymer exists as a dynamic equilibrium between euchromatin and heterochromatin, simultaneously allowing access to genetic information and compaction of the eukaryotic genome. We are beginning to understand the vital contributions and the dynamic regulation of this higher order chromatin organization to everyday cellular functions.

1.2 Histone Chaperones in Nucleosome Assembly and Disassembly

In eukaryotes, all biological processes involving genomic DNA occur on a chromatin template. Although the euchromatic structure promotes access, unwinding of DNA from the histone octamer is still necessary. Hence, the chromatin structure is constantly undergoing rounds of assembly and disassembly, allowing processes such as DNA replication, transcription, and DNA damage repair to occur without obstruction from the nucleosome.

Histone chaperones were initially perceived as passive histone binding proteins that facilitated histone transport into the nucleus and nucleosome assembly (Park and Luger 2008). Histone chaperones are now being recognized as key proteins that play an active role

in the formation of nucleosomes and contribute to the regulation of the dynamic structure of chromatin and its function. In fact, mixing DNA and free histones in the absence of their chaperones produces insoluble aggregates rather than nucleosomes. Histone chaperones can be broadly characterized as chaperones for H2A/H2B heterodimers or H3/H4 heterodimers (De Koning *et al.* 2007; Eitoku *et al.* 2008). In addition, some histone chaperones bind to variants of the canonical histones, such as the Chz1 histone chaperone that bind H2A.Z/H2B heterodimers preferentially over H2A/H2B heterodimers (Luk *et al.* 2007).

One important role for histones chaperones is guiding interactions between histones and DNA in the stepwise process of nucleosome assembly. In the current model, two H3/H4 heterodimers are first deposited onto DNA to form a tetrasome. Next, two pairs of H2A/H2B heterodimers are added and the DNA is wrapped around the resultant histone octamer, thus completing the nucleosome (Luger *et al.* 1997). During the nucleosome building process in the cell, histone chaperones are required for providing free histones for assembly, stabilizing charged histones until they are deposited onto the DNA and for promoting the correct points of contact between histones and DNA (Eitoku *et al.* 2008; Das *et al.* 2010; Ransom *et al.* 2010). In a similar manner, histone chaperones also coordinate every step of the nucleosome disassembly process. Additionally, histone chaperones are required for shuttling newly synthesized histones into the nucleus, promoting post-translational modification of histones, and maintaining a pool of free histone in the nucleus (Eitoku *et al.* 2008).

1.2.1 Asf1 Histone Chaperone

Not surprisingly, many classes of histone chaperones exist to perform the wide range of functions they are required for in the cell. Of particular interest in this dissertation is Asf1 (Anti-Silencing Function 1), a highly conserved histone chaperone for the H3/H4 heterodimer. First discovered in 1997 in a screen looking for disruptors of telomere silencing in *Saccharomyces cerevisiae,* Asf1 is now one of the best characterized histone chaperones (Le *et al.* 1997; Singer *et al.* 1998). Fundamentally, Asf1 is involved in the assembly of the H3/H4 heterodimer into chromatin during replication-dependent and replication-independent nucleosome assembly, as well as nucleosome assembly and disassembly during transcription (Tyler *et al.* 1999; Adkins *et al.* 2004; 2007; Adkins and Tyler 2004; Schwabish and Struhl 2006; Mousson *et al.* 2007; Gkikopoulos *et al.* 2009; Takahata *et al.* 2009). In the majority of these processes, Asf1 hands off the H3/H4 heterodimer to other histone chaperones and chromatin-remodellers for nucleosome assembly. Through its cooperation with multiple chromatin-modifying complexes, Asf1 is implicated in DNA replication, DNA damage response, telomere silencing and transcription (Mousson *et al.* 2007; Adkins *et al.* 2004; Raisner and Madhani 2008; Emili *et al.* 2001; Schwabish and Struhl 2006; Miller *et al.* 2010). In addition to nucleosome assembly, Asf1 also presents histone H3 for post-translational modification. Binding of Asf1 to the H3/H4 heterodimer is required for H3K56 acetylation by the histone acetyltransferase, Rtt109 (Recht *et al.* 2006; Tsubota *et al.* 2007; Schneider *et al.* 2006; Driscoll *et al.* 2007). Ultimately, the broad functions of histone chaperones can be attributed to their intimate relationship with a large range of chromatin-modifying complexes, which combined, direct nucleosome assembly and disassembly.

1.3 Nucleosome Positioning

As hinted at by the regulatory function of histone chaperones, nucleosomes are not randomly scattered in the genome but are often found in discreet increments and at fixed positions. It is now clear that the positioning of nucleosomes is a tightly regulated process of critical importance to various biological processes. High-resolution mapping of nucleosomes has revealed that nucleosomes are often depleted at enhancer, promoter and terminator regions, but enriched over genes and intergenic regions (Struhl and Segal 2013; Jiang and Pugh 2009; Lee *et al.* 2007; Mavrich *et al.* 2008; Shivaswamy *et al.* 2008; Whitehouse *et al.* 2007; Lam *et al.* 2008). It is apparent from these genome-wide experiments that nucleosomes are positioned in a very precise manner and that this is particularly true for genes. In the yeast genome, the majority of genes have a region just upstream of the transcriptional start site (TSS) that lacks nucleosomes, termed the nucleosome free region (NFR). The 5' NFR is approximately 150 bp in length and is flanked by two highly positioned nucleosomes referred to as the -1 and +1 nucleosomes (Jansen and Verstrepen 2011). However, while the nucleosomes near the 5' NFR adopt fixed positions, the position of nucleosomes becomes more random with increasing distance from the promoter. Interestingly, consistent with eviction of promoter nucleosomes by Pol II during transcription, highly expressed genes have less defined NFRs (Lee *et al.* 2004; Weiner *et al.* 2010; Cairns 2009).

Though there have been much debate regarding the underlying determinants of nucleosome positioning, collectively we now know that the combined effects of DNA sequence and chromatin-remodeling complexes are the two main factors influencing nucleosome

positioning in *Saccharomyces cerevisiae* (Struhl and Segal 2013). DNA sequence influences on nucleosome positioning are mainly attributed to the structural flexibility of the 147 bp that is wrapped around the histone octamer (Segal *et al.* 2006). G-C interactions are more rigid, whereas A-T interactions connected by two hydrogen bonds instead of three, offer more flexibility and facilitate DNA bending around the nucleosome. In addition, poly(dA:dT) tracts often found at gene promoters are important for nucleosome depletion and promoter accessibility (Segal and Widom 2009; Raveh-Sadka *et al.* 2012; Iyer and Struhl 1995).

Evidence that DNA sequence alone does not dictate nucleosome positioning comes from *in vitro* experiments demonstrating that chromatin-modifying complexes are required for nucleosomes to adopt their *in vivo* positioning patterns (Wippo *et al.* 2011). Furthermore, the Isw2 remodeler is required for positioning the +1 nucleosome onto unfavaourable DNA at select gene promoters *in vivo* (Whitehouse and Tsukiyama 2006; Whitehouse *et al.* 2007). The RSC remodeling complex is also important for sliding nucleosomes onto DNA sequences that are otherwise unfavorable for nucleosome assembly (Hartley and Madhani 2009). Thus, it appears that multiple chromatin remodelers in addition to the underlying DNA sequence are needed to confer specificity in establishing the position of nucleosomes. Although the precise contribution of each of these factors remains a key question in the field, there is no question that they all contribute to the positioning of nucleosomes.

The positions of promoter nucleosomes are highly regulated in part because of their ability to control the activation or repression of genes. Experiments with classical inducible genes such as *PHO5* and *GAL1* and genome-wide correlation experiments have demonstrated that

nucleosomes can regulate transcription by changing their positions (Almer and Hörz 1986; Fedor and Kornberg 1989; Lee *et al.* 2004; 2007). By physically blocking a transcription factor binding site or preventing docking of the PolII transcription machinery, the position of nucleosomes can indirectly control the activation of genes. Nevertheless, it is important to bear in mind that nucleosome position alone does not account for all transcriptional regulation but rather contributes to and plays an important role in the cellular dynamics of transcriptional control.

1.4 Modifications of the Chromatin Structure

In an effort to balance the need to compact DNA and the need to access genetic information contained within DNA, the chromatin structure must maintain a dynamic equilibrium of compaction and accessibility. The coordinated activities of various chromatin-modifying factors are crucial in maintaining distinct chromatin neighbourhoods, which ensure appropriate gene expression, as well as DNA replication, repair and recombination. Of the four main mechanisms regulating chromatin structures in eukaryotic cells, DNA methylation is the only alteration that does not exist in yeast. Methylation of cytosines in the context of CpG dinucleotides in gene promoter regions is generally associated with gene repression and heterochromatic regions. Another mechanism is the addition of post-translational modifications on histone proteins (Peterson and Laniel 2004; Turner 2005). Furthermore, nucleosomes can be moved in *cis* or in *trans* by ATP-dependent chromatin-remodeling complexes (Eberharter and Becker 2004; Lusser and Kadonaga 2003). Lastly, canonical histones can be replaced by histone variants to mark defined chromatin regions (Sarma and

Reinberg 2005; Zlatanova and Thakar 2008). The latter three mechanisms are of particular interest in this dissertation and their roles in chromatin regulation are expanded upon below.

1.4.1 Post-Translational Modification of Histones

A wealth of work has established that the addition of chemical groups or short protein peptides on histones provides an additional layer of regulatory control on the chromatin structure. Largely achieved by specialized "writer" enzymes, the types of post-translational modification (PTMs) on histones include acetylation, methylation, phosphorylation, ubiquitination, sumoylation, and ADP-ribosylation (Kouzarides 2007). The majority of PTMs occur on the N-terminal tails of histones that protrude from the nucleosome core particle. These tail modifications often serve as a docking platform or a signaling beacon for downstream factors. Nonetheless, some PTMs do occur on the globular domains of histones such as acetylation of H3K56 and these generally alter the overall stability of nucleosomes or regulate inter-nucleosome stability.

The first PTM reported, acetylation of lysine residues, remains one of the best understood (Allfrey *et al.* 1964). Lysine acetylation of histones is a reversible modification that is achieved by the combined actions of histone acetyltransferases (HATs) and histone deacetylases (HDACs). Characterized by a conserved acetyl-coA-factor binding domain, HATs catalyze the transfer of an acetyl group from acetyl-coA to a histone lysine residue (Li and Reinberg 2011; Shahbazian and Grunstein 2007). Acetylation of lysine neutralizes its positive charge, thereby weakening the interactions with the negatively charged DNA and resulting in a more open chromatin structure (Grunstein 1997). HATs can be classified into

two categories based on their substrate specificity. The first category of HATs acetylates histones within chromatin. For example, the essential NuA4 HAT of the MYST (MOZ, Ybf2, Sas2, and Tip60) family acetylates the lysine residues of nucleosomal H4, H2A, and H2A.Z (Allard *et al.* 1999; Eberharter *et al.* 1998; Babiarz *et al.* 2006; Doyon and Côté 2004; Keogh *et al.* 2006; Millar *et al.* 2006). These PTMs generally occur at specific chromatin locations and are critical in controlling the chromatin state at that region. For example, NuA4-targeted H4 acetylation at ribosomal gene promoters is required for the transcriptional activation of these genes (Reid *et al.* 2000). The second category of HATs acetylates newly synthesized histones that are associated with histone chaperones, and not nucleosomes. A fairly novel class of HATs, the activity and functions of these HATs are starting to be understood. Rtt109 is one particular example that has been extensively studied since its discovery (Masumoto *et al.* 2005; Han and Zhang 2007; Driscoll *et al.* 2007). In a mutually exclusive manner, Rtt109 requires the assistance of two histone chaperones, Vps75 and Asf1, to acetylate H3K9 and H3K56, respectively (Tsubota *et al.* 2007; Fillingham *et al.* 2008; Driscoll *et al.* 2007). Furthermore, PTMs sometimes play pivotal roles in the recognition of histone chaperones for their respective substrates. For instance, H3K36me reduces the binding of H3/H4 dimer to the histone chaperone Asf1, thereby suppressing histone exchange (Venkatesh *et al.* 2012).

Upon the discovery of the PTMs, scientists started looking for "readers" that would recognize and make use of the modified histone peptides. The first reading modules discovered were the chromodomains that recognized methylated lysines and the bromodomains that recognized acetylated lysines residues (Dhalluin *et al.* 1999; Bannister *et*

al. 2001). We now know that these "readers", together with PTMs, play key roles in mediating crosstalk between chromatin-modifying complexes and transcriptional regulators (Bannister and Kouzarides 2011). Rather than directing transcriptional activation or repression by altering chromatin structure, PTMs often serve as a signal platform to recruit downstream effectors (readers) responsible for underlying transcriptional changes. Combinatorial studies undertaken in recent years led to the proposal of a "histone code", where akin to the genetic code, the combination of PTMs on a single nucleosome would result in a unique downstream response (Strahl and Allis 2000). While it is still up for debate whether the histone code can be generalized, emerging evidence suggests that the combinatorial reading capacity of multi-subunit chromatin-modifying complexes increases binding strength and specificity (Huh *et al.* 2012; Li *et al.* 2009). In particular, recent structural analysis of NuA4 demonstrates that the HAT complex makes multiple contacts with the entire nucleosome, suggesting that it could recognize multiple PTMs on a single nucleosome (Chittuluru *et al.* 2011).

1.4.2 ATP-Dependent Chromatin-Remodeling Complexes

ATP-dependent chromatin-remodeling complexes are a specialized group of complexes that use the energy from ATP hydrolysis to disrupt DNA-histone contacts in order to carry out their respective functions (Cairns 2007). To facilitate crosstalk, chromatin remodelers have "reading" domain(s) that interact with other chromatin factors and recognize post-translational modifications of histones. Chromatin remodelers can be categorized into three main classes with specialized functions in either assembly of nucleosomes, restructuring the composition of nucleosomes or promoting genome access. Often working with histone

chaperones, the assembly class of chromatin remodelers facilitates the formation and positioning of nucleosomes. The second class of chromatin remodelers edits the compositions of nucleosomes, often replacing canonical histones with histone variants. The last class of chromatin remodeler enables access to chromatin, achieved either by sliding or ejecting the histone octamer. A major focus of this dissertation is the second class of chromatin remodelers, namely the SWR1-C ATP-dependent chromatin-remodeling complex. Part of the INO80 family of remodelers, SWR1-C alters the composition of a standard nucleosome by removal of H2A/H2B dimers and incorporation of histone variant H2A.Z/H2B dimers, resulting in the formation of unique chromatin neighbourhoods characterized by H2A.Z occupancy (Kobor *et al.* 2004; Krogan *et al.* 2004; Mizuguchi *et al.* 2004).

1.4.3 Histone Variants

Histone variants are non-allelic variants of canonical histones encoded by unique genes. Often possessing similar primary amino acid sequences and core structures, the incorporation of histone variants in place of canonical histones creates distinct chromosome neighbourhoods that confer specialized functions. In contrast to canonical histones whose expression is cell cycle regulated and peaks at S-phase during DNA replication, expression of histone variants is not cell cycle-dependent (Talbert and Henikoff 2010; Szenker *et al.* 2011). Instead, their expression is tightly regulated throughout the cell cycle in order to promote their availability and deposition. Histone variants exist for all canonical histones except for histone H4 (Talbert and Henikoff 2010). The H3 family of variants tends to be less diverse whereas the H2A and H2B families of variants have substantial sequence variations.

Similar to canonical histones, histone variants also associate with histone chaperones to regulate histone supply and chromatin incorporation (De Koning *et al.* 2007). For instance, the mammalian Asf1 histone chaperone must recognize the five amino acid differences between H3.1 and H3.3; handing off H3.1/H4 dimer to the CAF-1 complex for replication-dependent nucleosome assembly and delivering H3.3/H4 dimer to the HIRA complex for replication-independent assembly (Tagami *et al.* 2004). Furthermore, the sequence difference within histone variants can alter the molecular interactions between the histone octamer and DNA. In particular, many lines of evidence suggest that the incorporation of the H2A.Z histone variant reduces nucleosome stability (Ishibashi *et al.* 2009; Abbott *et al.* 2001; Watanabe *et al.* 2013; Bönisch and Hake 2012; Jin *et al.* 2009). Additionally, the acidic patch that is extended in H2A.Z compared to H2A regulates chromatin compaction by promoting chromatin fiber folding (Suto *et al.* 2000; Fan *et al.* 2002; 2004; Subramanian *et al.* 2013). Furthermore, histone variants often have different PTMs compared to their canonical counterparts, adding another level of complexity. For example, while H2A is acetylated at lysine 4 and 7, the H2A.Z histone variant is acetylated at lysine 3, 8, 10, and 14 (Babiarz *et al.* 2006; Millar *et al.* 2006; Suka *et al.* 2001; Vogelauer *et al.* 2000; Altaf *et al.* 2010). The unique features within histone variants provide specific interactions with binding partners, distinct biochemical properties to nucleosomes, and influence higher-level chromatin organization. Thus, histone variants are an exciting avenue of research to understand the creation and functions of distinct chromatin neighbourhoods.

1.5 Coordinated Activities of Chromatin-Modifying Factors

It is clear from recent observations that chromatin-modifying factors are not exclusive, but function in parallel with other remodelers to regulate chromatin organization and function. As a major focus in this dissertation, I decided to direct my attention on three specific chromatin-modifying processes that act on nucleosomes. In *Saccharomyces cerevisiae,* SWR1-C and NuA4 complexes converge on H2A.Z to generate distinct chromatin neighbourhoods (Figure 1.2). NuA4 first acetylates H4, which facilitates the recruitment of SWR1-C through its bromodomain-containing subunit, Bdf1 (Ranjan *et al.* 2013; Altaf *et al.* 2010). SWR1-C uses the energy from ATP hydrolysis to exchange canonical histone H2A for the histone variant H2A.Z, hence altering nucleosome composition (Kobor *et al.* 2004; Krogan *et al.* 2004; Mizuguchi *et al.* 2004). Once deposited, the N-terminus of H2A.Z is acetylated by NuA4 (Babiarz *et al.* 2006; Keogh *et al.* 2006; Millar *et al.* 2006). Intriguingly, yeast NuA4 and SWR1-C have four subunits in common, an observation that potentially accounts for their cooperative functions (Figure 1.3) (Lu *et al.* 2009).

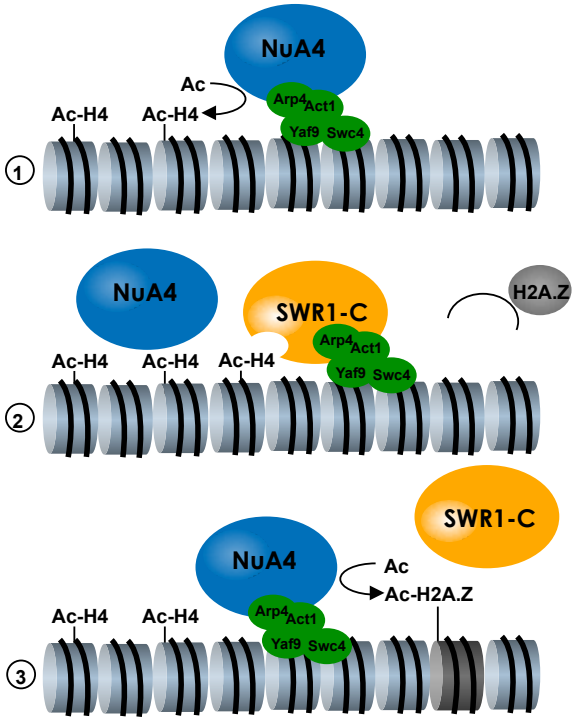

Figure 1.2 Sequential activity of NuA4 and SWR1-C on chromatin
Model of the sequential relationship between NuA4 and SWR1-C. 1: NuA4 is anchored to chromatin through the shared module and acetylates histone H4. 2: SWR1-C is recruited to chromatin with the help of the shared module and recognition of acetylated H4 by Bdf1. SWR1-C then deposits histone variant H2A.Z into chromatin. 3: NuA4 subsequently acetylates the newly deposited H2A.Z.

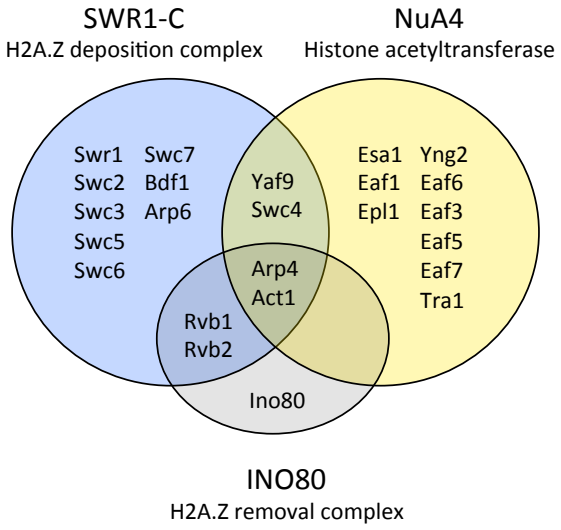

Figure 1.3 Shared subunits of SWR1-C, NuA4, and INO80
Venn diagram of the overlap between SWR1-C, NuA4, and INO80 subunits.

1.5.1 SWR1-C Structure and Function

SWR1-C was the first complex identified as solely dedicated to the deposition of histone variants in *S. cerevisiae* (Kobor *et al.* 2004; Krogan *et al.* 2004; Mizuguchi *et al.* 2004). To date, the only cellular function of this fourteen-subunit complex appears to be deposition of histone variant H2A.Z into chromatin at distinct regions such as the promoters of genes, double stranded breaks (DSB), and heterochromatin boundaries. It was recently elucidated that SWR1-C is recruited to gene promoters by recognition of NFRs flanked by nucleosomes by its Swr1 and Swc2 subunits (Ranjan *et al.* 2013; Yen *et al.* 2013). Beyond its central role in SWR1-C catalytic activity, Swr1 also acts as a scaffold for the assembly of numerous SWR1-C components (Nguyen *et al.* 2013; Wu *et al.* 2005; 2009). Swr1 is a large protein with several distinct regions such as the HSA (helicase-SANT-associated) and ATPase domains that are involved in diverse aspects of SWR1-C function (Figure 1.4). The HSA domain is often associated with helicases and mediates protein-protein interactions (Szerlong *et al.* 2008; Trotter *et al.* 2008). The ATPase domain of Swr1 is distinguished from canonical ATPase domains by the presence of an insertion region (Mizuguchi *et al.* 2004). These two domains are important for interactions with various members of SWR1-C. For example, the ATPase domain of Swr1 is required for binding to Swc2, Arp6, Swc6, Rvb1, and Rvb2, whereas the N-terminal portion is essential for association with Yaf9, Swc4, Act1, Arp4, Swc7, Bdf1, and H2A.Z (Wu *et al.* 2009; 2005; Nguyen *et al.* 2013). The N-terminal region of Swr1 can be further divided into two sections, N1 and N2, whereby N2 contains the HSA domain that physically associates with the shared module, composed of Act1, Arp4, Yaf9 and Swc4 (Szerlong *et al.* 2008). The majority of SWR1-C subunits have been functionally characterized and most of them have been found to be required for H2A.Z exchange *in vitro.*

Interestingly, SWR1-C can perform histone exchange in the absence of Bdf1, Swc7, and Swc3, suggesting that these subunits have auxiliary functions (Wu *et al.* 2009; 2005).

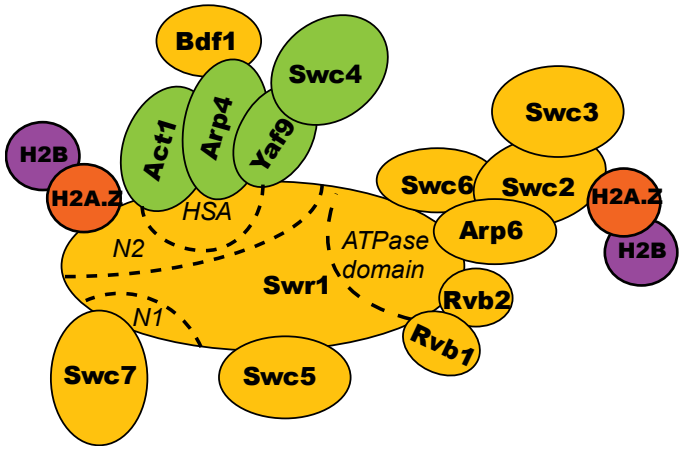

Figure 1.4 SWR1-C Structure
Schematic representation of the complex association map of SWR1-C showing Swr1 as the assembly platform.

1.5.2 NuA4 Structure and Function

NuA4 is a large thirteen-subunit complex that acetylates histones H2A, H2A.Z and H4 and is the only essential HAT in *S. cerevisiae* (Allard *et al.* 1999; Eberharter *et al.* 1998; Smith *et al.* 1998; Millar *et al.* 2006; Babiarz *et al.* 2006; Keogh *et al.* 2006). The essential function of NuA4 lies within its catalytic subunit, Esa1. In recent years, we are beginning to appreciate NuA4's role as a general lysine acetyltransferase for many non-histone targets (Mitchell *et al.* 2008; 2013; Lin *et al.* 2008; 2009). As a multifunctional HAT complex, NuA4 is implicated in transcriptional regulation, the DNA damage response (DDR), chromosome segregation, heterochromatin boundary establishment, life span, and cell autophagy (Boudreault *et al.* 2003; Bird *et al.* 2002; Downs *et al.* 2004; Lin *et al.* 2008; Krogan *et al.* 2004; Zhang *et al.* 2004; Babiarz *et al.* 2006; Zhou *et al.* 2010; Lin *et al.* 2009; Yi *et al.*

2012; Lu *et al.* 2011; Mitchell *et al.* 2011). The main scaffold component of NuA4 is Eaf1, which is required for binding of various NuA4 sub-modules via its distinct domains (Figure 1.5). For instance, the SANT region of Eaf1 is required for binding to Tra1 and the N-terminal region of Eaf1 associates with the Eaf3/5/7 sub-module (Auger *et al.* 2008). Furthermore, the HSA domain of Eaf1 is required for binding of the shared module composed of Act1, Arp4, Yaf9 and Swc4. In *S. cerevisiae*, NuA4 exists in two different forms within the cell. Namely, as the large thirteen-subunit NuA4 complex and as a smaller piccolo NuA4 complex consisting of only Esa1, Yng2, Eaf6, and Epl1 subunits (Auger *et al.* 2008; Boudreault *et al.* 2003; Chittuluru *et al.* 2011). Whereas NuA4 acetylates histones in a gene-specific manner, piccolo NuA4 is involved in global acetylation of H2A and H4 (Boudreault *et al.* 2003). In Chapter 4 of this dissertation, I expand upon our existing knowledge of the functional and structural relationship between picNuA4 and NuA4.

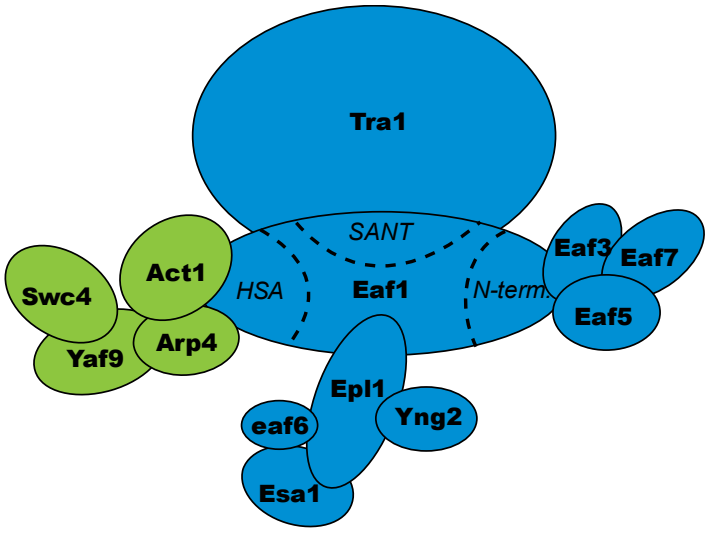

Figure 1.5 NuA4 Structure
Schematic representation of the complex association map of NuA4 showing Eaf1 as the scaffolding subunit for the modular complex.

1.5.3 H2A.Z at the Intersection between SWR1-C and NuA4

The histone variant H2A.Z is the most notable nexus between NuA4 and SWR1-C. Elucidation of the cellular function of H2A.Z has been greatly facilitated by its non-essential role in *S. cerevisiae.* Reassuringly, the majority of these functions were subsequently confirmed in higher eukaryotes in which H2A.Z is essential. In yeast, H2A.Z is involved in heterochromatin boundary formation, transcriptional activation and repression, chromosome stability, and chromosome segregation (Adam *et al.* 2001; Larochelle and Gaudreau 2003; Meneghini *et al.* 2003; Zhang *et al.* 2005; Santisteban *et al.* 2000; Sharma *et al.* 2013). Consistent with a role in transcriptional regulation, H2A.Z is primarily found in the promoter regions of genes where it often flanks the NFR proximal to the TSS (Guillemette *et al.* 2005; Li *et al.* 2005; Raisner *et al.* 2005). However, the exact role of H2A.Z in transcriptional regulation remains a puzzle, as genome-wide studies in yeast and metazoans do not reveal a simple regulatory relationship between loss of H2A.Z and gene activity (Abbott *et al.* 2001; Li *et al.* 2005; Meneghini *et al.* 2003; Suto *et al.* 2000; Zhang *et al.* 2005; Albert *et al.* 2007; Gévry *et al.* 2007; Buchanan *et al.* 2009; Hardy *et al.* 2009).

The role of H2A.Z at the boundary of heterochromatin and euchromatin is one example that nicely illustrates the functional interplay between NuA4 and SWR1-C. Global mRNA profiling indicated that H2A.Z is necessary for proper expression of many genes located in sub-telomeric regions (Meneghini *et al.* 2003). In the majority of cases, aberrant spreading of the heterochromatin SIR proteins into euchromatin regions caused reductions in gene expression in the absence of H2A.Z, suggesting that H2A.Z forms a barrier that limits SIR spread (Meneghini *et al.* 2003). Interestingly, the ability of H2A.Z to maintain proper

heterochromatin boundaries is dependent on its acetylation by NuA4 (Babiarz *et al.* 2006). The targeted deposition of H2A.Z into telomeres is also dependent on the acetylation of H4K16 by the SAS HAT complex, further demonstrating the interplay between H2A.Z deposition and H4 acetylation (Shia *et al.* 2006). As I will illustrate in Chapter 3, however, it appears that the SAS-mediated H2A.Z deposition activity is a telomere-specific mechanism.

SWR1-C is the principal complex responsible for the incorporation of H2A.Z into chromatin whereas NuA4 has two regulatory roles in H2A.Z biology. First, NuA4 is important for the association of H2A.Z and SWR1-C with chromatin. NuA4-dependent H2A and H4 acetylation stimulates and targets SWR1-C to specific gene promoters for H2A.Z exchange (Babiarz *et al.* 2006; Durant and Pugh 2007; Altaf *et al.* 2010). In addition to the acetylation of histones by NuA4, it appears that acetylation of the H3 N-terminal by another HAT, SAGA, also contributes to H2A.Z deposition (Raisner *et al.* 2005). Second, given NuA4's role in H2A acetylation and the high degree of homology between H2A and H2A.Z, it is perhaps not surprising that NuA4 also acetylates H2A.Z (Babiarz *et al.* 2006; Keogh *et al.* 2006; Millar *et al.* 2006). H2A.Z is first deposited into chromatin by SWR1-C, and then subsequently acetylated by NuA4 (Babiarz *et al.* 2006; Keogh *et al.* 2006). Interestingly, acetylation of H2A.Z becomes essential in the absence of H4 acetylation as seen in the synthetic lethality of a strain containing both the non-acetylable forms of H2A.Z (*htz1-K3, 8, 10, 14R*) and H4 (*hhf2-K5, 8, 12R*) (Babiarz *et al.* 2006). Lastly, it was recently shown that INO80 catalyzes the opposite reaction as SWR1-C; INO80 replaces nucleosomal H2A.Z for H2A (Papamichos-Chronakis *et al.* 2011).

Initial biochemical purifications of SWR1-C provided hints to its connection to NuA4 and INO80, as all three complexes share the Arp4 and Act1 subunits (Kobor *et al.* 2004; Krogan *et al.* 2004; Mizuguchi *et al.* 2004). During the DDR, there are intriguing physical and functional overlaps between SWR1-C, NuA4, and INO80 (Morrison and Shen 2009; van Attikum and Gasser 2009; Papamichos-Chronakis and Peterson 2013; Sinha and Peterson 2009; Papamichos-Chronakis *et al.* 2006). Upon DNA damage, one of the first PTMs that initiate the DDR cascade is the phosphorylation of H2A.X by the checkpoint kinases, Mec1 and Tel1 (Shroff *et al.* 2004). This modification covers a large region flanking the DSB that ranges from 50-100 kb (Rogakou *et al.* 1999). Arp4, a shared subunit of SWR1-C, NuA4, and INO80, is required for recruitment of these complexes to sites of DNA damage via direct physical interaction with phosphorylated H2A.X (Downs *et al.* 2004). NuA4 is recruited to DSBs in order to acetylate histone H4. This process results in a more accessible chromatin structure and allows for recruitment of DNA repair machinery and various chromatin-modifying complexes, including SWR1-C and INO80 (Bird *et al.* 2002; Downs *et al.* 2004; Tamburini and Tyler 2005; Bennett *et al.* 2013). In addition to acetylated H4, phosphorylated H2A.X also directly recruits SWR1-C and INO80 to DSBs (Morrison *et al.* 2004; Papamichos-Chronakis *et al.* 2006; van Attikum *et al.* 2007). H2A.Z is transiently and rapidly deposited into chromatin at DSBs immediately following DNA damage (Kalocsay *et al.* 2009). A strain lacking H2A.Z displays DNA resection defects and damage checkpoint defects, suggesting that H2A.Z has an early role in the DSB repair pathway (Kalocsay *et al.* 2009; Van *et al.* 2015). Following DDR, H2A.Z and H2A.X are subsequently removed from the DSB in an INO80-dependent manner (van Attikum *et al.* 2007; Papamichos-Chronakis *et al.* 2011).

1.6 Conservation of NuA4 and SWR1-C in Mammals

Many components of SWR1-C and NuA4 are structurally and functionally conserved throughout eukaryotic evolution, highlighting the importance of these complexes in various cellular processes of eukaryotic development. The SRCAP complex functions as the human counterpart of the yeast SWR1-C to deposit H2A.Z into chromatin (Wong *et al.* 2007). Similar to NuA4, the primary function of human TIP60 complex is to acetylate histones H2A and H4, but it can also exchange H2A.Z/H2B for H2A/H2B dimers (Ikura *et al.* 2000; Cai *et al.* 2003; Doyon *et al.* 2004). H2A.Z exchange is mediated by two distinct subunits in mammals, p400 (in the TIP60 complex) and the SRCAP subunit (in the SRCAP complex) (Gévry *et al.* 2007; Svotelis *et al.* 2009; Martinato *et al.* 2008). TIP60 and SRCAP complexes share several subunits in addition to the unique subunits that differentiate the two complexes. Biochemical and structural evidence suggests that NuA4 and SWR1-C exist as a single, massive complex in higher eukaryotes (Doyon *et al.* 2004). It is speculated that the two major scaffold proteins for NuA4 and SWR1-C, Eaf1 and Swr1, fused to form the p400 protein in higher eukaryotes, since p400 contains SANT, HSA, and ATPase domains (Auger *et al.* 2008; Doyon *et al.* 2004; Lu *et al.* 2009). Evidently, a fusion protein containing distinguishable domains of Swr1 and Eaf1 in *S. cerevisiae* can partially replace the function of both subunits in H2A.Z deposition and H4 acetylation (Auger *et al.* 2008). Furthermore, a TIP60-like complex is reconstituted in yeast in the presence of the Eaf1-Swr1 fusion protein, suggesting a physical merger of SWR1-C and NuA4.

1.7 Summary

The chromatin structure is essential for the compaction of the eukaryotic genome into the cell nucleus. A wide variety of chromatin-modifying complexes regulate this organizational structure in order to maintain an equilibrium of accessibility and compaction. While we are beginning to appreciate the complex mechanisms underlying chromatin biology, there still remain many more questions on how these factors work together. In this dissertation, I examined the cooperative activities of the Asf1 histone chaperone and SWR1-C chromatin-remodeling complex at heterochromatic regions and gene promoters. Furthermore, I dissected the complex dynamics of the NuA4 histone acetyltransferase and its catalytic module using a variety of genome-wide and biochemical approaches.

In Chapter 2, I describe the genetic and functional connections between Asf1 and SWR1-C in the maintenance of native heterochromatin structures and nucleosome composition at promoters. Asf1 and a subunit of SWR1-C, Yaf9, are both required for maintaining expression of heterochromatin-proximal genes and they worked cooperatively to prevent repression of telomere-proximal genes by limiting the spread of SIR complexes to nearby regions. Furthermore, genetic and molecular analysis revealed that H3K56 acetylation was required for efficient deposition of H2A.Z at subtelomeric and euchromatic gene promoters, pointing to a role for Asf1-dependent H3K56 acetylation in SWR1-C biology.

In Chapter 3, I investigate the functional connection between Asf1 and SWR1-C on H2A.Z containing nucleosomes. Loss of H2A.Z at heterochromatin boundaries was not due to loss

of SAS recruitment by Asf1. By examining H2A.Z occupancy genome-wide, I found that the acetylation of lysine 56 on histone H3 was required for H2A.Z occupancy at a subset of promoters. Furthermore, loss of H3K56 acetylation resulted in alterations of H2A.Z position at gene promoters normally enriched for this histone modification.

In Chapter 4, I examined the consequences on NuA4 structure and function in the presence of two genetic perturbations, loss of the entire Eaf1 protein and loss of the Epl1 C-terminus. Eaf1 is the main scaffold protein of NuA4 and the C-terminus of Epl1 anchors the catalytic module to Eaf1. Large-scale genetic and gene expression analysis and comprehensive biochemical assays identified the Eaf1 HSA domain and the Epl1 C-terminus as two key domains in the NuA4 complex that regulate the cellular equilibrium of NuA4 and picNuA4.

In Chapter 5, I discuss my results in Chapter 2-4 and highlight how my findings fit within and contribute to our current understanding of chromatin biology. I explore the implications of my findings and discuss future experiments that would elucidate the molecular mechanisms governing the coordinated activities of chromatin-modifiers on the chromatin structure.

Chapter 2: Maintenance of Heterochromatin Boundary and Nucleosome Composition at Promoters by the Asf1 Histone Chaperone and SWR1-C Chromatin Remodeler in *Saccharomyces cerevisiae*[1]

2.1 Introduction

The fundamental building block of chromatin is a nucleosome composed of 146 bp of DNA wrapped around a histone octamer. Protein complexes involved in post-translational modification of histones, nucleosome movement or replacement alter chromatin dynamics to regulate various chromosomal processes. Often, these chromatin-modifying processes intersect and interact cooperatively to regulate chromatin structure.

Transcriptionally silent heterochromatin structures are a prime example of the multilayered activities of chromatin modifying complexes. In budding yeast *Saccharomyces cerevisiae*, there are three well-defined regions of silent chromatin: the mating loci (*HMR* and *HML*), the rDNA locus and telomeres. These regions are characterized by a distinct set of histone modifications and associated factors that distinguish them from adjacent transcriptionally active euchromatin (Rusche *et al.* 2003). Chief among these is the Silent Information Regulator (SIR) complex, which not only constitutes the main structural component during

[1] This chapter is published in Genetics. Lu, P.Y.T. and Kobor, M.S., 2014. Maintenance of heterochromatin boundary and nucleosome composition at promoters by the Asf1 histone chaperone and SWR1-C chromatin remodeler in *Saccharoymyces cerevisiae.Genetics.* 197(1): 133-145

establishment and maintenance of heterochromatin but also harbors an enzymatic function (Rusche *et al.* 2003). Specifically, the Sir2 subunit is a NAD+ dependent histone deacetylase (HDAC) that deacetylates H4K16, a process critical for promoting initial SIR complex formation at heterochromatin loci as well as for formation of heterochromatin boundaries. The establishment of heterochromatin boundaries is biologically important to prevent antagonistic silencing of neighbouring euchromatic genes by encroaching heterochromatic structures (Rusche *et al.* 2003; Imai *et al.* 2000).

Several additional histone modifying enzymes contribute to demarcating the boundary between heterochromatin and euchromatin, including the Something About Silencing 2 (SAS2) complex, the Dot1 histone methyltransferase, and the highly conserved histone variant H2A.Z (Takahashi *et al.* 2011; Verzijlbergen *et al.* 2009; Shia *et al.* 2006; Meijsing and Ehrenhofer-Murray 2001; Osborne *et al.* 2009). Similar to the other factors, loss of H2A.Z from the heterochromatin-euchromatic boundary results in the spread of SIR complexes to nearby subtelomeric genes and subsequent repression of these genes (Meneghini *et al.* 2003). In part, the role of H2A.Z at boundaries is mediated by acetylation of its N-terminal lysine residues, although the magnitude of this effect varies among different studies (Babiarz *et al.* 2006; Millar *et al.* 2006; Keogh *et al.* 2006).

Like many of the factors sculpting heterochromatin boundaries, H2A.Z also has roles in euchromatic regions. H2A.Z, for instance, is enriched at the majority of gene promoters and often resides in the two nucleosomes flanking the nucleosome free region (NFR) (Raisner *et al.* 2005). H2A.Z is more commonly localized to lowly expressed gene promoters and is

largely absent from highly expressed genes (Guillemette *et al.* 2005; Li *et al.* 2005; Zhang *et al.* 2005). Despite these strong correlations, the causal role of H2A.Z for gene expression is more nebulous as genome-wide expression studies found that loss of H2A.Z affects only a minority genes in yeast (Meneghini *et al.* 2003). Rather than affecting steady-state gene expression, H2A.Z may facilitate the induction of genes in response to changing environments (Adam *et al.* 2001; Larochelle and Gaudreau 2003; Lemieux *et al.* 2008; Halley *et al.* 2010).

H2A.Z is deposited into chromatin by SWR1-C, an ATP-dependent chromatin remodeling complex that recognizes the NFR and exchanges H2A-H2B dimers with H2A.Z-H2B dimers at the two flanking nucleosomes (Ranjan *et al.* 2013; Yen *et al.* 2013; Kobor *et al.* 2004; Krogan *et al.* 2004; Mizuguchi *et al.* 2004). Illustrative of the crosstalk between chromatin remodelers, SWR1-C and the NuA4 histone acetyltransferase (HAT) have interconnected activities converging on H2A.Z chromatin neighbourhoods. Acetylation of H4 lysine residues by NuA4 promotes the recruitment of SWR1-C for H2A.Z deposition, and subsequent acetylation of newly incorporated H2A.Z by NuA4 is required for gene activation and heterochromatin formation (Altaf *et al.* 2010; Ranjan *et al.* 2013; Durant and Pugh 2007; Babiarz *et al.* 2006). The interplay between SWR1-C and NuA4 likely involves a module of four subunits that is shared between the two complexes (Lu *et al.* 2009). For instance, at a subset of telomeres, the Yaf9 shared subunit is vital to H2A.Z incorporation, H4 acetylation, and proper telomere-specific gene expression changes (Zhang *et al.* 2004; Wang *et al.* 2009).

Yaf9 contains an evolutionary conserved YEATS domain, whose closest structural relative in budding yeast is Asf1(Wang *et al.* 2009). These two proteins share a common essential function, although the nature thereof has yet to be defined. Asf1 plays a number of roles in heterochromatin function, transcription regulation, and cellular response to DNA damage (Mousson *et al.* 2007; Lin and Schultz 2011; Chen *et al.* 2008; Williams *et al.* 2008; Sharp *et al.* 2001). Asf1 functions as an anti-silencing factor as both its deletion and overexpression have an antagonistic effect on silencing of yeast mating type loci (Le *et al.* 1997; Singer *et al.* 1998). Regulation of silencing by Asf1 occurs through a redundant pathway with chromatin assembly factor 1 (CAF-1) (Sharp *et al.* 2001; Sutton *et al.* 2001). Mechanistically, Asf1 functions as a highly conserved histone chaperone for the H3/H4 heterodimer to mediate nucleosome assembly and disassembly, and is required to facilitate the acetylation of lysine 56 on H3 by the HAT, Rtt109 (Kolonko *et al.* 2010; Recht *et al.* 2006; Tsubota *et al.* 2007; Fillingham *et al.* 2008). Similar to Asf1, the acetylation state of H3K56 is important for the maintenance of silent chromatin structures at yeast mating loci and telomeres (Miller *et al.* 2008; Värv *et al.* 2010; Xu *et al.* 2007). Remarkably, Asf1 and SWR1-C are functionally linked as H3K56 acetylated nucleosomes alter the substrate specificity of SWR1-C to cause promiscuous exchange of H2A.Z (Watanabe *et al.* 2013).

The functional and genetic linkages between Asf1 and SWR1-C suggest that their cellular roles are closely related. Our works revealed that while Asf1 and SWR1-C had distinct functions for the expression of heterochromatin-proximal genes, they had overlapping roles in H2A.Z deposition. Consistent with locus–specific layers of chromatin modifications at heterochromatin, Asf1 was required for normal expression of HMR-proximal but not

telomere-proximal genes, whereas Yaf9 regulated silencing of both HMR- and telomere-proximal genes. Furthermore, we found Asf1 worked cooperatively with Yaf9 at the telomeric heterochromatin boundary to restrict SIR complexes at a subset of telomeres. The growth defect of *asf1Δyaf9Δ* cells could not be attributed to defects in maintaining heterochromatin structure. Instead, we established that Asf1-mediated H3K56 acetylation was required to maintain normal levels of H2A.Z at promoters of subtelomeric genes, hinting that Asf1 may regulate subtelomeric gene expression by influencing H2A.Z occupancy at promoters. We also elucidated that acetylation of H3K56 by Asf1 was also required for H2A.Z occupancy at euchromatic promoters, which suggests a broader role for this histone modification in H2A.Z biology.

2.2 Materials and Methods

2.2.1 Yeast Strains and Plasmids

All strains used in this study are listed in Table 2.1. Yeast strains were generated using standard genetic techniques including homologous recombination and genetic crosses followed by tetrad dissection (Ausubel 1987). Complete deletion of genes and 3' end integration of an in frame 3xFLAG tag were achieved using one-step gene integration PCR-amplified modules (Gelbart *et al.* 2001). Mating of the *sir2Δ* strain was achieved with the aid of the *URA3* plasmid pRS316[SIR2], 5-FOA was used as a counter-selection agent to evict plasmid following tetrad dissection. Plasmid shuffle experiments were performed using 5-FOA to evict *URA3* plasmid pRS316[H3 H4], and select for pRS316[H3K56R H4], pRS316[H3K56Q H4], pRS316[H3K9R H4], pRS316[H3K9Q H4], and

pRS316[H3K9RK56R H4]. These plasmids were a generous gift from Ann Kirchmaier (Purdue University). The p*ASF1*, p*asf1 H36A/D37A* and p*asf1 H39A/K41A* plasmids were generous gifts from Paul Kaufman (University of Massachusetts Medical School). The p*asf1 V94R* mutant was obtained from Carl Mann (CEA).

Table 2.1 Yeast strains used in this study

Strain number	Relevant Genotype
MKY5	W303*, MATα ade2-1 can1-100 his3-11 leu2-3,112 trp1-1 ura3-1 LYS2*
MKY6	W303*, MATA, ADE2, can1-100 his3-11 leu2-3,112 trp1-1 ura3-1 lys2Δ*
MKY7	W303*, MATA, ade2-1, can1-100 his3-11 leu2-3,112 trp1-1 ura3-1 LYS2*
MKY399	W303*, MATα, ADE2, can1-100 his3-11 leu2-3,112 trp1-1 ura3-1 lys2Δ*
MKY352	MKY6, *asf1Δ::NATMX*
MKY1596	MKY6, *yaf9Δ::KANMX*
MKY1597	MKY6, *asf1Δ::NATMX yaf9Δ::KANMX*
MKY1598	MKY6, *htz1Δ::HYGMX6*
MKY1599	MKY6, *asf1Δ::NATMX6 htz1Δ::HYG*
MKY646	MKY6, *swr1Δ::HIS*
MKY754	MKY6, *asf1Δ::NATMX swr1Δ::HIS*
MKY672	MKY6, *swc2Δ::HIS*
MKY385	MKY6, *asf1Δ::NATMX swc2Δ::HIS*
MKY394	MKY6, *swc3Δ::HIS*
MKY396	MKY6, *asf1Δ::NATMX swc3Δ::HIS*
MKY903	MKY6, *swc5Δ::HIS*
MKY467	MKY6, *asf1Δ::NATMX swc5Δ::HIS*
MKY463	MKY6, *swc6Δ::HIS*
MKY458	MKY6, *asf1Δ::NATMX swc6Δ::HIS*
MKY1600	MKY7, *SIR2-FLAG::KANMX*
MKY1601	MKY7, *SIR2-FLAG::KANMX asf1Δ::HIS*

Strain number	Relevant Genotype
MKY1602	MKY7, *SIR2-FLAG::KANMX yaf9Δ::NATMX*
MKY1603	MKY7, *SIR2-FLAG::KANMX asf1Δ::HIS yaf9Δ::NATMX*
MKY1605	MKY6, *asf1Δ::NATMX yaf9Δ::HIS sir2Δ::KANMX*
MKY1606	MKY6, *asf1Δ::NATMX swr1Δ::HIS sir2Δ::KANMX*
MKY1607	MKY6, *asf1Δ::NATMX sir2Δ::KANMX*
MKY1608	MKY6, *yaf9Δ::HIS sir2Δ::KANMX*
MKY1609	MKY6, *swr1Δ::HIS sir2Δ::KANMX*
MKY1610	MKY399, *asf1Δ::NATMX [pRS414, ASF1]*
MKY1611	MKY399, *asf1Δ::NATMX [pRS414, asf1 H36A/D37A]*
MKY1612	MKY399, *asf1Δ::NATMX cac2Δ::HYGMX [pRS414, ASF1]*
MKY1613	MKY399, *asf1Δ::NATMX yaf9Δ::KANMX [pRS414, ASF1]*
MKY1614	MKY399, *asf1Δ::NATMX cac2Δ::HYGMX [pRS414, asf1 H36A/D37A]*
MKY1615	MKY399, *asf1Δ::NATMX yaf9Δ::KANMX [pRS414, asf1 H36A/D37A]*
MKY1616	MKY399, *asf1Δ::NATMX cac2Δ::HYGMX yaf9Δ::KANMX [pRS414, ASF1]*
MKY1617	MKY399, *asf1Δ::NATMX cac2Δ::HYGMX yaf9Δ::KANMX [pRS414, asf1 H36A/D37A]*
MKY1618	MKY399, *asf1Δ::NATMX [pRS414, asf1 H39A/K41A]*
MKY1619	MKY399, *asf1Δ::NATMX cac2Δ::HYGMX [pRS414, asf1 H39A/K41A]*
MKY1620	MKY399, *asf1Δ::NATMX yaf9Δ::KANMX [pRS414, asf1 H39A/K41A]*
MKY1621	MKY399, *asf1Δ::NATMX cac2Δ::HYGMX yaf9Δ::KANMX [pRS414, asf1 H39A/K41A]*
MKY1622	MKY6 *[pRS314]*
MKY1623	MKY6, *asf1Δ::NATMX [pRS314]*
MKY1624	MKY6, *yaf9Δ::KANMX [pRS314]*
MKY1625	MKY6, *asf1Δ::NATMX yaf9Δ::KANMX [pRS314]*
MKY1626	MKY6, *asf1Δ::NATMX [pRS314, ASF1-MYC]*
MKY1627	MKY6, *asf1Δ::NATMX [pRS314, asf1 V94R-MYC]*
MKY1628	MKY6, *asf1Δ::NATMX yaf9Δ::KANMX [pRS314, ASF1-MYC]*
MKY1629	MKY6, *asf1Δ::NATMX yaf9Δ::KANMX [pRS314, asf1 V94R-MYC]*
MKY1630	MKY6, *hht1-hhf1::LEU2 hht2-hhf2::HIS [pRS314, HHT2-HHF2]*
MKY1631	MKY6, *hht1-hhf1::LEU2 hht2-hhf2::HIS yaf9Δ::KANMX [pRS314, HHT2-HHF2]*

Strain number	Relevant Genotype
MKY1632	MKY6, *hht1-hhf1::LEU2 hht2-hhf2::HIS [pRS314, HHT2 K56Q HHF2]*
MKY1633	MKY6, *hht1-hhf1::LEU2 hht2-hhf2::HIS [pRS314, HHT2 K56R HHF2]*
MKY1634	MKY6, *hht1-hhf1::LEU2 hht2-hhf2::HIS yaf9Δ::KANMX [pRS314, HHT2 K56Q HHF2]*
MKY1635	MKY6, *hht1-hhf1::LEU2 hht2-hhf2::HIS yaf9Δ::KANMX [pRS314, HHT2 K56R HHF2]*
MKY555	MKY6, *rtt109Δ::KANMX*
MKY1636	MKY6, *rtt109Δ::KANMX yaf9Δ::HIS*
MKY677	MKY6, *rtt109Δ::KANMX swr1Δ::HIS*
MKY674	MKY6, *rtt109Δ::KANMX swc2Δ::HIS*
MKY696	MKY6, *rtt109Δ::KANMX swc3Δ::HIS*
MKY763	MKY6, *rtt109Δ::KANMX swc5Δ::HIS*
MKY690	MKY6, *rtt109Δ::KANMX swc6Δ::HIS*
MKY1637	MKY6, *rtt109Δ::KANMX, htz1Δ::HYGMX*
MKY1638	MKY6, *hht1-hhf1::LEU2 hht2-hhf2::HIS [pRS314, HHT2 K9R HHF2]*
MKY1639	MKY6, *hht1-hhf1::LEU2 hht2-hhf2::HIS [pRS314, HHT2 K9Q HHF2]*
MKY1640	MKY6, *hht1-hhf1::LEU2 hht2-hhf2::HIS yaf9Δ::KANMX [pRS314, HHT2 K9Q HHF2]*
MKY1641	MKY6, *hht1-hhf1::LEU2 hht2-hhf2::HIS yaf9Δ::KANMX [pRS314, HHT2 K9R HHF2]*
MKY1642	MKY6, *hht1-hhf1::LEU2 hht2-hhf2::HIS [pRS314, HHT2 K9R K56R HHF2]*
MKY1643	MKY6, *hht1-hhf1::LEU2 hht2-hhf2::HIS yaf9Δ::KANMX [pRS314, HHT2 K9R K56R HHF2]*
MKY353	MKY5, *HTZ1-FLAG::KANMX*
MKY355	MKY5, *HTZ1-FLAG::KANMX asf1Δ::NATMX*
MKY354	MKY5, *HTZ1-FLAG::KANMX yaf9Δ::HIS*
MKY356	MKY5, *HTZ1-FLAG::KANMX asf1Δ::NATMX yaf9Δ::HIS*
MKY1644	MKY7, *hht1-hhf1::LEU2 hht2-hhf2::HIS [pRS314, HHT2-HHF2]*
MKY1645	MKY7, *HTZ1-FLAG::KANMX hht1-hhf1::LEU2 hht2-hhf2::HIS [pRS314, HHT2-HHF2]*
MKY1646	MKY7, *HTZ1-FLAG::KANMX hht1-hhf1::LEU2 hht2-hhf2::HIS yaf9Δ::NATMX [pRS314, HHT2-HHF2]*
MKY1647	MKY7, *HTZ1-FLAG::KANMX hht1-hhf1::LEU2 hht2-hhf2::HIS [pRS314, HHT2 K56R HHF2]*
MKY1648	MKY7, *HTZ1-FLAG::KANMX hht1-hhf1::LEU2 hht2-hhf2::HIS yaf9Δ::NATMX [pRS314, HHT2 K56R HHF2]*

2.2.2 Growth and Genotoxic Sensitivity Assays

Overnight cultures grown in YP-dextrose were diluted to OD_{600} 0.5. Cells were 10-fold serially diluted and spotted onto solid YPD plates or plates with 10mM hydroxyurea. For strains containing *TRP1* plasmids, the cultures were grown in SC –TRP media and serially diluted cells were spotted onto SC –TRP plates or plates containing 10mM hydroxyurea. The plates were then incubated at the indicated temperature for 36 hours. The 16°C plates were incubated for 96 hours.

2.2.3 RT-qPCR

Overnight cultures were diluted to OD_{600} of 0.15 and grown in YP-dextrose to an OD_{600} of 0.5. Ten OD_{600} units were harvested for RNA extraction and purification using a Qiagen RNeasy minikit as per manufacturer protocol. cDNA was synthesized using QuantiTect Reverse Transcription Kit (Qiagen). cDNA was analyzed using a Rotor-Gene 6000 (Qiagen) and PerfeCTa SYBR green FastMix (Quanta Biosciences). mRNA levels were normalized to *TUB1* mRNA levels. Samples were analyzed in triplicates for three independent RNA preparations. Statistical significance was assessed using Student's *t* test. Primer sequences are listed in Table 2.2.

Table 2.2 Primer sequences used in this study

Name	Method	Primer sequence (5'-3')
YCR094W ORF F	RT-qPCR	TTTCACTCTTTGGTGGCACA
YCR094W ORF R	RT-qPCR	TCGCTCTTGGTTGGAAGATT
YCR095C ORF F	RT-qPCR	CTTTGCAGAGAGCCAGAAGTG
YCR095C ORF R	RT-qPCR	TCAAATCGTCTCCTAGAACTCCAC
GIT1 ORF F	RT-qPCR	ATCGGTTCTGTAGTAGGCG
GIT1 ORF R	RT-qPCR	TTACCAGTCCAGCCATTGG
YCR099C ORF F	RT-qPCR	TCAGATTGCCCTTTCCGATA
YCR099C ORF R	RT-qPCR	GGAATGTTCATGGCCTCAAT
YCR100C ORF F	RT-qPCR	CCAGATGGATCAGGCTCAAA
YCR100C ORF R	RT-qPCR	TCGATCGCATACAGGACACT
RDS1 ORF F	RT-qPCR	AAGCCGTGAGATTGAAATGG
RDS1 ORF R	RT-qPCR	CTCCATCTGGCACAACAGAA
TUB1 ORF F	RT-qPCR	TCTTGGTGGTGGTACTGGTT
TUB1 ORF R	RT-qPCR	TGGATTTCTTACCGTATTCAGCG
ChrIII 286.5kbp F	ChIP	CGCACTGCGAACAAAGAATA
ChrIII 286.5kbp R	ChIP	CGCTGTGTTAGGAGGCTTTT
ChrIII 288kbp F	ChIP	TGAGGATGTACACGCAGAGAA
ChrIII 288kbp R	ChIP	AGCAAACCCTGGGAGTTCTT
ChrIII 289.5kbp F	ChIP	ATTGGGCTTCTGGATGACAG
ChrIII 289.5kbp R	ChIP	AGGAAGGCATGCATTGAACT
ChrIII 291kbp F	ChIP	TGATTTAAGCGTGCGTGAAG
ChrIII 291kbp R	ChIP	GGTCAACATAAAGTGGCGAGA
HMR ORF F	ChIP	TGGCGGAAAACATAAACAGA
HMR ORF R	ChIP	TGCTTGGGGTGATATTGATG
ChrIII 296.5kbp F	ChIP	TCAACATGGTGTTCCAAAGC
ChrIII 296.5kbp R	ChIP	TGATGCAGTGGCGATATCAT
ChrIII 298kbp F	ChIP	GAACACACTCAATGGCCAGA
ChrIII 298kbp R	ChIP	TGGTCCATTTGCTACGATCA

Name	Method	Primer sequence (5'-3')
ChrIII 299.5kbp F	ChIP	TTTCGACGGCTGATAACCTT
ChrIII 299.5kbp R	ChIP	AAAGAAGGGGAGCGAAAAAG
ChrIII 301kbp F	ChIP	GGAATGTTCATGGCCTCAAT
ChrIII 301kbp R	ChIP	TCAGATTGCCCTTTCCGATA
ChrIII 309kbp F	ChIP	GGTATTTCCAACGCAAAGGA
ChrIII 309kbp R	ChIP	CGGCCAATTATTTCATGTCC
ChrIII 310.5kbp F	ChIP	CGAGCATGTCTGATGAGGTC
ChrIII 310.5kbp R	ChIP	CCGAATGCAAAAATGTGAAG
ChrIII 312kbp F	ChIP	TGAGCCCCACTAACTTGCTT
ChrIII 312kbp R	ChIP	TACCAGCATCACCTTCAGCA
ChrIII 313.5kbp F	ChIP	TTTGATGCCTTCTGGGATTT
ChrIII 313.5kbp R	ChIP	TTACATTCCGCCTGCCTAAC
YCR094W Prom F	ChIP	GCAAACCCCTCTACAATCCA
YCR094W Prom R	ChIP	CAAAAGTGAAAGCGACCCATA
YCR095C Prom F	ChIP	TACCGTATGCGGTATAATGA
YCR095C Prom R	ChIP	GTCTCCACTTTAGAACATCT
GIT1 Prom F	ChIP	TTCATGAATTTCCTTACTGGAC
GIT1 Prom R	ChIP	GTTGACTAGTCACAAGAAACAG
YCR099C Prom F	ChIP	TGCTACTGGTGATCTGGGAAA
YCR099C Prom R	ChIP	CTGATCCATCTGGCGTTGTA
YCR100C Prom F	ChIP	GCAAGGATTCTGACTTTACTGG
YCR100C Prom R	ChIP	CTCGTTATGCCCGTCATCTT
RDS1 Prom F	ChIP	TGTGCTATCTAAGAGGATGGTTCA
RDS1 Prom R	ChIP	CAGCAGCCAATTTCATGTTC
PRP8 ORF F	ChIP	GGATGTATCCAGAGGCCAAT
PRP8 ORF R	ChIP	AACCCGCGTATTAAGCCATA
GID7 Prom F	ChIP	CTTGTGTGCGCTTGTAGCAT
GID7 Prom R	ChIP	CCCGTTTCCGATGATATTGT
STE50 Prom F	ChIP	AATGGTAGACACCGGACTCG

Name	Method	Primer sequence (5'-3')
STE50 Prom R	ChIP	AGTGGAGCAGGCTGTACGTT
BUD3 Prom F	ChIP	GAGATTTCGATCACCATCGT
BUD3 Prom R	ChIP	CTTCCTCATTGAAGATCAAAGC
MRK1 Prom F	ChIP	AGGGGCAGCATTATCCGTTA
MRK1 Prom R	ChIP	CTTCCCCGCAGTATGGTAGA
BZZ1 Prom F	ChIP	CGCTTAGCAAAGGAATAGACAGA
BZZ1 Prom R	ChIP	TGCTCAATGTCCTTCAACCA
YDC1 Prom F	ChIP	CGGAGAGTGGCATAGCATG
YDC1 Prom R	ChIP	TGCAATAGAAAGAAAGCAAGCG

2.2.4 ChIP-qPCR and ChIP-on-chip

Chromatin immunoprecipitation (ChIP) experiments were performed as described previously (Schulze *et al.* 2009). In brief, 250 ml of cells were grown in YP-dextrose to an OD_{600} of 0.5-0.6 from OD_{600} of 0.15 and were crosslinked with 1% formaldehyde for 20 minutes before chromatin was extracted. The chromatin was sonicated (Bioruptor, Diagenode, Spart, NJ: 10 cycles, 30s on/off, high setting) to yield an average DNA fragment of 500bp. Anti-FLAG antibody (4.2µl, Sigma) was coupled to 60µl of protein A magnetic beads (Invitrogen). After reversal of the crosslinking and DNA purification, the immunoprecipitated and input DNA were analyzed by quantitative real-time PCR (qPCR). Samples were analyzed in triplicate for three independent ChIP experiments. Statistical significance was assessed using Student's *t* test. Primer sequences are listed in Table 2.2. For microarray analysis, after reversal of crosslinking and DNA purification, the DNA was amplified with two rounds of T7 RNA polymerase amplification and hybridized to Affymetrix 1.0R *S. cerevisiae* tiling microarray.

A modified version of the model-based analysis of tiling arrays (MAT) algorithm was used to reliable detect Sir2 occupancy across the genome. The data was normalized using both input DNA and a mock IP control.

2.3 Results

2.3.1 *ASF1* Genetically Interacted with Genes Encoding for Subunits of SWR1-C

Yeast lacking both *ASF1* and *YAF9* have an exacerbated growth defect compared to cells with a single deletion of either gene, suggesting these genes share a redundant function (Figure 2.1) (Wang *et al.* 2009). Given that *YAF9* is required for H2A.Z deposition by SWR1-C, we asked if the synthetically sick phenotype of *asf1Δyaf9Δ* double mutants broadly reflected defects in SWR1-C function. We characterized genetic interactions between *ASF1* and genes that encode all unique subunits of SWR1-C. Under unperturbed growth conditions, loss of *ASF1* resulted in synthetic sick genetic interactions with genes encoding eight SWR1-C subunits (Figure 2.1). The growth fitness of the double mutants was further reduced when cells were grown at 16°C or in conditions that induce DNA replication stress (HU). The decrease in fitness of all double mutants under stressed conditions was generally comparable to *asf1Δyaf9Δ* double mutants, although nuanced differences were present (Figure 2.1). Although *ASF1* showed strong synthetic interaction with genes encoding for the entire SWR1-C complex, a similar pattern and severity of genetic interactions was not observed with members of the NuA4 complex (data not shown). Taken together, the genetic data suggested that the synthetic lethality between *ASF1* and *YAF9* primarily reflected Yaf9's

function within SWR1-C, and that SWR1-C in its entirety had an important functional relationship with the Asf1 histone chaperone.

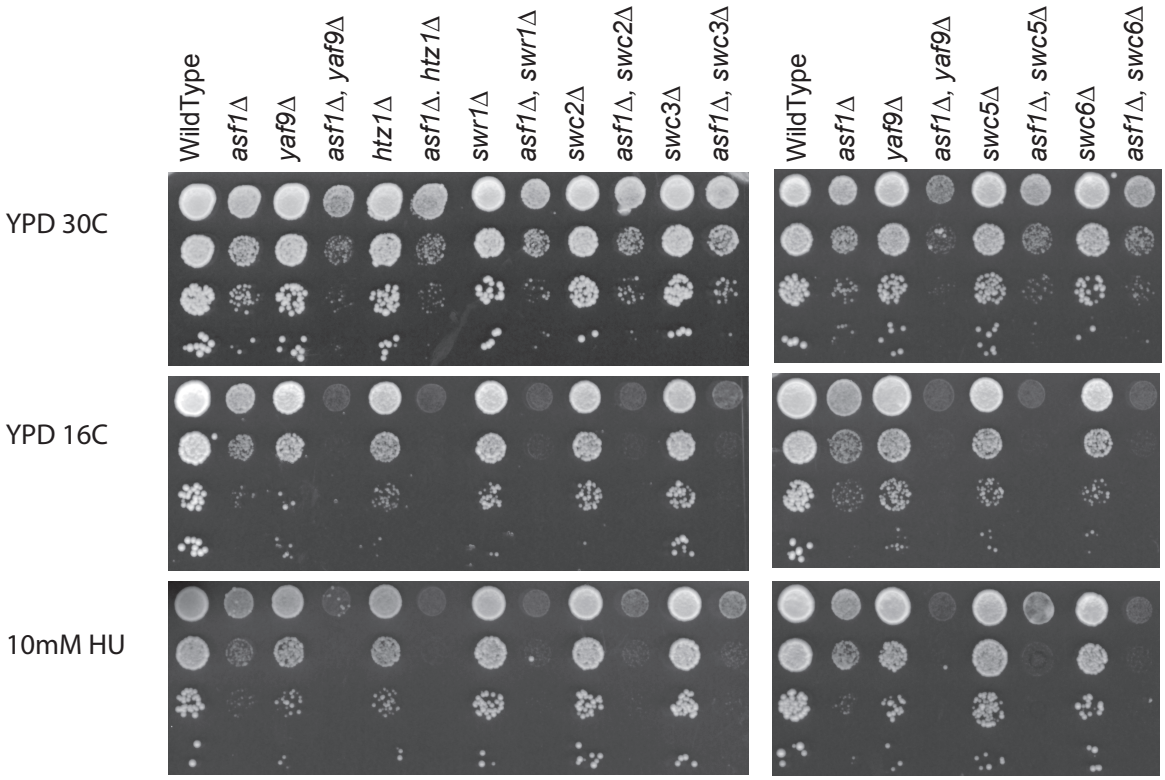

Figure 2.1 *ASF1* genetically interacted with genes encoding for non-essential subunits of SWR1-C subunits
Double mutants containing *asf1Δ* and a subunit of SWR1-C grew significantly more slowly than the respective single mutants. Ten-fold serial dilutions of the indicated strains were plated on YPD media, with or without 10mM HU and incubated at the indicated temperatures.

2.3.2 *ASF1* and *YAF9* were Required for Maintaining Heterochromatin-Proximal Gene Expression

To further examine the interplay between Asf1 and Yaf9, we dissected their roles at heterochromatin boundaries, focusing on the well-characterized subtelomeric region encompassing the right telomere of chromosome III and the *HMR* locus. NuA4 does not

acetylate H4 at Chr III R, which allowed us to assay SWR1-C-specific activities of Yaf9 (Zhang *et al.* 2004). A unique aspect of this 35kb region of DNA is that it encompasses three distinct heterochromatin boundaries: two located on either side of the *HMR* and one at the telomere heterochromatin boundary (Figure 2.2A). By RT-qPCR, we quantified expression levels of endogenous genes to interrogate native silencing defects, circumventing issues associated with embedded reporter genes such as *URA3*. Consistent with previous work, gene expression at all loci tested was significantly reduced in *yaf9Δ* strains (Figure 2.2B) (Zhang *et al.* 2004). Surprisingly, the effect of *ASF1* in this 35kb region differed depending on the gene's proximity to either the *HMR* or the telomere. Loss of *ASF1* led to reduced expression of genes flanking the *HMR*, while *ASF1* was dispensable for proper expression of subtelomeric genes (Figure 2.2B). Based both on proximity to the *HMR*/telomere and differential expression patterns in *asf1Δ* cells, we classified *YCR094, YCR095* and *GIT1* as *HMR*-influenced genes and *YCR099, YCR100* and *RDS1* as telomere-influenced genes. Interestingly, changes in transcript levels in the *asf1Δ yaf9Δ* double mutant did not reflect the genetic interaction phenotype. mRNA levels of the three genes flanking the *HMR* in the *asf1Δ yaf9Δ* double mutant were comparable to either of the single mutants alone, whereas mRNA levels of *YCR099C, YCR100C,* and *RDS1* in the double mutant were reduced to the same level as the *yaf9Δ* mutant (Figure 2.2B).

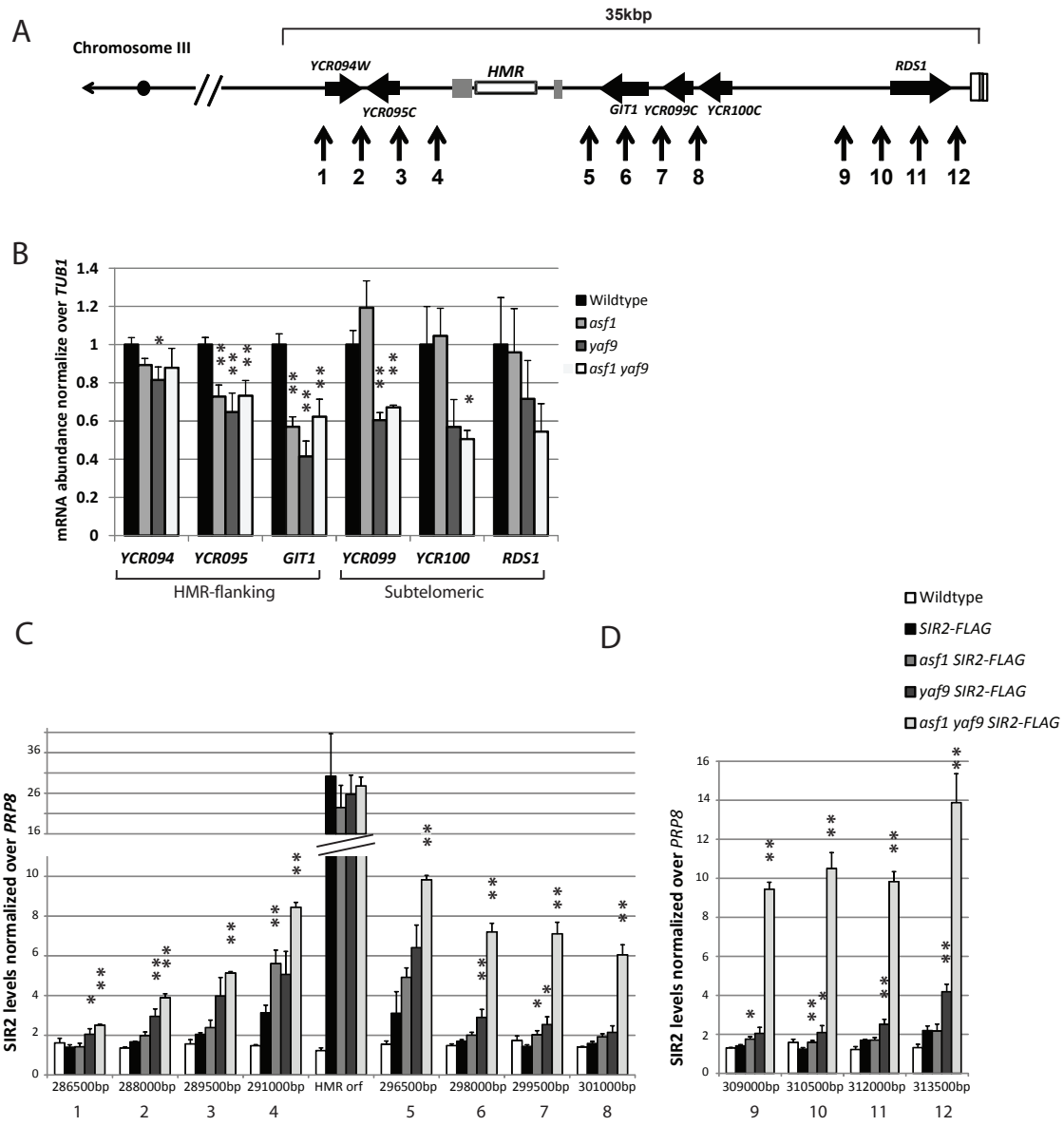

Figure 2.2 *ASF1* and *YAF9* were required for maintaining heterochromatin-proximal gene expression
(A) Schematic representation of ORFs at the boundaries of the *HMR* locus and the right telomere of Chromosome III. Arrows represent ORFs and provide transcriptional direction information. Locations of PCR primers for Sir2-FLAG ChIP analysis are indicated with arrows 1 to 12 spaced in 1.5kb increments. (B) As measured by RT-qPCR, mRNA levels of the indicated genes in wildtype, *asf1Δ, yaf9Δ* and *asf1Δ yaf9Δ* strains are represented by black, light gray, dark gray and white bars, respectively. *asf1Δ* strains exhibited reduced mRNA levels of *HMR*-flanking genes. Loss of *YAF9* led to the repression of all heterochromatin-proximal genes tested. mRNA levels for all genes were normalized to levels of *TUB1* mRNA. (C) Sir2 spread beyond the telomere and *HMR* in *yaf9Δ* and *asf1Δ yaf9Δ* strains. *yaf9Δ* exhibited a small but significant increase in Sir2 levels at regions previously devoid of Sir2. *asf1Δ yaf9Δ* showed a synergistic increase in Sir2 levels immediately adjacent to the telomere that spread up to 15kb away. Sir2 levels measured by ChIP-qPCR were normalized to Sir2 level at the *PRP8* ORF. (B), (C) (D) Error bars represent standard error of values of three biological replicates. *, p-value < 0.10; **, p-value < 0.05 when compared with the Wildtype strain using a two-tailed student t-test.

We then asked whether repression of *HMR*-influenced genes in *asf1Δ* cells was due to the spread of SIR complexes beyond the *HMR* locus. We examined Sir2 levels via ChIP-qPCR in 1.5kb increments on either side of the *HMR* locus and outside of the Chr III R telomeric region (Figure 2.2A). Sir2 levels were enriched at the *HMR* locus and depleted at all other sites tested in wildtype cells as expected (Figure 2.2C). In agreement with previous studies, loss of *YAF9* led to Sir2 spreading into regions previously devoid of SIR complexes, with the highest levels of Sir2 occupancy occurring on both sides flanking the *HMR* (Figure 2.2C) (Meneghini *et al.* 2003). Even though cells lacking *ASF1* exhibited reduced transcriptional activity of *HMR*-adjacent genes, significant enrichment of Sir2 was not observed more than 1.5kb away from the *HMR* nor at the subtelomeric regions (Figure 2.2C and Figure 2.2D). In particular, the promoters of *YCR094W, YCR095C and GIT1* were not enriched for Sir2 in *asf1Δ* cells (Figure 2.2C). Strikingly, while *yaf9Δ* cells showed significant increases in Sir2 levels at the subtelomeric regions, *asf1Δ yaf9Δ* cells exhibited dramatic Sir2 spreading immediately adjacent to the telomere (Figure 2.2C and Figure 2.2D). These data suggested that Asf1 works cooperatively with SWR1-C to regulate SIR occupancy adjacent to the telomere. The increase in local concentrations of Sir2 was not reflected in gene expression levels since mRNA levels of telomere-associated genes in *asf1Δ yaf9Δ* double mutants were similar to *yaf9Δ* single mutants.

2.3.3 Cooperative Regulation of SIR Occupancy by Asf1 and Yaf9 was Telomere-Specific

To ascertain how Asf1 and Yaf9 regulate Sir2 positioning, we characterized genome-wide Sir2 occupancy by ChIP-on-chip in the mutant strains. We focused our analysis on telomere-

proximal regions 30kb away from the chromosomal ends. In accordance with our ChIP-qPCR analysis of Chr III R, Sir2 occupancy was restricted to the *HMR* and to the region immediately adjacent to the telomere in wildtype and *asf1Δ* cells whereas in both the *yaf9Δ* strain and the double mutant, Sir2 spread beyond the normal heterochromatic regions (Figure 2.3A). We also demonstrated that over the 17kb region between the telomere and *HMR,* the genome-wide ChIP analysis recapitulated the dramatic increase in Sir2 levels when *ASF1* was deleted in a *yaf9Δ* background. Across all chromosomal ends, the loss of *ASF1* did not significantly alter Sir2 occupancy although the loss of *YAF9* led to an increase in Sir2 occupancy at subtelomeres (data not shown). Interestingly, the principles derived from Chr III R appeared to not be limited to this unique region. We found similar patterns on three more chromosomal ends where both Asf1 and Yaf9 were required to restrict the spread of Sir2 (Figure 2.3B). Conversely, the patterns of Sir2 occupancy on the remaining 28 telomere ends were highly comparable between the *yaf9Δ* and the *asf1Δ yaf9Δ* mutants (data not shown). We also noted that Asf1 was important for regulating Sir2 occupancy over the highly conserved Y' element that is present in the majority of yeast telomeres. Loss of *YAF9* led to minimal changes to Sir2 occupancy within the Y' element but the combined deletion of *ASF1* and *YAF9* led to a synergistic increase in Sir2 occupancy over the telomere element (Figure 2.3C). The highly repetitive nature of telomeric DNA makes it difficult to verify whether our observed trend holds true for all Y' elements.

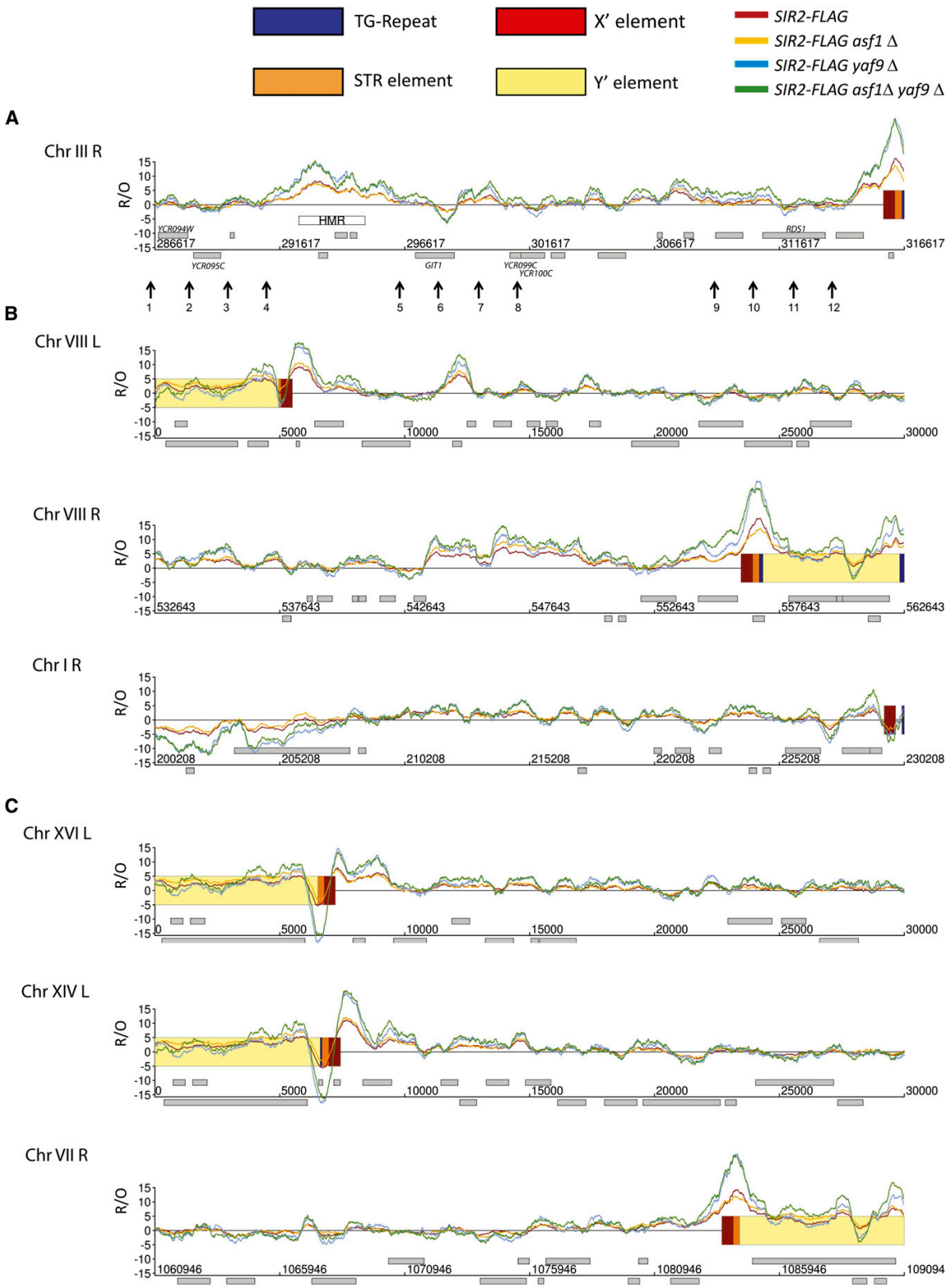
TG-Repeat
X' element
STR element
Y' element
SIR2-FLAG
SIR2-FLAG asf1 Δ
SIR2-FLAG yaf9 Δ
SIR2-FLAG asf1Δ yaf9 Δ
A
Chr III R
R/O
HMR
YCR094W
YCR095C
GIT1
YCR099C
YCR100C
RDS1
286617
291617
296617
301617
306617
311617
316617
1
2
3
4
5
6
7
8
9
10
11
12
B
Chr VIII L
0
5000
10000
15000
20000
25000
30000
Chr VIII R
532643
537643
542643
547643
552643
557643
562643
Chr I R
200208
205208
210208
215208
220208
225208
230208
C
Chr XVI L
Chr XIV L
Chr VII R
1060946
1065946
1070946
1075946
1080946
1085946
1090946

Figure 2.3 Regulation of Sir2 occupancy by Asf1 and Yaf9 was telomere-specific
ChIP-on-chip profiles of Sir2. Thirty kilo-basepairs of chromosome ends were plotted along the x-axis against the relative occupancy (R/O) of Sir2 in wildtype, *asf1Δ, yaf9Δ* and *asf1Δ yaf9Δ* cells. ORFs are indicated as light gray rectangles above the x-axis for Watson genes and below the x-axis for Crick genes. (A) ChIP-on-chip profile of Sir2 along the right telomere of Chr III. Arrows 1 through 12 represent locations assayed by ChIP-qPCR in Figure 2. (B) Telomere-proximal profiles of Chr VIII L, VIII R, and IR showed increased Sir2 occupancy in *asf1Δ yaf9Δ* cells similar to Chr III R. (C) Genome-wide profiling of Sir2 highlighted differences in Asf1 and Yaf9 function over heterochromatin-specific Y' elements. Chr XVI L, XIV L, and VII R are shown.

2.3.4 Asf1 and SWR1-C Affected Heterochromatin-Proximal Gene Expression through Different Mechanisms

We next tested whether Sir2 accumulation caused gene expression changes across the right arm of chromosome III by measuring mRNA levels in cells lacking *SIR2*. To test whether Yaf9's role at the Chr III R telomere was indeed linked to its function in SWR1-C as our previous experiments suggested, we included strains lacking *SWR1,* the catalytic subunit of SWR1-C. Not surprisingly, strains lacking *YAF9* or *SWR1* had very similar expression profiles at the Chr III R region suggesting that the decreased mRNA levels of these genes resulted from reduced SWR1-C activity (Figure 2.4A and Figure 2.4B). The combined analysis of gene expression in double and triple mutants highlighted distinct functions and causal interdependencies in this region. Firstly, loss of *SIR2* restored expression levels of all six genes in *yaf9Δ* and *swr1Δ* cells (Figure 2.4A and Figure 2.4B). In agreement with our Sir2 ChIP results, loss of *SIR2* did not restore mRNA levels of *HMR*-flanking genes in *asf1Δ* cells, indicating that repression of these genes was not mediated by the spread of Sir2 into adjacent euchromatin (Figure 2.4C). Secondly, deletion of *SIR2* in *asf1Δ yaf9Δ* and *asf1Δ swr1Δ* strains restored the mRNA levels of the genes between the *HMR* and telomere, but not those flanking the left side of the *HMR* (Figure 2.4D and Figure 2.4E). Both *YCR094W* and *YCR095C* that depended on Asf1 for expression remained repressed even when *SIR2* was

deleted (Figure 2.4D and Figure 2.4E). Unlike the other two *HMR*-flanking genes, the expression of *GIT1* was restored to at least wildtype levels in both *asf1Δ yaf9Δsir2Δ* and *asf1Δ swr1Δsir2Δ* (Figure 2.4D and Figure 2.4E). *YCR099C* and *YCR100C* exhibited higher than wildtype levels of mRNA in the *asf1Δ swr1Δ sir2Δ* triple mutant (Figure 2.4E). Together, these data suggested that in the absence of a functional SWR1-C, SIR complexes spread into nearby euchromatic regions, whereas *asf1Δ*-dependent repression of *HMR*-flanking genes was not due to SIR activity.

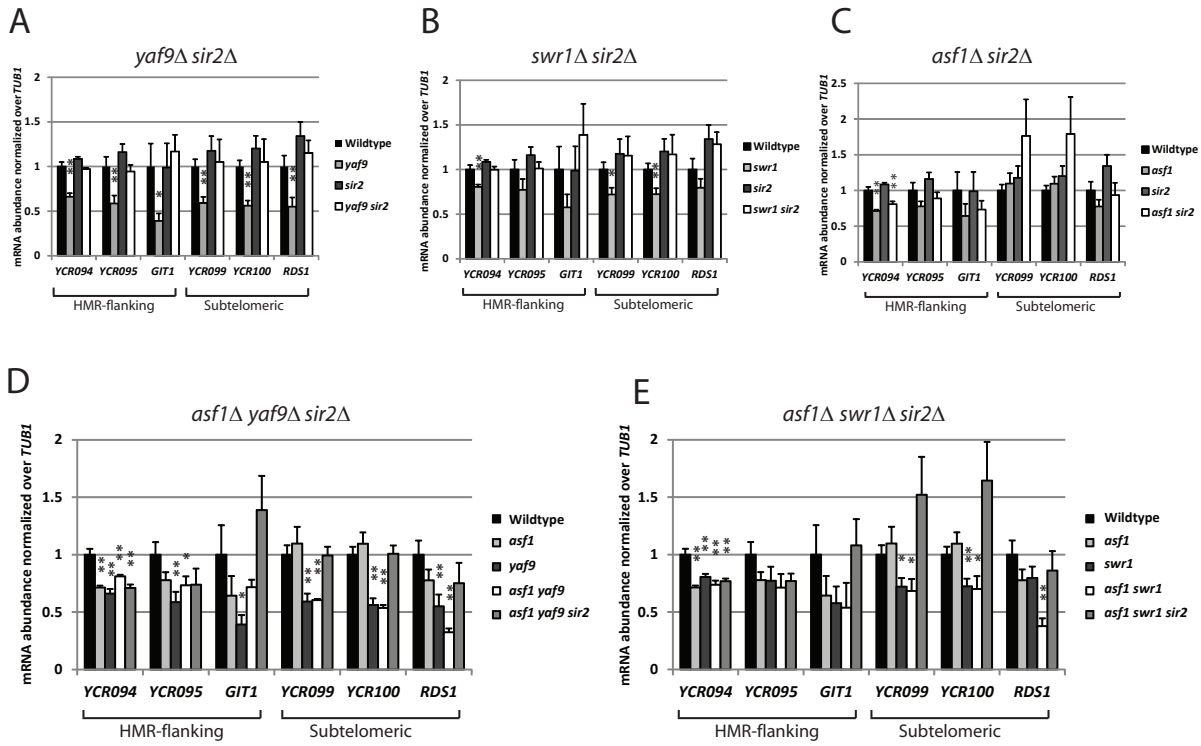

Figure 2.4 Asf1 regulated *HMR*-proximal gene expression in a Sir2-independent manner
mRNA levels of heterochromatic genes in the indicated strains were carried out in parallel. mRNA levels were determined by qRT-PCR and normalized to *TUB1*. Data shown are the average of three independent experiments. Error bars represent standard error of values of the three biological replicates. *, p-value < 0.10; **, p-value < 0.05 when compared with the Wildtype strain using a two-tailed student t-test. (A) Deletion of *SIR2* rescued all expression defects observed in *yaf9Δ* strains. mRNA levels of wildtype (black), *yaf9Δ* (light gray), *sir2Δ* (dark gray) and *yaf9Δ sir2Δ* (white) strains. (B) Expression profile of tested genes in cells lacking *SWR1* resembled those lacking *YAF9*. Loss of *SIR2* in *swr1Δ* background also rescued the expression of all tested genes to wildtype levels. mRNA levels of wildtype (black), *swr1Δ* (light gray), *sir2Δ* (dark gray) and *swr1Δ sir2Δ* (white) strains. (C) Loss of *SIR2* in strains lacking *ASF1* was unable to rescue the repression of *HMR*-flanking genes. mRNA levels of wildtype (black), *swr1Δ* (light gray), *asf1Δ* (dark gray) and *asf1Δ sir2Δ* (white) strains. (D) Loss of *SIR2* in an *asf1Δ yaf9Δ* background was able to rescue all Yaf9-specific transcriptional defects but not Asf1-specific defects around the *HMR*. mRNA levels of wildtype (black), *asf1Δ* (light gray), *yaf9Δ* (dark gray), *asf1Δ yaf9Δ* (white) and *asf1Δ yaf9Δ sir2Δ* (medium gray) strains. (E) Similarly, deletion of *SIR2* rescued gene expression of subtelomeric genes to wildtype levels in *asf1Δ swr1Δ* strains, but not the *HMR*-flanking genes. mRNA levels of wildtype (black), *asf1Δ* (light gray), *swr1Δ* (dark gray), *asf1Δ swr1Δ* (white) and *asf1Δ swr1Δ sir2Δ* (medium gray) strains.

2.3.5 Dysregulation of Heterochromatin Boundaries in *asf1Δ yaf9Δ* was not the Underlying Cause of the Severe Growth Defects

The complex relationship between Sir2 localization and gene expression described above raised the possibility that the growth phenotype of *asf1Δ yaf9Δ* was a reflection of additional

cellular processes. We therefore expected that aberrant SIR chromatin structures, caused by the simultaneous loss of *ASF1* and *YAF9,* did not contribute to the pronounced growth defects. Indeed, loss of *SIR2* did not suppress the synergistic genetic interaction between *ASF1* and *YAF9*, indicating that the growth defect was due to other functions of Asf1 and SWR1-C (Figure 2.5A).

To gain a better mechanistic understanding of the genetic interaction between *ASF1* and *YAF9*, we focused on Asf1's role in nucleosome assembly at heterochromatin by using two *asf1* alleles (H36A/D37A and H39A/K41A) that exhibit reduced silencing at telomeres when CAF-1 is mutated (Sharp *et al.* 2001; Daganzo *et al.* 2003). Plasmids containing the *asf1* alleles were transformed into strains lacking both *ASF1* and a gene encoding for the *CAC2* subunit of CAF-1. As expected, *asf1H36A/D37A* and *asf1H39A/K41A* mutants alone did not exhibit a significant growth defect (Figure 2.5B) (Daganzo *et al.* 2003). Strains lacking *CAC2* with an *asf1* allele showed slight growth defects compared to wildtype strains (Figure 2.5B). Consistent with previous work, the *asf1H39A/K41A* allele exhibited a stronger phenotype than *asf1H36A/D37A* (Figure 2.5B). *cac2Δ yaf9Δ asf1H36A/D37A* and *cac2Δ yaf9Δ asf1H39A/K41A* strains, however, did not demonstrate a strong synergistic interaction (Figure 2.5B). Our genetic data therefore revealed that the synergistic genetic interaction between *ASF1* and *YAF9* was not due to Asf1's functions in various aspects of heterochromatin biology.

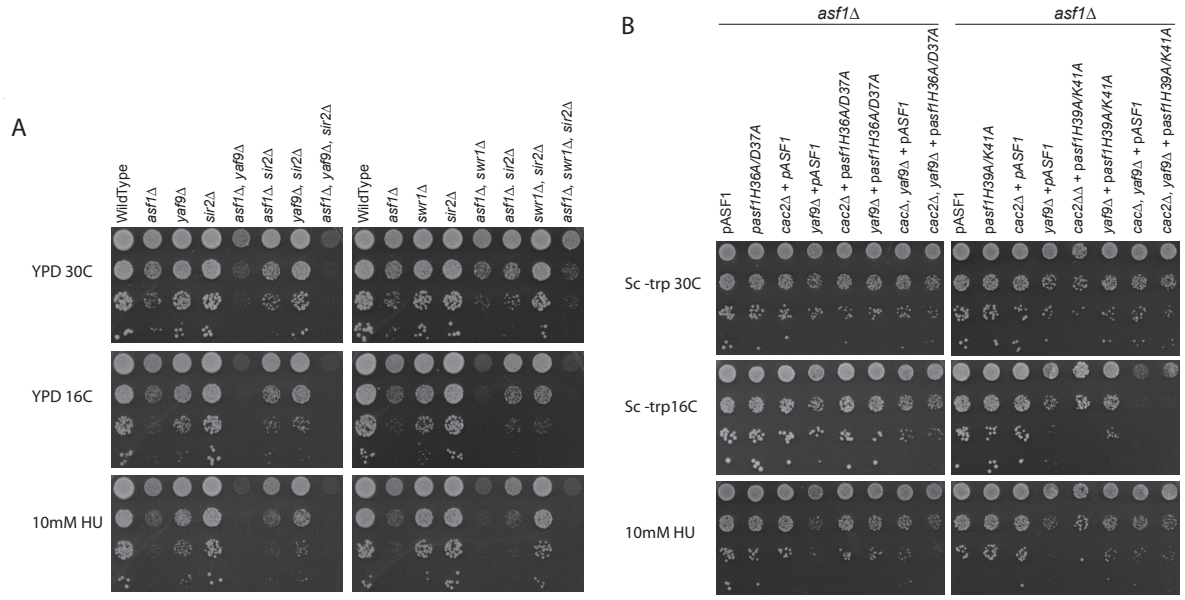

Figure 2.5 Silencing defects were not causal for *asf1Δ yaf9Δ* synthetic growth defect
(A) Deletion of *SIR2* did not suppress the growth defects observed in *asf1Δ yaf9Δ* and *asf1Δ swr1Δ* strains. Ten-fold serial dilution of strains were plated and incubated at the indicated condition. (B) Heterochromatin-specific nucleosome assembly mutants of *ASF1* did not genetically interact with *YAF9.* Ten-fold serial dilutions of indicated strains carrying p*ASF1,* p*asf1 H36A/D37A,* or p*asf1H39A/K41A* were plated on SC-TRP media and incubated for two to three days at the indicated conditions.

2.3.6 The Synergistic Genetic Interaction between *ASF1* and *YAF9* was Mediated via Rtt109-Dependent H3K56 Acetylation

To test if Asf1's ability to act as a global chaperone in nucleosome assembly was important for its genetic interaction with *YAF9,* we used the well-characterized *asf1V94R* mutant to assay whether a complete loss of histone H3/H4 binding can replicate the synergistic interaction between *ASF1* and *YAF9* (Mousson *et al.* 2005). We found that similar to *asf1Δyaf9Δ, asf1V94R yaf9Δ* grew much slower at 16°C and showed increased sensitivity to a low concentration of hydroxyurea, implicating Asf1 and H3 interaction in this pathway (Figure 2.6A). Since the physical association between Asf1 and H3 is important to mediate the acetylation of lysine 56 on H3 by Rtt109, we subsequently tested whether *RTT109* also displayed a genetic interaction with *YAF9* and genes encoding for other subunits of SWR1-C.

As previously seen in the *asf1Δyaf9Δ* double mutants, *RTT109* displayed a synthetic genetic interaction with *YAF9.* Furthermore, the growth fitness of all double mutants was significantly compromised compared to their respective single mutants under stress-induced conditions (Figure 2.6B).

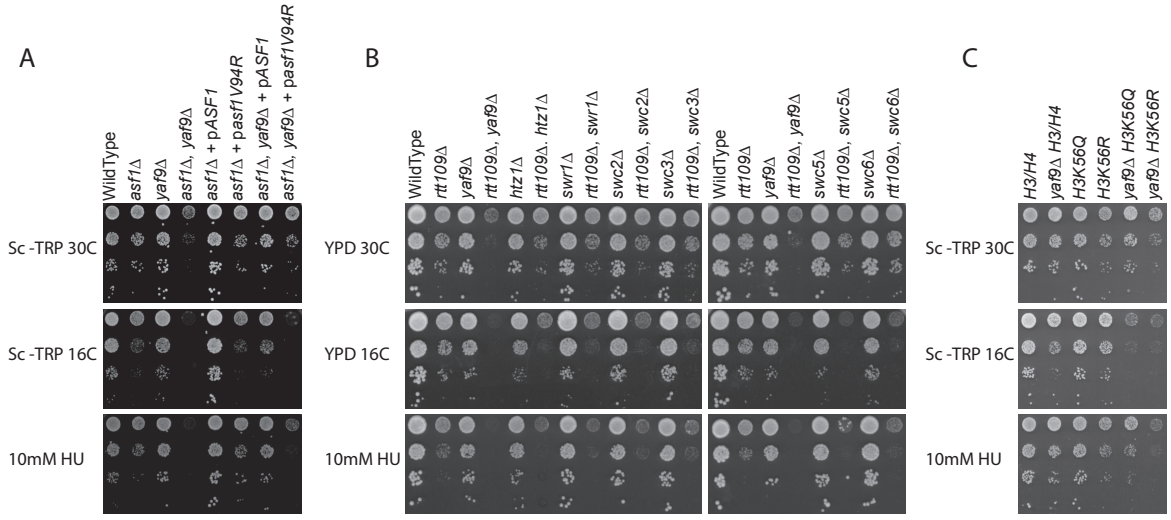

Figure 2.6 Synergistic genetic interaction between *ASF1* and *YAF9* was mediated by Rtt109-dependent H3K56 acetylation
(A) *YAF9* genetically interacted with *asf1V94R*. (B) *RTT109* genetically interacted with all non-essential genes encoding for SWR1-C subunits. (C) H3K56R genetically interacted with *YAF9*. Ten fold-serial dilutions of strains were plated and incubated at the labeled conditions.

To confirm if the genetic interaction we observed was mediated via acetylation of H3K56, we took advantage of existing H3K56 alleles containing a point mutation at lysine 56 to either glutamine or arginine, mimicking a constitutively hyperacetylated lysine or constitutively hypoacetylated lysine, respectively (Miller *et al.* 2008). In agreement with published data, the *yaf9ΔH3K56R* strain had significantly reduced growth fitness compared to either of the single mutants alone, while the *yaf9ΔH3K56Q* strain did not display a strong

growth defect (Figure 2.6C) (Wang *et al.* 2009). Furthermore, similar experiments testing for H3K9 acetylation, which is also mediated by Rtt109, revealed that the genetic interaction was specific to Asf1's role in H3K56 acetylation and not Rtt109-mediated H3K9 acetylation (data not shown). These results indicated that the genetic interaction between *ASF1* and *YAF9* was a result of failure to acetylate H3K56 in an Asf1/Rtt109-dependent manner.

2.3.7 Asf1 and H3K56 Acetylation Promoted H2A.Z Occupancy at Subtelomeric Gene Promoters

We again utilized our six genes of interest to explore the genetic connection between H3K56 acetylation and SWR1-C in more detail, since all but *YCR099* have robust H2A.Z promoter occupancy. Because we previously demonstrated that H3K56ace-containing promoters preferentially lose H2A.Z in a *yaf9* hypomorph, we next addressed whether H3K56 acetylation and Asf1 are involved in H2A.Z occupancy at gene promoters (Wang *et al.* 2009). We used ChIP-qPCR to assay H2A.Z localization at the promoters of heterochromatin-proximal genes in strains that contain either *asf1Δ* or the H3K56R non-acetylable mutation. H2A.Z was enriched to varying degrees at the promoters of all genes we examined and as expected, a loss of *YAF9* led to a total depletion of H2A.Z at each promoter (Figure 2.7A). Remarkably, deletion of *ASF1* resulted in a significant decrease in H2A.Z levels across all promoters tested; this result demonstrated that Asf1 enhanced H2A.Z deposition but was not required (Figure 2.7A). Next, we asked if the reduction of H2A.Z at subtelomeric gene promoters seen in *asf1Δ* cells was due to a loss of H3K56ace. We found that H2A.Z enrichment in the H3K56R mutant was reduced to levels similar to those of

asf1Δ, suggesting that Asf1-mediated H3K56 acetylation promoted H2A.Z localization at the promoters of heterochromatin-proximal genes (Figure 2.7B).

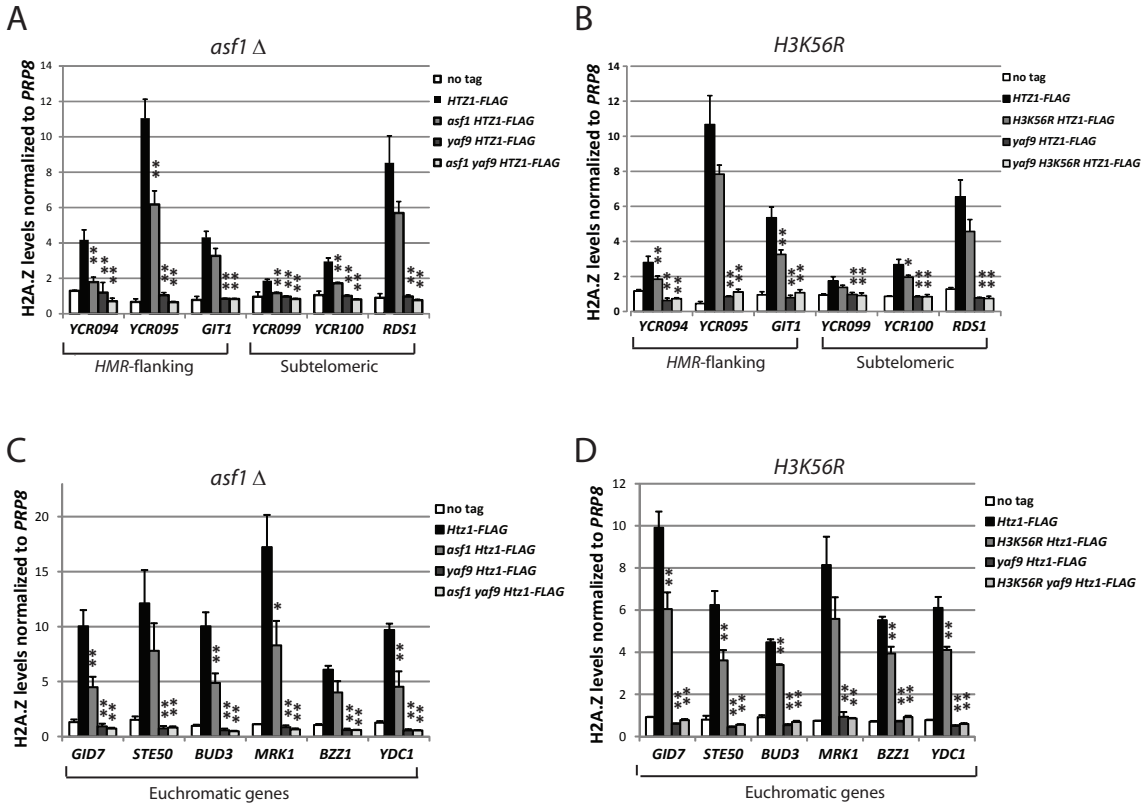

Figure 2.7 Asf1 and H3K56 acetylation promoted H2A.Z occupancy at subtelomeric and euchromatic gene promoters

H2A.Z occupancy at promoters of indicated genes was measured by ChIP-qPCR using the anti-FLAG antibody (Sigma). H2A.Z enrichment was normalized to the reference gene *PRP8.* Error bars represent standard error of three biological replicates. *, p-value < 0.10; **, p-value < 0.05 when compared with the Wildtype strain using a two-tailed student t-test. (A) Occupancy of H2A.Z at heterochromatin-proximal gene promoters was reduced significantly in cells lacking *ASF1.* (B) Similarly, promoter H2A.Z levels of subtelomeric genes were significantly reduced in a H3K56R mutant. (C) (D) Asf1 and H3K56 acetylation are both required for normal H2A.Z occupancy at euchromatic promoters. Loss of *YAF9* led to a complete loss of H2A.Z at gene promoters.

Since our genetic data suggested that the relationship between Asf1 and H2A.Z was not exclusive to the heterochromatic region, we extended the analysis to include euchromatic promoters that are H2A.Z-enriched. We selected six genes from either previously published primer sets or genome-wide H2A.Z ChIP data sets. As expected, H2A.Z was highly enriched at the promoter of these genes in wildtype cells (Figure 2.7C and Figure 2.7D). Analogous to the effects at heterochromatic gene promoters, loss of *ASF1* also led to a reduction in H2A.Z levels at all six genes we assayed (Figure 2.7C). Furthermore, H2A.Z levels were also significantly reduced in the H3K56R mutant, suggesting that the acetylation of H3K56 by Asf1 is important for H2A.Z occupancy at euchromatic gene promoters (Figure 2.7D).

2.4 Discussion

We have teased apart the region-specific and global interactions between Asf1 and SWR1-C, particularly its Yaf9 subunit, and expanded upon the established linkages between them. First, we identified region-specific changes in gene expression in the absence of either Asf1 or Yaf9 within a 35kb region on the right telomere of chromosome III. Whereas loss of SWR1-C function resulted in repression of heterochromatin-proximal genes as a result of Sir2 spread, loss of Asf1 led to repression of only *HMR*-proximal genes in a Sir2-independent manner. Nevertheless, we found that Asf1 cooperated with Yaf9 to modulate the telomere-heterochromatin boundary of Chr III R to prevent the spread of SIR complexes into the subtelomeric region. This interaction was recapitulated at three additional telomere ends upon genome-wide analysis of Sir2 occupancy. In agreement with these effects likely being region-specific, genetic analysis revealed that global loss of *SIR2* did not rescue the growth

defect in *asf1Δ yaf9Δ* double mutants. Next, we demonstrated that a strong synergistic genetic interaction existed between genes encoding for SWR1-C and factors in the H3K56 acetylation pathway. Loss of H3K56 acetylation, either by the deletion of the Asf1 histone chaperone or mutation of the K56 residue, diminished H2A.Z levels at the promoters of subtelomeric and euchromatic genes.

Maintenance of euchromatin-heterochromatin boundaries requires the concerted activities of chromatin remodeling complexes. RT-qPCR analysis of genes adjacent to the right telomere of Chr III showed that SWR1-C, but not Asf1, regulated this heterochromatin boundary. After careful dissection of how Asf1 and Yaf9 function in restricting Sir2 spread around the *HMR* and the Chr III R subtelomeric region, however, we found that the connection between Asf1 and SWR1-C was more complex. Repression of telomere-proximal genes in *yaf9Δ* cells was due to the loss of a functional heterochromatin boundary, which resulted in a spread of SIR complexes over nearby genes. On the other hand, loss of *ASF1* alone did not affect the function of the heterochromatin boundary, as evidenced by the lack of Sir2 spread in *asf1Δ* cells and normal expression levels of subtelomeric genes. We demonstrated by ChIP-qPCR and by ChIP-on-chip that combined loss of *ASF1* and *YAF9* led to increased spread of Sir2 and elevated levels of Sir2, suggesting that Yaf9 and Asf1 cooperated to restrict the spread of SIR proteins into nearby subtelomeres. Despite the dramatic enhancement of Sir2 occupancy over the subtelomeric region, mRNA levels of the three telomere-proximal genes we examined were reduced to the same level in the *asf1Δ yaf9Δ* double mutant as compared to the *yaf9Δ* single mutant. It has been suggested that SIR complexes function in a dosage-dependent manner in a reporter gene assay when *SIR3* and *SIR4* are overexpressed (Strahl-

Bolsinger *et al.* 1997). However, our combined occupancy and expression approach at Chr III R supported a threshold effect for SIR-dependent silencing. Specifically, the presence of Sir2 over the locus, regardless of whether it constitutes a two-fold increase of Sir2 occupancy in *yaf9Δ* or up to five-fold increase of Sir2 occupancy in *asf1Δ yaf9Δ,* led to the same level of gene repression of subtelomeric genes. Our genome-wide analysis of Sir2 occupancy patterns also demonstrated that the functional connection between Asf1 and SWR1-C was telomere-specific. Altogether, our findings showed that SWR1-C and Asf1 act cooperatively at a subset of telomere-proximal ends to limit the spread of SIR complexes onto nearby subtelomeric regions and that the SIR complex mediated silencing through a threshold mechanism.

The *HMR* is unique in that the silent cassette is flanked by silencers that initiate the formation of silenced chromatin (Guillemette *et al.* 2005). H2A.Z protects genes on either sides of the *HMR* from SIR-mediated silencing and loss of the histone variant leads to repression of the nearby genes (Meneghini *et al.* 2003; Babiarz *et al.* 2006; Li *et al.* 2005). Consistent with this, we found that deletion of *YAF9* and *SWR1* led to decreased transcript levels of *HMR*-proximal genes. Furthermore, *asf1Δ* and *asf1Δ yaf9Δ* cells also exhibited the same level of transcriptional defects, suggesting that SWR1-C and Asf1 regulate gene expression in the same pathway. Further analysis, however, revealed that repression of *YCR094, YCR095* and *GIT1* in SWR1-C mutants resulted from a defective heterochromatin boundary and Asf1-dependent expression defects were not a result of Sir2 spreading. The lack of correlation between SIR occupancy and changes in gene expression indicated that the silencing of *HMR*-proximal genes in *asf1Δ* cells was not due to SIR spread. Moreover, the persistence of a

transcriptional defect in *asf1Δ yaf9Δ sir2Δ* and *asf1Δ swr1Δ sir2Δ* triple mutants further supported that decreased mRNA levels of *YCR094* and *YCR095* resulted from an Asf1-specific transcriptional defect that was not linked to either Sir2 or H2A.Z-dependent boundary activity. Therefore, even though loss of *ASF1* and *YAF9* both led to gene repression around the *HMR*, Asf1 and SWR1-C mediated these effects through distinct mechanisms. Perhaps, by promoting H3K56 acetylation, Asf1 is directly involved in transcriptional activation of these subtelomeric genes by promoting nucleosome clearance at promoters (Adkins *et al.* 2004; Korber *et al.* 2006; Williams *et al.* 2008; Tolkunov *et al.* 2011).

In addition to region-specific effects, we also systematically characterized the genetic interaction profiles of *ASF1* and *RTT109* with all non-essential genes encoding for subunits of the SWR1-C complex. We found that all SWR1-C-encoding genes displayed a synthetically sick genetic interaction with *ASF1* and *RTT109* in an H3K56 acetylation-dependent manner. Given the severity of the genetic interaction, our data suggest that the functional relationship between H3K56 acetylation and SWR1-C goes beyond their interaction at heterochromatin. To add to our current understanding of SWR1-C-mediated H2A.Z deposition, we demonstrated that the level of chromatin-associated H2A.Z was also dependent on the histone chaperone Asf1. Deletion of *ASF1* or introduction of an unacetylable allele of H3K56 (H3K56R) resulted in an intermediate reduction in H2A.Z levels at promoters of heterochromatin-proximal and euchromatic genes. Based on previous genome-wide expression data in *htz1Δ,* it was not surprising that changes in H2A.Z levels in cells lacking *ASF1* were not correlated to changes in the expression of these lowly expressed genes. We speculate based on our data that Asf1 might directly influence the deposition of

H2A.Z through an H3K56ace-dependent pathway. Reduced H2A.Z occupancy in the H3K56R mutant suggests that acetylation promotes H2A.Z deposition. Alternatively, it is possible that H2A.Z-containing nucleosomes are more stable when H3K56 is also acetylated within the same nucleosome. While our study focused on specific heterochromatin-proximal and euchromatic loci, a recent publication demonstrated that the H3K56Q mutant promotes removal of the H2A.Z/H2B heterodimer by SWR1-C across the yeast genome (Watanabe *et al.* 2013). Hence, it remains to be seen whether the locus-specific effects of H3K56 acetylation-dependent H2A.Z deposition extends into all genomic regions similar to H3K56Q. Moreover, further studies are required to elucidate how both the absence and the presence of this histone modification can lead to loss of H2A.Z at promoters.

Chapter 3: H3K56 Acetylation is Required for Positioning H2A.Z and for Maintaining H2A.Z Occupancy at Gene Promoters

3.1 Introduction

The eukaryotic genome is packaged into the nucleus as a compact structure called chromatin. The fundamental repeating unit of chromatin is the nucleosome, a 146 bp DNA fragment wrapped around a histone core containing two copies each of H2A, H2B, H3 and H4. Over the last few years, it has become clear that nucleosomes are not assembled randomly across the genome (Brogaard *et al.* 2012; Jiang and Pugh 2009; Lee *et al.* 2007; Mavrich *et al.* 2008; Shivaswamy *et al.* 2008; Whitehouse and Tsukiyama 2006). Instead, they are highly organized and tightly regulated by a number of factors. The underlying DNA sequence, dedicated chromatin remodeling complexes and various transcription factors all contribute to and influence the position of nucleosomes. This is particularly true at yeast gene promoters where two highly positioned nucleosomes flank the nucleosome free region (NFR) just upstream of the transcriptional start site (TSS) (Mavrich *et al.* 2008; Shivaswamy *et al.* 2008).

In addition to the four canonical histones that constitute the major protein component of the nucleosome, nucleosomes may also contain histone variants that mark unique chromatin domains. H2A.Z is one of the most highly conserved histone variants throughout eukaryotic

evolution and its three-dimensional structure is very similar to canonical cousin, H2A (Suto *et al.* 2000). Studies in yeast have shown that H2A.Z is required for a wide range of genome functions including gene expression, maintenance of silencing boundaries, DNA repair, cell cycle progression and chromosome stability (Malik and Henikoff 2003; Meneghini *et al.* 2003; Kobor *et al.* 2004; Mizuguchi *et al.* 2004; Kalocsay *et al.* 2009; Dhillon *et al.* 2006; Krogan *et al.* 2004; Rangasamy *et al.* 2004). As evidence of its central role in a variety of cellular functions, H2A.Z is essential for viability in higher eukaryotes such as flies, frogs and mice (Faast *et al.* 2001; Iouzalen *et al.* 1996; van Daal and Elgin 1992).

H2A.Z is considered a genome-wide signature of eukaryotic promoters and enhancer elements. Despite being found in only 10% of all nucleosomes, the majority of chromatin-bound H2A.Z variants are deposited at the +1 and -1 nucleosomes flanking the NFR (Albert *et al.* 2007; Barski *et al.* 2007; Mavrich *et al.* 2008). Deposition of H2A.Z at specific genomic regions is solely catalyzed by the multi-subunit SWR1-C ATPase-dependent chromatin-remodeling complex (Kobor *et al.* 2004; Krogan *et al.* 2004; Mizuguchi *et al.* 2004). Using the energy from ATP hydrolysis, SWR1-C evicts two nucleosomal H2A/H2B units for two H2A.Z/H2B heterodimers, resulting in a variant nucleosome containing two copies of H2A.Z (Luk *et al.* 2010). While the mechanism of SWR1-C mediated H2A.Z exchange is well understood from *in vitro* experiments, the mechanisms of SWR1-C recruitment to sites of H2A.Z exchange *in vivo* remains an area of significant interest. Early studies demonstrated that NFR formation by the Reb1 general transcription regulatory protein and the RSC chromatin remodeler is sufficient to induce H2A.Z deposition (Raisner *et al.* 2005; Hartley and Madhani 2009). In addition, it was recently elucidated that the NFR

and the adjoining nucleosome plays a direct role in targeting SWR1-C to sites of H2A.Z exchange at gene promoters (Ranjan *et al.* 2013; Yen *et al.* 2013).

Consistent with H2A.Z's role in maintaining telomeric boundaries, SWR1-C also catalyzes H2A.Z exchange at the boundaries of euchromatin and heterochromatin (Meneghini *et al.* 2003; Zhang *et al.* 2004). Loss of H2A.Z and SWR1-C activity at heterochromatin boundaries result in repression of subtelomeric genes as a consequence of SIR complex spread (Meneghini *et al.* 2003; Lu and Kobor 2014). Intriguingly, two post-translational modifications have been shown to be critical for H2A.Z occupancy at telomeres. Firstly, H4K16 acetylation by the SAS histone acetyltransferase is required targeting H2A.Z deposition at the right telomere of ChrVI (Shia *et al.* 2006). Secondly, in Chapter 2 of this dissertation, we identified that Asf1-dependent H3K56 acetylation is required for maintaining H2A.Z levels at subtelomeric regions of ChrIII R (Lu and Kobor 2014). Physical interaction between Asf1 and the SAS complex suggests the two complexes might act in the same pathway to regulate H2A.Z deposition (Osada *et al.* 2005; 2001).

The primary role of Asf1 is a histone chaperone for the H3/H4 heterodimer. However, research in the last decade has revealed a key role of Asf1 in many auxiliary functions. For example, Asf1 is part of a class of histone chaperones that promote post-translational modifications (PTM) of histones. Binding of the H3/H4 heterodimer by Asf1 exposes the globular domain to Rtt109 thus allowing for acetylation of H3K56 (Recht *et al.* 2006; Tsubota *et al.* 2007; Schneider *et al.* 2006; Driscoll *et al.* 2007; Adkins *et al.* 2007). Furthermore, Asf1 is connected to a number of biological functions from DNA replication,

DNA repair, and transcription-coupled nucleosome assembly and disassembly (Tyler *et al.* 1999; Adkins *et al.* 2004; Adkins and Tyler 2004; Schwabish and Struhl 2006; Adkins *et al.* 2007; Mousson *et al.* 2007; Gkikopoulos *et al.* 2009; Takahata *et al.* 2009). By promoting physical interactions with various chromatin-remodeling complexes, Asf1 plays a key role in establishing unique chromatin neighbourhoods.

Here, we examined the functional connection between H3K56 acetylation and H2A.Z occupancy with respect to known regulatory mechanisms for H2A.Z deposition. Firstly, we studied whether Asf1-mediated H2A.Z occupancy at heterochromatin boundaries is dependent on H4K16 acetylation by the SAS complex, and secondly, whether H3K56 acetylation is required for H2A.Z occupancy genome-wide. We determined that H3K56 acetylation did not regulate H2A.Z occupancy in a SAS-dependent manner. Instead, H3K56 acetylation was required for maintaining promoter H2A.Z levels genome-wide. Our data suggested a key role for H3K56 acetylation in positioning H2A.Z nucleosomes flanking the NFR at a subset of gene promoters.

3.2 Materials and Methods

3.2.1 Yeast Strains and Plasmids

All strains used in this study are listed in Table 3.1. Yeast strains were generated using standard genetic techniques including homologous recombination and genetic crosses followed by tetrad dissection (Ausubel 1987). Complete deletion of genes and 3' end integration of an in frame 3xFLAG tag (Gelbart *et al.* 2001) were achieved using one-step

gene integration PCR-amplified modules. Plasmid shuffle experiments were performed using 5-FOA to evict *URA3* plasmid pRS316[H3 H4], and select for pRS316[H3K56R H4], pRS316[H3K56Q H4], pRS316[H3K9R H4], pRS316[H3K9Q H4], and pRS316[H3K9RK56R H4]. These plasmids were a generous gift from Ann Kirchmaier (Purdue University).

Table 3.1 Yeast strains used in this study

Strain number	Relevant Genotype
MKY6	W303*, MATA, ADE2, can1-100 his3-11 leu2-3,112 trp1-1 ura3-1 lys2Δ*
MKY1754	MKY6, *HTZ1-FLAG::KAN*
MKY1755	MKY6, *HTZ1-FLAG::KAN, asf1::NAT*
MKY1756	MKY6, *HTZ1-FLAG::KAN, sas2::HIS*
MKY1757	MKY6, *HTZ1-FLAG::KAN, asf1::NAT, sas2::HIS*
MKY1758	MKY6, *SWC2-VSV::KAN*
MKY1759	MKY6, *SWC2-VSV::KAN, asf1::HIS*
MKY1760	MKY6, *SWC3-VSV::KAN*
MKY1761	MKY6, *SWC3-VSV::KAN, asf1::HIS*
MKY1630	MKY6, *hht1-hhf1::LEU2 hht2-hhf2::HIS [pRS314, HHT2-HHF2]*
MKY1633	MKY6, *hht1-hhf1::LEU2 hht2-hhf2::HIS [pRS314, HHT2 K56R HHF2]*

3.2.2 Growth and Genotoxic Sensitivity Assays

Overnight cultures grown in YP-dextrose were diluted to OD_{600} 0.5. Cells were 10-fold serially diluted and spotted onto solid YPD plates or plates with 10mM hydroxyurea. The plates were then incubated at the indicated temperature for 36 hours. The 16°C plates were incubated for 96 hours.

3.2.3 ChIP-qPCR and ChIP-on-chip

Chromatin immunoprecipitation (ChIP) experiments were performed as described previously (Schulze *et al.* 2009). In brief, 250 ml of cells were grown in YP-dextrose to an OD_{600} of 0.5-0.6 from OD_{600} of 0.15 and were crosslinked with 1% formaldehyde for 20 minutes before chromatin was extracted. The chromatin was sonicated (Bioruptor, Diagenode, Spart, NJ: 10 cycles, 30s on/off, high setting) to yield an average DNA fragment of 500bp. Anti-FLAG antibody (4.2µl, Sigma) was coupled to 60µl of protein A magnetic beads (Invitrogen). After reversal of the crosslinking and DNA purification, the immunoprecipitated and input DNA were analyzed by quantitative real-time PCR (qPCR). Samples were analyzed in triplicate for three independent ChIP experiments. Statistical significance was assessed using Student's *t* test. Primer sequences are listed in Table 3.2.

For microarray analysis, after reversal of crosslinking and DNA purification, the DNA was amplified with two rounds of T7 RNA polymerase amplification and hybridized to Affymetrix 1.0R *S. cerevisiae* tiling microarray. Experiments were carried out in duplicates. A modified version of the model-based analysis of tiling arrays (MAT) algorithm was used to normalize and average the duplicates. The data was normalized using both input DNA and a mock IP control. Relative occupancy scores were calculated for each probe using a 300bp sliding window. Enriched features had at least 50% of the probes contained in the feature above the 1.5 threshold. Promoters were defined as the 500bp upstream of the ORF.

Table 3.2 Primer sequences used in this study

Name	Method	Primer sequence (5'-3')
HMR left F	ChIP	CTACCTTGTTGTATATAGGC
HMR left R	ChIP	AACAGCGATAGTGCGAGGAT
HMR right F	ChIP	TCTACAATGCAACCCCACAA
HMR right R	ChIP	TTGAACCGATGATCTCCACA
ChrIII tel R F	ChIP	AAGGCGGTGTTATTTGTTGC
ChrIII tel R R	ChIP	TTATGCGGCCGAATGATACT
YCR094W Prom F	ChIP	GCAAACCCCTCTACAATCCA
YCR094W Prom R	ChIP	CAAAAGTGAAAGCGACCCATA
YCR095C Prom F	ChIP	TACCGTATGCGGTATAATGA
YCR095C Prom R	ChIP	GTCTCCACTTTAGAACATCT
GIT1 Prom F	ChIP	TTCATGAATTTCCTTACTGGAC
GIT1 Prom R	ChIP	GTTGACTAGTCACAAGAAACAG
YCR099C Prom F	ChIP	TGCTACTGGTGATCTGGGAAA
YCR099C Prom R	ChIP	CTGATCCATCTGGCGTTGTA
YCR100C Prom F	ChIP	GCAAGGATTCTGACTTTACTGG
YCR100C Prom R	ChIP	CTCGTTATGCCCGTCATCTT
RDS1 Prom F	ChIP	TGTGCTATCTAAGAGGATGGTTCA
RDS1 Prom R	ChIP	GAATCCATCAGAGCATTTCA
PRP8 ORF F	ChIP	GGATGTATCCAGAGGCCAAT
PRP8 ORF R	ChIP	AACCCGCGTATTAAGCCATA
T6R-H F	ChIP	GAAAGTTTGGATGCTAGCAAGGGC
T6R-H R	ChIP	GCATAGCCTTTGAAAACGGCG
T6R-E F	ChIP	GTCTCGTAGGTAGCTTTCAC
T6R-E R	ChIP	CGGTGTTCCTTTACAAACCC
T6R-C F	ChIP	CGTTCTTCTTGGCCCTTATC
T6R-C R	ChIP	CATCATCGGTGGTTTTGTCGTG

3.2.4 Chromatin Association Assay

Chromatin association assays were performed as previously described (Wang *et al.* 2009). In brief, cells were diluted to OD_{600} 0.15 and collected at logarithmic phase. Following collection, cells were incubated in pre-spheroblast buffer (100 mM PIPES/KOH [pH 9.4], 10 mM DTT, 0.1% sodium azide) for 10 minutes at room temperature rotating, then spheroblasted for 20 minutes at 37C with 20mg/ml Zymoylase-100T (Seikagaku Corporation). Spheroblasts were washed with wash buffer (50 mM HEPES/KOH [pH 7.5], 100mM KCl, 2.5 mM $MgCl_2$, 0.4 M sorbitol) and resuspended in equal volume of EB (50 mM HEPES/KOH [pH 7.5], 100mM KCl, 2.5 mM $MgCl_2$, 1 mM DTT, 1 mM PMSF, and Complete Protease Inhibitor cocktail [Roche]). Cells were lysed with 1% Triton X-100. Whole cell extracts were saved and the remaining lysate were separated into the chromatin pellet and supernatant fraction by centrifugation through EBSX (EB + 0.25% Triton X-100 and 30% sucrose). The three fractions were subsequently analyzed by SDS-PAGE and immunoblotted.

3.3 Results

3.3.1 Asf1-Dependent H2A.Z Promoter Occupancy was not Mediated by the SAS Histone Acetyltransferase

In chapter 2, we found that H2A.Z occupancy at subtelomeric promoters is dependent partly on the Asf1 histone chaperone. Loss of H3K56 acetylation, either by deleting *ASF1* or by introducing an unacetylable mutation (*H3K56R),* resulted in a decrease in H2A.Z levels at

the promoters of genes proximal to the telomere of Chr III. Based on previous work, we tested whether Asf1 recruits the SAS complex to promote H2A.Z deposition at ChrIII R (Osada *et al.* 2005; Shia *et al.* 2006). We first created strains that lacked genes encoding for *ASF1* and the catalytic subunit of the SAS complex, *SAS2.* While strains lacking *SAS2* grew better than the *asf1Δ* strain*,* we found that the *asf1Δ sas2Δ* double mutant more closely resembled the *asf1Δ* strain (Figure 3.1A).

The acetylation of H4K16 by the SAS histone acetyltransferase complex is a key chromatin modification that restricts the spread of SIR silencing complexes at heterochromatin boundaries (Kimura *et al.* 2002; Suka *et al.* 2002; Oki and Kamakaka 2004). To examine if Asf1 was required for H4K16 acetylation at the well-characterized heterochromatin boundaries of ChrIII R, we first compared levels of H4K16 acetylation in strains lacking *ASF1* or *SAS2* (Figure 3.1B). Normalized for nucleosome content, we found that upon *ASF1* deletion, there was a significant reduction of H4K16 acetylation at all three boundaries (Figure 3.1C). As expected, *sas2Δ* cells had very low levels of acetylated H4K16 at the heterochromatin boundaries of ChrIII R. To test whether the SAS complex is required for H2A.Z occupancy in a similar manner to Asf1, we assessed the levels of H2A.Z at the ChrIII R heterochromatin boundaries in *sas2Δ* strains. Unlike *asf1Δ,* a strain lacking *SAS2* had H2A.Z levels similar to that of a wildtype strain, indicating that neither the SAS complex nor H4K16 acetylation was required for H2A.Z deposition at the boundaries of ChrIII R (Figure 3.1D).

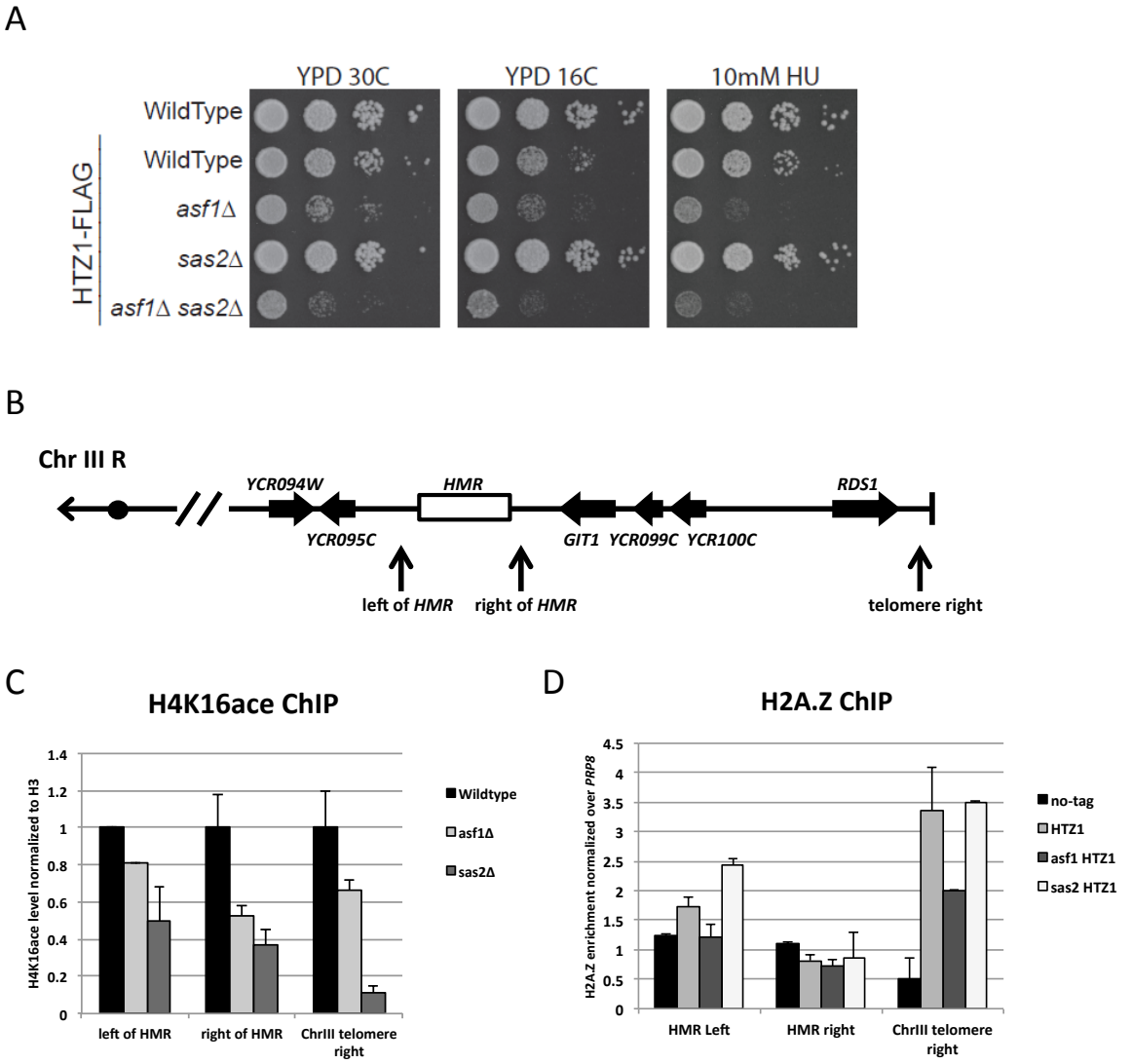

Figure 3.1 Asf1-dependent H2A.Z promoter occupancy did not require the SAS histone acetyltransferase
(A) Ten-fold serial dilution assay of indicated strains plated on YPD media with or without HU and incubated at the labeled temperatures. (B) Schematic representation of the boundaries of the *HMR* locus and the ChrIII R telomere. (C) H4K16 acetylation partially depended on Asf1. ChIP-qPCR of H4K16 acetylation at heterochromatin boundaries of ChrIII R in wildtype, *asf1Δ,* and *sas2Δ* strains. Enrichment of H4K16 acetylation was normalized to nucleosome density as measured by H3. (D) H2A.Z deposition at heterochromatin boundaries of ChrIII R does not depend on *SAS2.* ChIP-qPCR of H2A.Z-FLAG in wildtype, *asf1Δ,* and *sas2Δ* strains. H2A.Z enrichment was normalized to enrichment level at the *PRP8* ORF. (C)(D) Error bars represent standard errors of the means for three independent experiments.

In Chapter 2, we found that Asf1 was also required for maintaining H2A.Z levels at the promoters of subtelomeric genes, therefore, we also examined whether the SAS complex was involved in this aspect of H2A.Z occupancy (Figure 3.2A). Unlike Asf1, Sas2 was also not required for maintaining H2A.Z levels at subtelomeric gene promoters, with the exception of the *RDS1* gene that lies closest to the ChrIII R telomere (Figure 3.2B). Our observations at the right telomere of ChrIII suggested that the SAS complex might have distinct H2A.Z regulatory functions at different telomeres. We next examined the role of Asf1 and its relationship with the SAS complex at ChrVI since the SAS complex is required for H2A.Z deposition at this heterochromatin domain (Figure 3.2C) (Shia *et al.* 2006). We verified that H2A.Z was lost in the subtelomeric region of ChrVI upon *SAS2* deletion in a distance-dependent manner (Figure 3.2D). However, the profile of H2A.Z occupancy differed between *asf1Δ* and *sas2Δ* cells. When the histone chaperone was deleted, there was a consistent reduction in overall H2A.Z levels across all sites assayed, irrespective of their distance away from the heterochromatin boundary (Figure 3.2D). In accordance with our findings at the subtelomeric genes of ChrIII R, the levels of H2A.Z were reduced by half (Lu and Kobor 2014). Furthermore, H2A.Z level in the *asf1sas2* double mutant was reduced to the same level as the *asf1Δ* mutant at both ChrIII R and ChrVI R telomeric ends. Taken together, this set of experiments suggested that Asf1 does not promote H2A.Z occupancy through a SAS complex-mediated mechanism. Furthermore, Asf1 seems to be important for maintaining H2A.Z levels across telomeres.

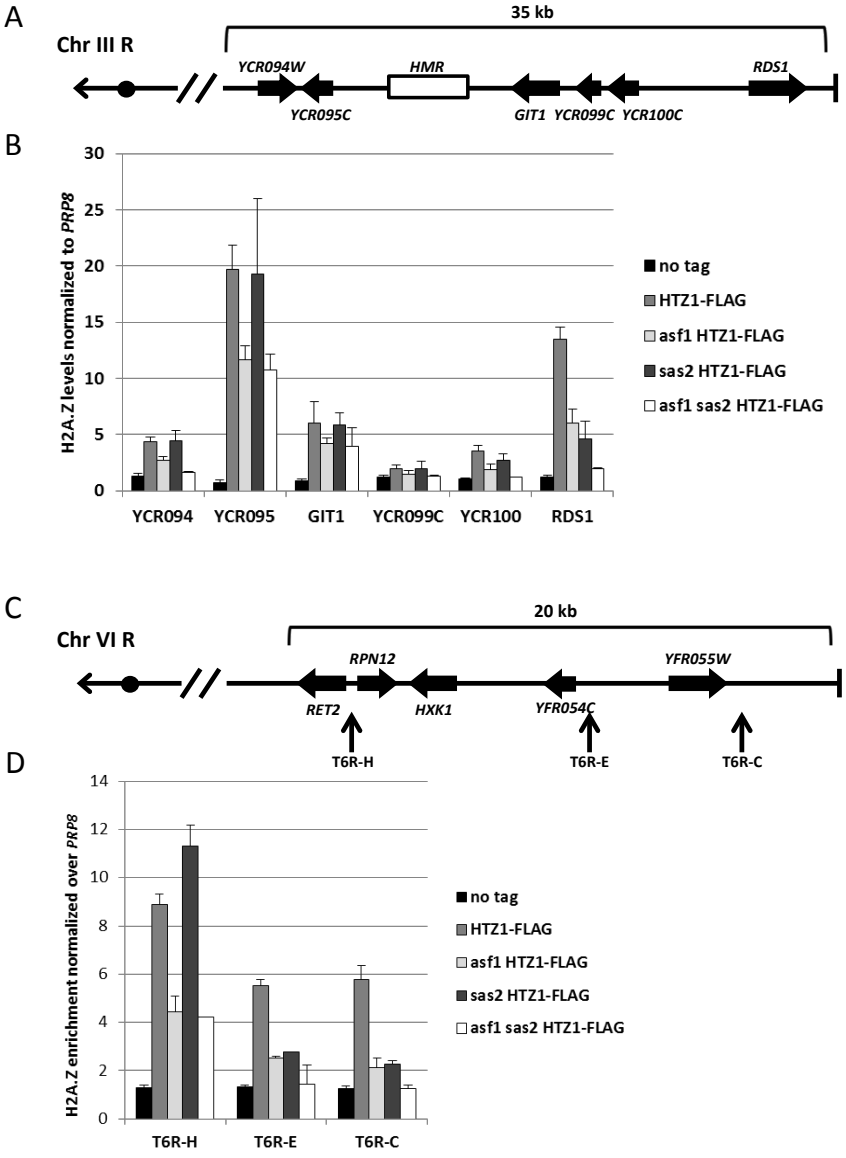

Figure 3.2 Asf1-dependent H2A.Z deposition at ChrIII R was not mediated by SAS
(A) Schematic representation of ORFs at the right telomere of ChrIII. (B) H2A.Z promoter enrichment at ChrIII R subtelomeric region did not depend on *SAS2*. (C) Schematic representation of ORFs at the right telomere of ChrVI. (D) H2A.Z promoter enrichment at ChrVI R subtelomeric regions depended on *ASF1* and *SAS2*. (B) (D) ChIP-qPCR of H2A.Z was performed in the indicated strains and normalized to H2A.Z enrichment over *PRP8*. Error bars represent standard errors of the means for three independent experiments.

3.3.2 Loss of Asf1 did not Alter Global H2A.Z Levels in Chromatin

The consistent reduction in H2A.Z levels in *asf1Δ* cells at subtelomeric promoters prompted us to ask if bulk H2A.Z deposition and SWR1-C recruitment was dependent on Asf1. In wildtype cells, the majority of cellular H2A.Z is chromatin bound (Wang *et al.* 2009). Using a centrifugation-based assay to separate chromatin-associated proteins from the rest of the whole cell lysate (referred to as the supernatant fraction), we found that cells lacking the Asf1 histone chaperone had similar levels of H2A.Z in the supernatant and chromatin fractions as compared to wildtype cells (Figure 3.3A). Similarly, Asf1 did not seem to play a role in the recruitment of the SWR1-C complex to chromatin, as chromatin association of key subunits of the SWR1-C complex (Swc2 and Swc3) was not significantly altered upon deletion of *ASF1* (Figure 3.3B). Unlike H2A.Z, the majority of Swc2 and Swc3 proteins were found in the chromatin fraction and there were no detectable amounts of these SWR1-C subunits in the supernatant (Figure 3.3B).

As H3K56 acetylation is a hallmark of newly deposited histones during DNA replication, we were prompted to investigate the relationship between Asf1 and H2A.Z during S-phase (Kaplan *et al.* 2008; Masumoto *et al.* 2005; Recht *et al.* 2006; Han and Zhang 2007). Cells lacking *ASF1* are particularly sensitive to hydroxyurea (HU), a genotoxic agent commonly used to arrest cells during S-phase (Tyler *et al.* 1999; Franco and Kaufman 2005; Ramey *et al.* 2004). Therefore, cells were synchronized in G1-phase by alpha-factor arrest and collected at S-phase as determined by fluorescence assisted cell sorting (FACS). In wildtype cells, the bulk of cellular H2A.Z was in chromatin in both asynchronous and S-phase cells (Figure 3.3C). Despite the prominence of H3K56 acetylation in S-phase, in *asf1Δ* cells, the

majority of H2A.Z was associated with chromatin in both asynchronous and S-phase (Figure 3.3C). Furthermore, the levels of H2A.Z in the supernatant were comparable between the cell cycle phases in *asf1Δ* cells (Figure 3.3C). Taken together, our data suggested that Asf1 was not required for global SWR1-C recruitment or bulk H2A.Z deposition and that the relationship between the histone chaperone and H2A.Z was not cell cycle-dependent.

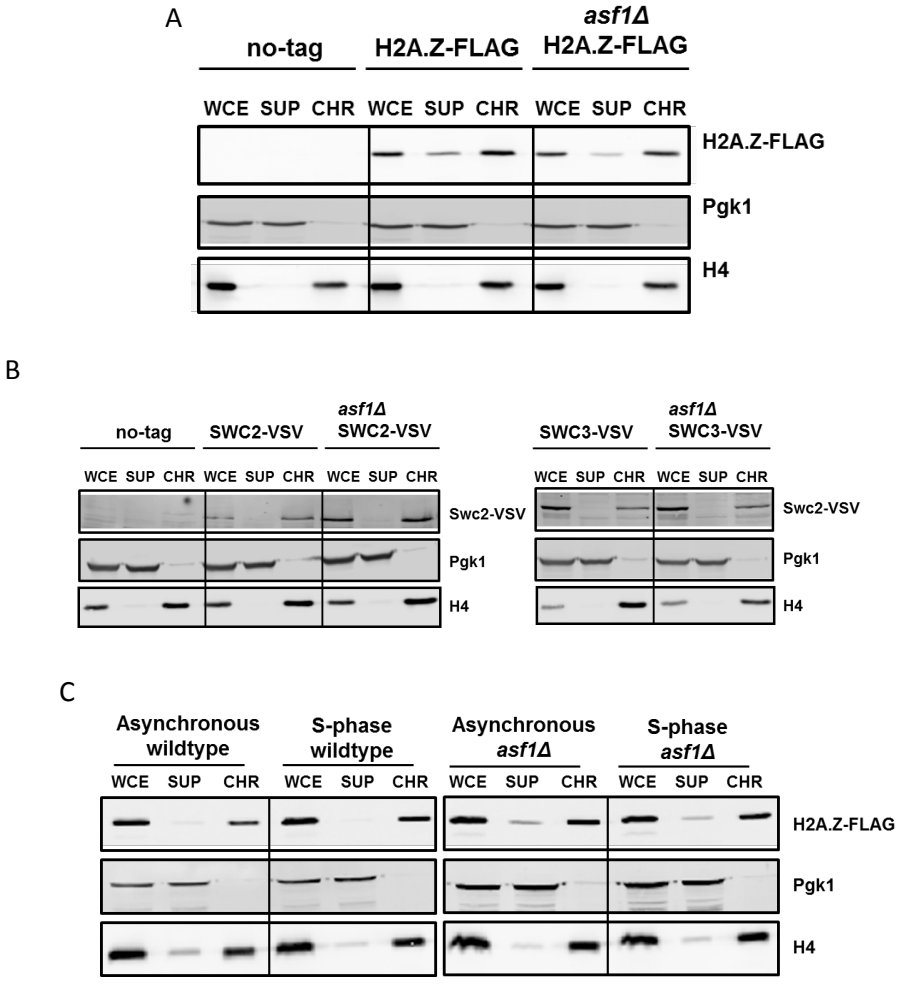

Figure 3.3 Loss of Asf1 does not alter global H2A.Z levels in chromatin
Chromatin association assay was performed on the indicated strains. WCE, whole cell extract; SUP, supernatant; CHR, chromatin pellet. (A) Loss of *ASF1* did not alter H2A.Z association to chromatin. (B) Loss of *ASF1* did not alter Swc2 and Swc3 recruitment to chromatin. (C) Loss of *ASF1* did not alter H2A.Z association to chromatin during S-phase. The relative amounts of H2A.Z-FLAG, Swc2-VSV, and Swc3-VSV were determined by immunoblotting with anti-FLAG and anti-VSV antibodies. Antibodies against histone H4 and Pgk1 were used as loading controls for the chromatin pellet and supernatant, respectively.

3.3.3 Genome-Wide H2A.Z Occupancy was Altered by Loss of H3K56 Acetylation

To reconcile the differences between our observations of H2A.Z deposition at bulk levels versus promoter-specific differences, we explored the relationship between Asf1 and H2A.Z more thoroughly by analyzing H2A.Z occupancy genome-wide. ChIP-on-chip (Chromatin Immunoprecipitation on microarray) was used to precisely map changes in H2A.Z occupancy in cells lacking *ASF1* and in cells containing an unacetylable substitute for lysine 56, H3K56R. Consistent with previous studies, H2A.Z was predominantly found at gene promoters using our enrichment criteria, with 3508 promoters enriched for H2A.Z in wildtype cells (Figure 3.4A). In both *asf1Δ* and *H3K56R* cells, the majority of H2A.Z peaks were found to be associated with gene promoters (Figure 3.4B). However, the H2A.Z profiles of both mutants had notable distinctions from the wildtype H2A.Z profile. At a subset of gene promoters, H2A.Z was completely lost, whereas at some promoters there was a reduction in the level of promoter-associated H2A.Z (Figure 3.4B). Overall, H2A.Z was completely lost in roughly 15% of promoters that were enriched for H2A.Z in the wildtype, with 3032 and 2940 enriched promoters enriched in *asf1Δ* and *H3K56R* cells, respectively (Figure 3.4A).

A

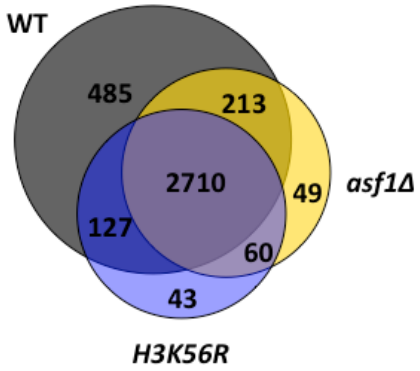

B

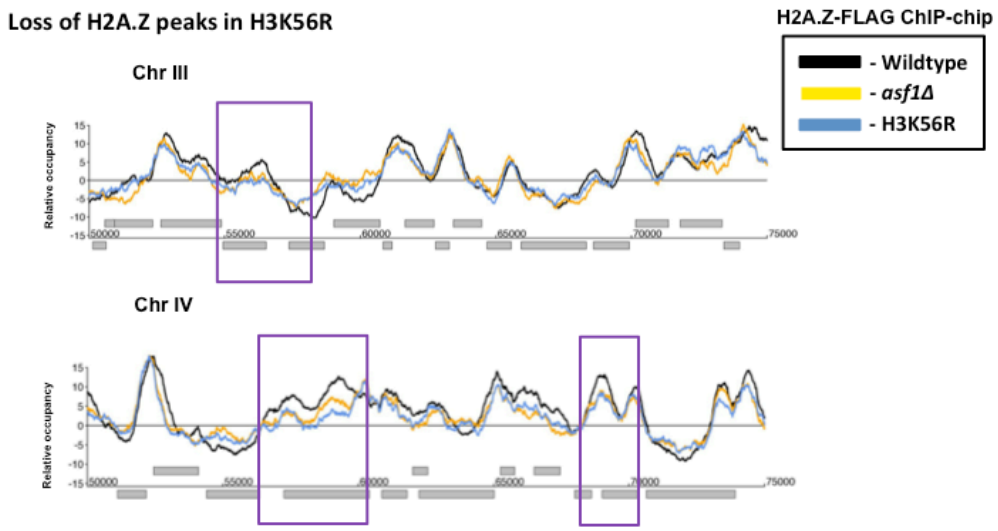

Figure 3.4 Genome-wide H2A.Z occupancy was altered by loss of H3K56 acetylation
Averaged H2A.Z profiles over the entire yeast genome were obtained from two independent experiments. (A) Venn diagram of gene promoters enriched for H2A.Z in wildtype, *asf1Δ,* and *H3K56R.* (B) ChIP-chip profile of H2A.Z-FLAG-enriched regions in wildtype, *asf1Δ,* and *H3K56R* strains. Sample genomic regions were plotted for ChrIII and ChrIV along the x-axis against the relative occupancy of H2A.Z. ORFs are indicated as light gray rectangles above the x-axis for Watson genes and below the axis for Crick genes.

Correspondingly, there was a slight overall decrease in H2A.Z occupancy in cells lacking *ASF1* or H3K56 acetylation when all genes were visualized by CHROMATRA (Figure 3.5A, Figure 3.5B, and Figure 3.5C) (Hentrich *et al.* 2012). As expected, the majority of H2A.Z in wildtype cells was found in close proximity to the TSS of genes and was in low abundance along the ORF (Figure 3.5A). Very little H2A.Z was observed at the promoters of highly transcribed genes in all strains assayed (Figure 3.5A). Unlike the robust H2A.Z 500bp signal on either side of the TSS in wildtype cells, there appeared to be an overall decrease in H2A.Z enrichment at the 5' end of all genes in cells lacking *ASF1* or H3K56 acetylation (Figure 3.5B and Figure 3.5C). Furthermore, changes in H2A.Z levels were independent of transcription rate and transcript length (Figure 3.5B and Figure 3.5C). The striking similarity of the H2A.Z profiles of *asf1*Δ and *H3K56R* cells suggested a common mechanism in H2A.Z regulation. The H2A.Z profiles of the two mutants had a Spearman correlation of 0.946, suggesting that the acetylation of H3K56 was the key regulatory mechanism mediating their effects on H2A.Z occupancy (Figure 3.5D).

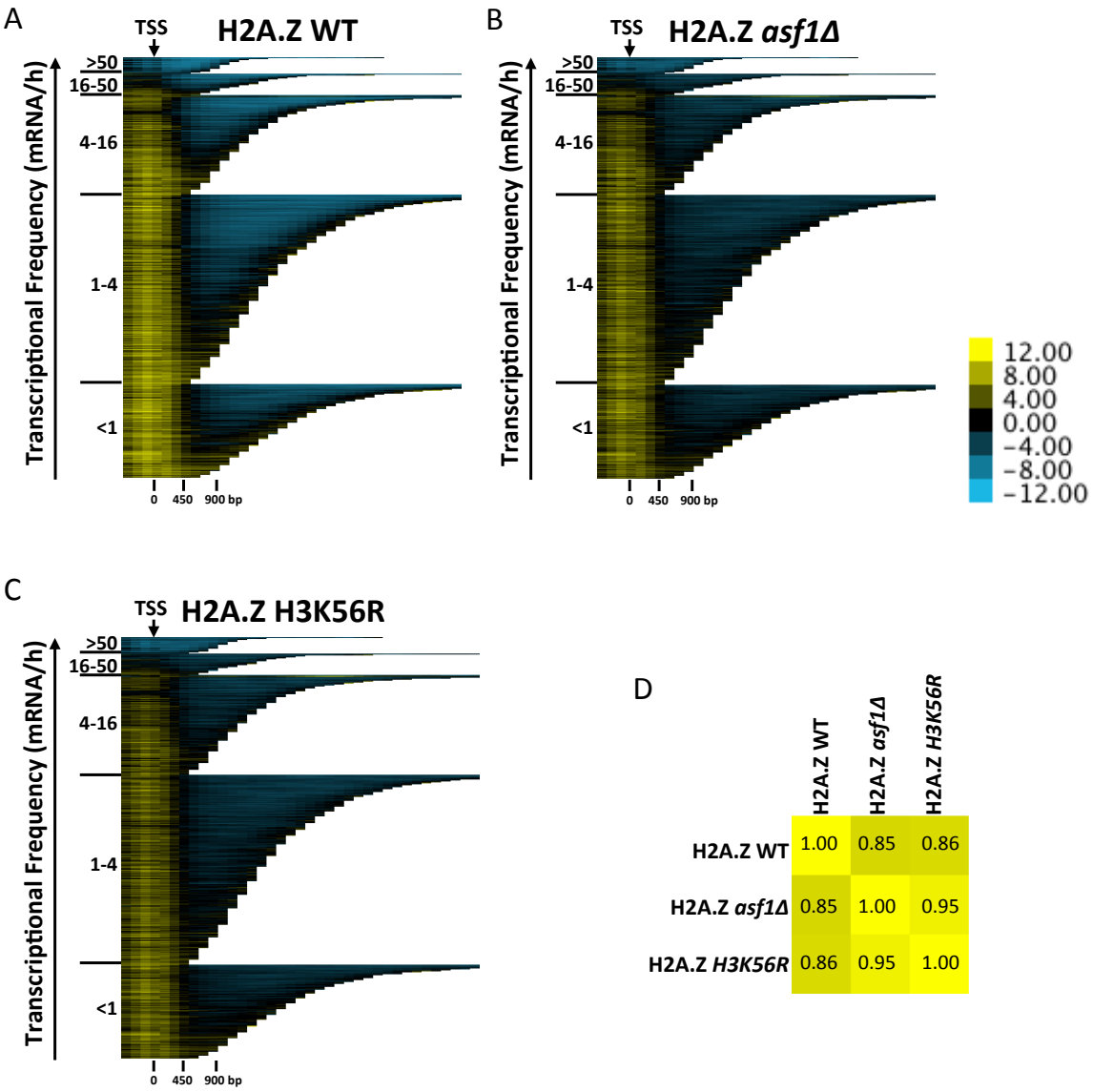

Figure 3.5 Loss of H3K56 acetylation led to an overall decrease in H2A.Z levels
(A) (B) (C) Comparison of H2A.Z enrichment of all genes in wildtype, *asf1Δ,* and *H3K56R*. CHROMATRA plots of relative H2A.Z occupancy across all transcripts sorted by length and transcriptional frequency. All genes are aligned by their TSS and include a 500bp region upstream of the TSS. Enrichment scores are binned into 150bp segments. Transcripts were grouped into five classes according to their transcriptional frequency as per Holstege *et al.* (1998). (D) Spearman correlation of H2A.Z enrichment profile of WT, *asf1Δ,* and *H3K56R.*

3.3.4 Defects in H3K56 Acetylation Resulted in Reduced H2A.Z Promoter Occupancy

Next, differences in H2A.Z relative occupancy were considered, with a specific focus on promoters that were significantly enriched for the H2A.Z variant in wildtype cells. As expected, an average gene profile of all genes whose promoters were enriched for H2A.Z revealed that H2A.Z was highly enriched around the TSS, depleted over the ORF, and enriched to a small degree at the 3' end of genes (Figure 3.6A). The average gene profile of H2A.Z enrichment in cells lacking *ASF1* clearly demonstrated an overall reduction in H2A.Z levels at both the 5' IGR (intergenic region) and the 3'IGR (Figure 3.6A). In addition, cells containing an unacetylable arginine in place of lysine 56 exhibited a similar H2A.Z average gene profile, with a strong decrease in H2A.Z levels at the 5' end of genes and a similar decrease at the 3' end of genes (Figure 3.6A). Comparing the relative H2A.Z occupancy, in a gene-by-gene manner, of all 3509 H2A.Z-containing promoters revealed an overall decrease in H2A.Z occupancy in *asf1Δ* and *H3K56R* cells (t-test p-value = 4.54e-117 in *asf1Δ* mutant and p-value = 8.41e-172 in *H3K56R* mutant) (Figure 3.6B and Figure 3.6C). Demonstrating that while the majority of genes were still considered enriched under our selection criteria, there was a significant decrease in the relative occupancy of H2A.Z at these promoters.

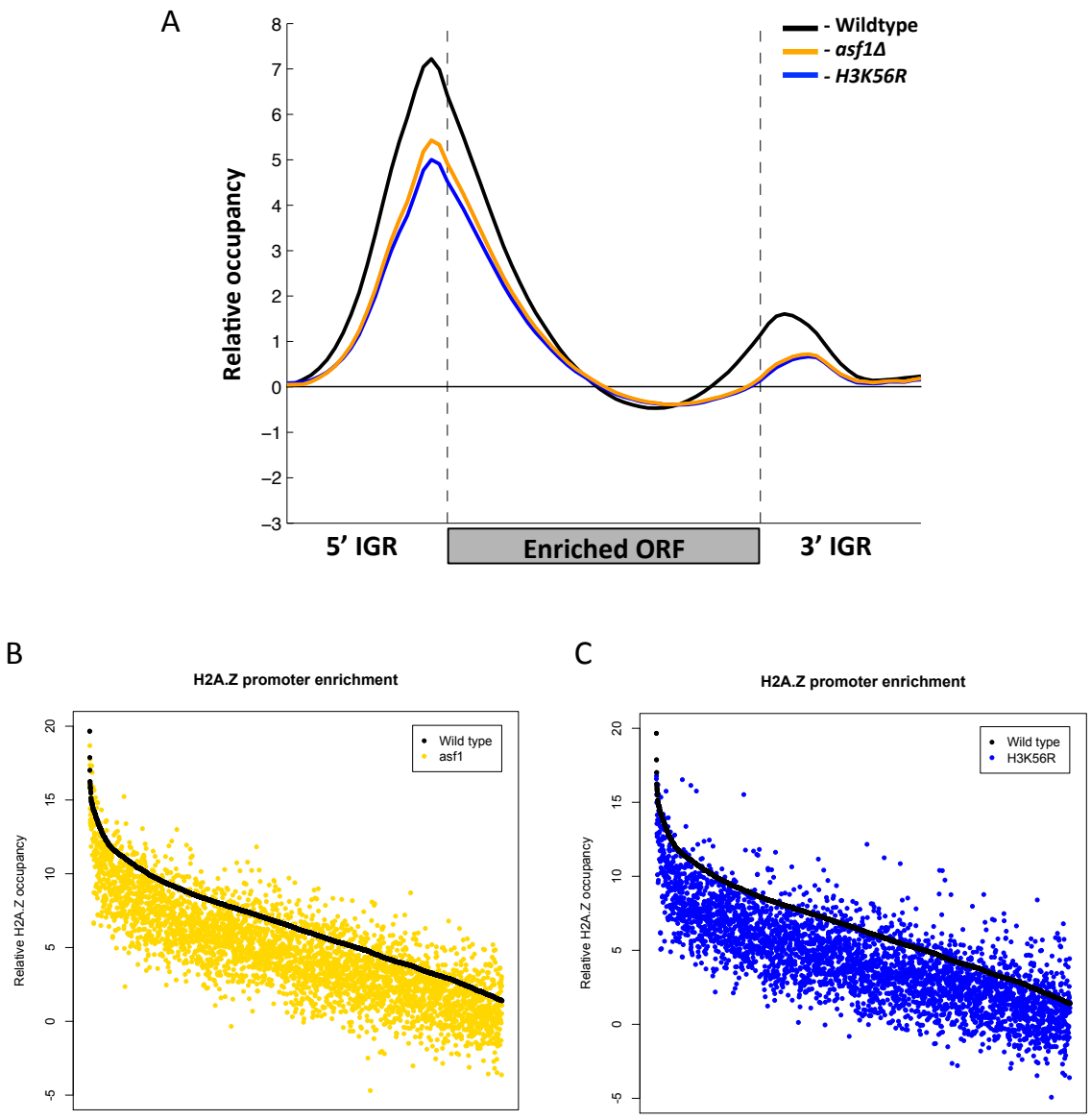

Figure 3.6 Defects in H3K56 acetylation resulted in reduced H2A.Z promoter occupancy
(A) Average gene profile of H2A.Z enrichment of all genes enriched at its promoters in wildtype cells. Each ORF was divided into 40 bins (independent of gene length), and average enrichment values were calculated for each bin. 1500bp upstream of the TSS and 1500bp downstream of the 3' UTR were assigned to 20 bins. The average enrichment value for each bin was plotted. (B)(C) H2A.Z promoter occupancy scores were significantly decreased in *asf1Δ* (p-value = 4.54e-117) and *H3K56R* (p-value = 8.41e-172) cells. Promoter occupancy scores for H2A.Z were plotted for all promoters enriched for H2A.Z in wildtype cells. Promoters are ordered from highest to lowest based on the H2A.Z enrichment score of wildtype.

3.3.5 H3K56 Acetylation Positioned H2A.Z at Gene Promoters

While a subset of H2A.Z peaks were lost or reduced when H3K56 acetylation was abolished, the majority of gene promoters remained enriched for H2A.Z in *asf1Δ* and *H3K56R* mutants. Closer examination of the H2A.Z genome-wide profile revealed that there was a subtle yet clear shift in the genomic location of H2A.Z peaks in *asf1Δ* and *H3K56R* mutants compared to wildtype. Representative regions in ChrIII and ChrIX highlighted a shift in the H2A.Z enrichment profile towards the left arm of both chromosomes (Figure 3.7A). Analogous to all earlier analyses of the H2A.Z profiles of *asf1Δ* and *H3K56R* in this chapter, the shift patterns observed in the two mutants were also strikingly similar. Additionally, the magnitude of the shifted peaks remained consistent with wildtype cells despite the change in their location (Figure 3.7A).

To determine the significance of the observed shift between wildtype and the H3K56 acetylation mutant strains, we developed a new method to define the change in location of the H2A.Z peak relative to the TSS of its corresponding gene (for the analysis, this is defined as the closest gene). Using the TSS of genes as a reference point, we calculated the distance from TSS to the midpoint of H2A.Z peaks in wildtype and mutants, and compared the differences in H2A.Z position. Only genes whose promoters were enriched for H2A.Z in wildtype, *asf1Δ,* and *H3K56R* cells were used. Furthermore, a criterion was set so that the midpoint of the associated H2A.Z peak must be within 500bp upstream or downstream of the TSS. Following this set of selection criteria, 2399 genes were left whose promoter had an associated H2A.Z peak in all three strains.

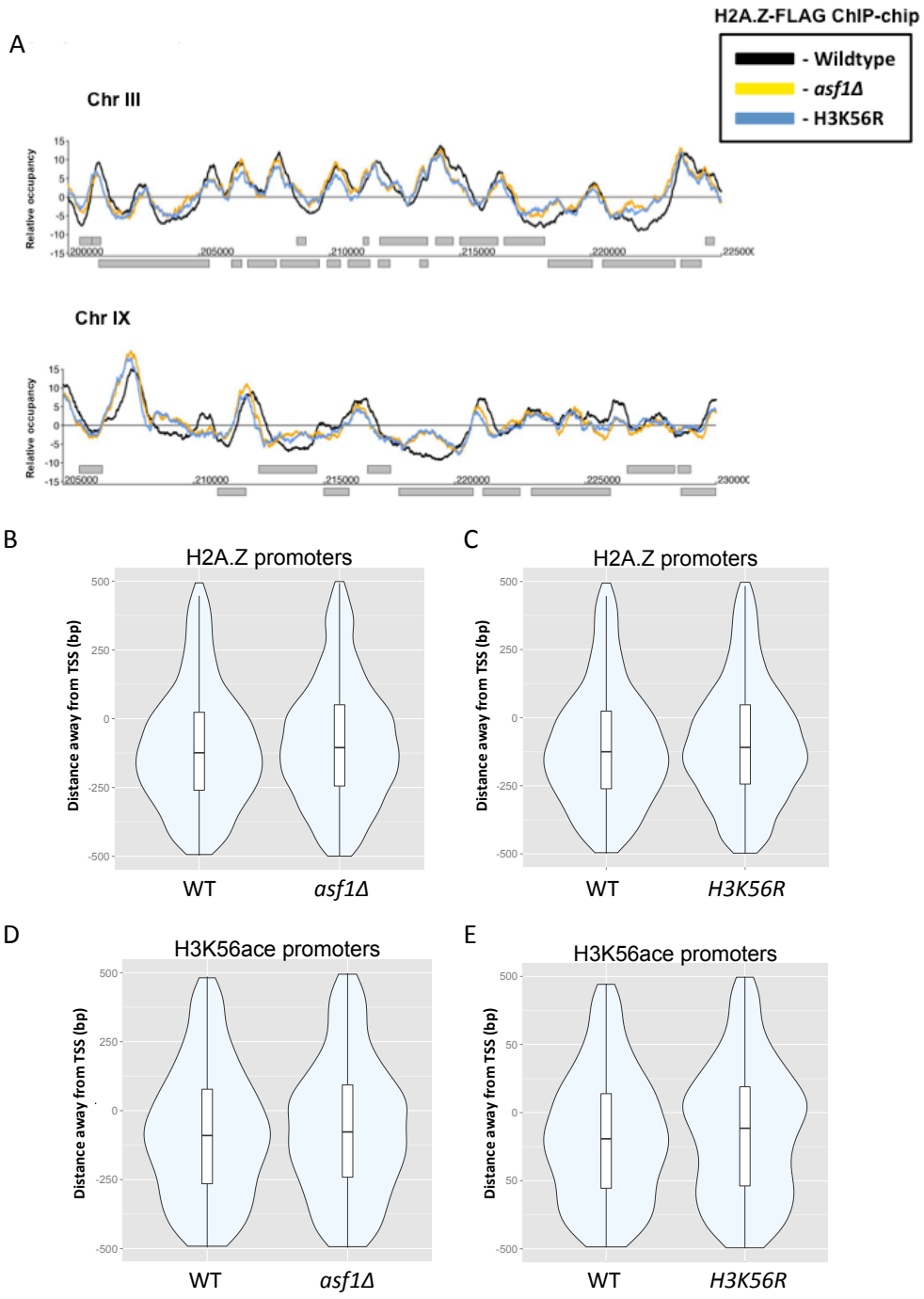

Figure 3.7 Loss of H3K56 acetylation resulted in a shift of H2A.Z position at gene promoters
(A) Representative genomic regions were plotted for ChrIII and ChrIX along the x-axis against the relative occupancy of H2A.Z normalized to input in wildtype, *asf1Δ,* and *H3K56R* strains. ORFs are indicated as light gray rectangles above the x-axis for Watson genes and below the axis for Crick genes. (B) (C) Distribution of H2A.Z positions did not change at H2A.Z-enriched promoters (D) (E) Position of H2A.Z peaks were significantly shifted at H3K56 acetylated promoters in *H3K56R* cells (p-value = 0.021). (B) (C) (D) (E) Violin plot representing the distribution of H2A.Z peak position relative to TSS for each strain.

First, we examined H2A.Z position in these 2399 genes enriched for the histone variant in all three mutant strains. As expected, for the majority of genes in wildtype cells, H2A.Z was located just upstream of the TSS, with a mean position of -103bp relative to the TSS (Figure 3.7B). Thus, it is likely that the single large peak from our microarray analysis represents an average profile of the -1 and +1 H2A.Z containing nucleosomes. Comparable to the wildtype distribution, the majority of H2A.Z was found approximately 100bp upstream of the TSS in *asf1Δ* and *H3K56R* (Figure 3.7B and Figure 3.7C). Taken together, the distribution of promoter H2A.Z position in *asf1Δ* and *H3K56R* resembled the wildtype distribution suggesting that H2A.Z position did not change.

Next, since a shift in H2A.Z upon loss of H3K56 acetylation was expected only at promoters that are normally acetylated at H3K56, we examined genes whose promoter was normally enriched for H3K56 acetylation (Rufiange *et al.* 2007). Using the genome-wide H3K56 acetylation profile of asynchronous wildtype cells, we identified 1369 promoters enriched for H3K56 acetylation, of which 452 also had an associated H2A.Z peak in WT, *asf1Δ* and *H3K56R* cells (Rufiange *et al.* 2007). Strikingly, there was a notable shift in the positions of H2A.Z peaks in both *asf1Δ* and *H3K56R* mutants at H3K56 acetylated promoters (Figure 3.7 D, 7E). The distribution of H2A.Z peak position was significantly shifted towards the TSS in the *H3K56R* mutant with a p-value of 0.021, whereas the change in position of the *asf1Δ* mutant had a p-value of 0.086 (Wilcox test for paired, non-normal distribution) (Figure 3.7E). On average, H2A.Z position in *H3K56R* shifted closer to the TSS than in the *asf1Δ* mutant.

Similar to before, a gene-by-gene approach was taken to examine the 452 promoters where H2A.Z and H3K56ace colocalized. To get a sense of the magnitude and direction of the change in H2A.Z position upon *ASF1* deletion and H3K56 mutation, we plotted the distance to TSS for this subset of H2A.Z peaks and compared the wildtype profile against the mutant (Figure 3.8). As a whole, there was a large range in the change of H2A.Z peak positions in the mutants when compared to the wildtype. In both *asf1Δ* and *H3K56R,* there was a proportion of H2A.Z peaks that remained relatively unchanged compared to wildtype H2A.Z position as well as a subset of H2A.Z peaks that shifted drastically away from the wildtype position (Figures 3.8A and Figure 3.8B). Importantly, the H2A.Z peaks shifted both upstream and downstream of its wildtype position with loss of *ASF1* or H3K56 acetylation (Figure 3.8A and Figure 3.8B). Taken together, our data demonstrated that H3K56 acetylation was required for H2A.Z positioning at a subset of gene promoters.

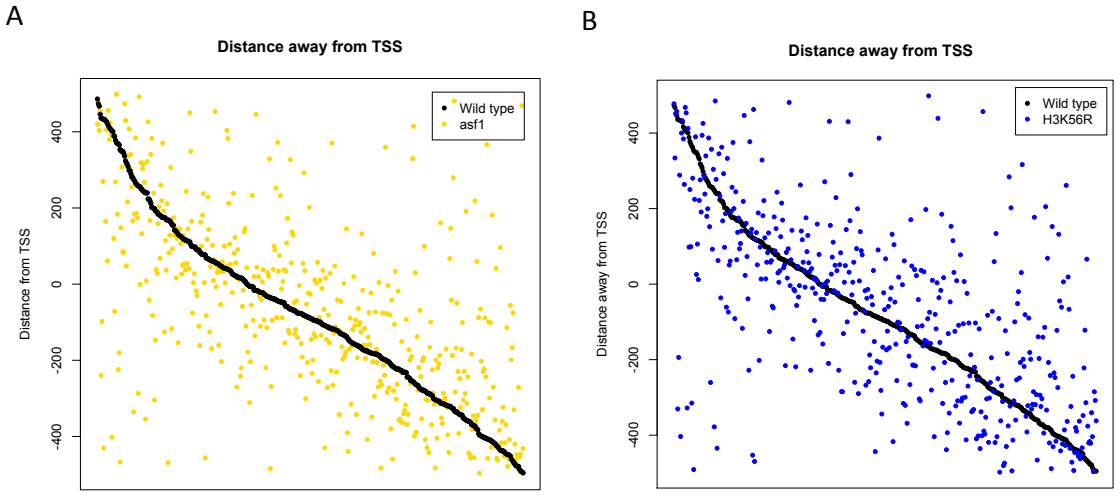

Figure 3.8 H3K56 acetylation defects led to a shift in H2A.Z position
Scatterplot of H2A.Z position relative to the TSS of the corresponding gene in wildtype, *asf1Δ,* and *H3K56R* cells. (A) Loss of *ASF1* resulted in a shift of H2A.Z peaks both upstream and downstream of the wildtype position. (B) A change in H2A.Z position was observed in *H3K56R* compared to wildtype.

3.4 Discussion

In this chapter, we provide evidence that Asf1 regulated H2A.Z occupancy and positioning at gene promoters by promoting H3K56 acetylation. Despite indications from previous studies, Asf1-dependent H2A.Z occupancy at ChrIII was not mediated through H4K16 acetylation by the SAS HAT complex. Instead, H2A.Z deposition at telomeres was dependent on H3K56 acetylation and the Asf1 histone chaperone. We mapped the genome-wide occupancy profile of H2A.Z in *asf1Δ* and *H3K56R* cells by ChIP-chip to gain a comprehensive and detailed understanding of how H3K56 acetylation could be regulating H2A.Z occupancy. Loss of H3K56 acetylation resulted in a slight, albeit significant, reduction in H2A.Z levels and alterations in H2A.Z position at gene promoters. At a subset of genes, H2A.Z was depleted at promoters that were occupied by the histone variant in the wildtype. At the majority of affected promoters, there was significant decrease in the level of H2A.Z in strains that lack H3K56 acetylation. Interestingly, we also observed a significant shift in the position of promoter H2A.Z upon the loss of H3K56 acetylation, suggesting a key role for the histone modification in positioning H2A.Z. Taken together, the results in this chapter present a model in which H3K56 acetylation at gene promoters played a key role in governing H2A.Z biology, both in regulating the levels and position of this histone variant.

In Chapter 2 of this dissertation, we uncovered that Asf1 was required to maintain normal H2A.Z levels at the promoters of both subtelomeric and euchromatic genes. In this chapter, we explored this relationship further to tease apart the mechanistic and functional relationship between the Asf1 H3/H4 histone chaperone and the H2A.Z histone variant.

Previous reports proposed a recruitment-based model in which Asf1 recruited the SAS complex, a H4K16 histone acetyltransferase, to the heterochromatin boundary (Osada *et al.* 2005; 2001). H4K16ace by the SAS complex has been shown to be required for SWR1-C-dependent H2A.Z deposition at one heterochromatin boundary (Shia *et al.* 2006). We found that while H2A.Z occupancy at the ChrVI heterochromatin boundary was indeed dependent on the SAS complex, this did not hold true at the heterochromatin boundaries of ChrIII R. At ChrIII R, even though loss of *ASF1* resulted in reduced H4K16 acetylation levels, loss of H4K16ace through *sas2Δ* did not alter H2A.Z levels. While the reduction in H4K16 acetylation was likely due to a role for Asf1 in recruiting the SAS complex to heterochromatic boundaries, our findings suggested that the relationship between the SAS complex and H2A.Z was telomere-specific. Furthermore, H2A.Z occupancy level at subtelomeric gene promoters in *asf1Δsas2Δ* was similar to *asf1Δ* at ChrVI R and ChrIII, supporting the model that Asf1 acts upstream of the SAS complex. While the focus of this chapter was in H2A.Z at heterochromatin, the functional relationship between Asf1 and the SAS complex likely extends beyond their roles in H2A.Z regulation. A number of earlier publications highlight this relationship as cells lacking Asf1 or SAS function exhibit similar growth deficiencies, defects in establishing silent chromatin structure, and genetic interaction partners (Miller *et al.* 2010; Raisner and Madhani 2008; Osada *et al.* 2005; Meijsing and Ehrenhofer-Murray 2001).

Analysis of the relationship between Asf1 and the bulk levels of chromatin-bound H2A.Z suggested that bulk H2A.Z occupancy and SWR1-C recruitment did not depend on Asf1. This differed from our region-specific examination of the subtelomeric gene promoters, as

we saw a consistent decrease in H2A.Z levels at multiple telomeres as well as euchromatic genes (Lu and Kobor 2014). One possible explanation for this may be due to the differences between the two assays. A centrifugation-based separation of chromatin from whole cell lysate may not be able to distinguish SWR1-C bound H2A.Z that are associated to chromatin, but not deposited, from H2A.Z incorporated into the nucleosome. Similar observations in cells lacking *YAF9* support this idea and indicate that a chromatin association assay cannot pick up the differences between H2A.Z that are associated with chromatin versus H2A.Z that are incorporated in the nucleosome (Wang *et al.* 2009).

Using ChIP-on-chip, we generated a detailed global H2A.Z occupancy profile in the absence of H3K56 acetylation. The genome-wide H2A.Z profile highlighted three distinct effects that the loss of H3K56 acetylation had on H2A.Z biology in chromatin. The loss of H3K56 acetylation resulted in either the absolute loss of H2A.Z at gene promoters, a reduction in the levels of H2A.Z at gene promoters, or a shift in H2A.Z position at gene promoters; highlighting a key role for this histone modification in the regulation of chromatin-bound H2A.Z. The most exciting observation that we uncovered as a result of our genome-wide H2A.Z profiling was the observed shift in H2A.Z occupancy peaks in H3K56 acetylation mutants. In wildtype cells, almost 50% of H3K56 acetylated promoters are also enriched with H2A.Z, supporting a functional overlap of these two chromatin marks. While nucleosomes with or without acetylated H3K56 have the same stability *in vitro*, $(H3/H4)_2$ tetrasomes are more stable than $(H3K56ace/H4)_2$ tetrasomes, suggesting that the modified tetrasome has the capacity to promote nucleosome movement (Andrews *et al.* 2010; Muthurajan *et al.* 2004). It is tempting to speculate the heightened chromatin fluidity of

H3K56-acetylated tetrasomes allow for fine-tuning of nucleosome position during H2A.Z/H2B exchange by SWR1-C, whereas this capability is lost in cells lacking H3K56 acetylation. Indeed, *in vitro* FRET experiments have shown that the constitutive acetyl mimic, K56Q, have heightened nucleosome thermal mobility compared to unmodified nucleosomes (Ferreira *et al.* 2007). This proposed mechanism is distinct from a recent report demonstrating that H3K56 acetylation promotes the removal of H2A.Z by SWR1-C by disrupting the locking mechanism of Swc2 (Watanabe *et al.* 2013). It is interesting that H3K56 acetylation has such a dynamic role in the regulation of H2A.Z. This could be the underlying reason for why H3K56 acetylation is such a transient and highly regulated histone modification (Maas *et al.* 2006; Kaplan *et al.* 2008; Ozdemir *et al.* 2006).

Interestingly a recent paper demonstrated that the H3K56Q, designed to mimic H3K56 acetylation, also lead to reduced H2A.Z occupancy (Watanabe *et al.* 2013). Furthermore, our own ChIP-on-chip data also revealed a similar reduction in H2A.Z level in a *H3K56Q* mutant (Lu, data not shown). Taken together with the data presented in this chapter, it seems as if both the constitutive presence and absence of H3K56 acetylation regulate H2A.Z occupancy. It is tempting to speculate that perhaps, it is the tight regulation of this transient histone modification that is the key in its role in H2A.Z position and occupancy. Indeed, while H3K56 acetylation is required for chromatin reassembly after DNA damage repair, removal of the histone modification is also required for release from cell cycle checkpoint after repair (Hyland *et al.* 2005; Tjeertes *et al.* 2009; Chen *et al.* 2008; Masumoto *et al.* 2005; Wurtele *et al.* 2012; Celic *et al.* 2006; Maas *et al.* 2006). Further research is needed to determine if a

similar requirement for regulating the status of H3K56 acetylation exist in regulating H2A.Z occupancy.

In this chapter, we utilized two distinct genetic perturbations that lead to loss of H3K56 acetylation and their effect on H2A.Z biology. Surprisingly, deletion of *ASF1* and the unacetylable H3 allele, *H3K56R,* both exhibited very similar defects in H2A.Z occupancy. That being said, loss of H3K56 acetylation through *H3K56R* consistently resulted in a stronger decrease in H2A.Z levels and a bigger shift in H2A.Z nucleosomes compared to the *asf1Δ* mutant. Considering that *H3K56R* mutant very specifically compromises Asf1's role as a chaperone in promoting H3K56 acetylation, it is possible that a complete deletion of the histone chaperone would lead to compensation by other chromatin remodeling factors. Nevertheless, the overall effect on H2A.Z position and occupancy between the two mutations were quite similar. With a Spearman correlation of 0.946 and over 90% overlap of promoters enriched for H2A.Z between *asf1Δ* and *H3K56R*, our data emphasizes the importance H3K56 acetylation plays in regulating the position and occupancy level of H2A.Z at a subset of gene promoters.

It is exciting to think that perhaps a more precise method of measuring nucleosome position would yield a better understanding of the precise mechanism of H2A.Z positioning by acetylated H3K56. With our current data set from the ChIP-chip analysis, we developed a method to analyze the change in location of each H2A.Z peak found at gene promoters. As it currently stands, the peak shift analysis also includes all H2A.Z peaks even if they were not shifted. This was due to the inability to set objective cutoffs deeming significantly shifted

peaks. By mapping H2A.Z containing nucleosomes through MNase digestion followed by ChIP-seq, we would better understand and appreciate the significance of H3K56 acetylation in H2A.Z nucleosome positioning.

Chapter 4: Eaf1 HSA Domain and Epl1 C-terminus Coordinate NuA4 Stability and Function

4.1 Introduction

Chromatin structure facilitates DNA compaction inside the cell nucleus and contributes to the regulation of nuclear processes such as transcription, DNA repair and DNA replication (Ehrenhofer-Murray 2004; Rando and Chang 2009). In eukaryotes, the structure of chromatin can be modified by several fundamental mechanisms, often involving specialized and dedicated protein complexes. For instance, ATP-dependent remodeling enzymes use energy derived from ATP hydrolysis to slide or exchange nucleosomes on the DNA template (Eberharter and Becker 2004; Clapier and Cairns 2009). Additionally, the composition of nucleosomes can be altered by incorporation of the less abundant histone variants, who differ from their canonical counterparts in their primary amino acid sequence and function (Sarma and Reinberg 2005; Zlatanova and Thakar 2008). Finally, both canonical histones and their variants are subjected to numerous post-translational chemical modifications, including acetylation, methylation, phosphorylation, ubiquitination and ADP-ribosylation (Bannister and Kouzarides 2011).

Budding yeast, *Saccharomyces cerevisiae,* contain several histone acetyltransferase (HAT) complexes, including NuA4 (Nucleosome acetyltransferase of H4). NuA4, the only essential HAT in yeast, is composed of 13 subunits and not only acetylates the N-terminal tails of

histones H4, H2A, and H2A.Z but also additional non-histone substrates (Babiarz *et al.* 2006; Doyon *et al.* 2004; Jeong *et al.* 2011; Keogh *et al.* 2006; Lin *et al.* 2008; 2009; Mitchell *et al.* 2011). NuA4 is required for a diverse set of cellular functions, including cell cycle progression, DNA double-stranded break repair, establishment of heterochromatin-euchromatin boundaries at subtelomeric regions, and transcription of ribosomal genes (Bird *et al.* 2002; Boudreault *et al.* 2003; Clarke *et al.* 1999; Reid *et al.* 2000; Smith *et al.* 1998; Zhang *et al.* 2004). Its catalytic activity resides within the Esa1 subunit, while other subunits coordinate specific functions of NuA4 and contribute to its structural stability. NuA4 is a modular complex that assembles on the Eaf1 subunit and as such, different regions of the Eaf1 protein mediate the association of distinct components of NuA4. For example, the N-terminal region of Eaf1 is responsible for the association of the Eaf5/7/3 sub-module, while its SANT (SWI3-ADA2-N-CoR-TFIIIB) domain binds Tra1, a subunit involved in NuA4 recruitment to specific promoters via Tra1's interaction with acidic transcription activators such as Gcn4, Hap4, and Gal4 (Auger *et al.* 2008; Brown *et al.* 2001). In addition, the HSA (helicase-SANT-associated) domain of Eaf1 interacts with a module containing Swc4, Arp4, Yaf9, and Act1 (Auger *et al.* 2008; Szerlong *et al.* 2008). The Swc4/Arp4/Act1/Yaf9 module provides an intriguing link to the H2A.Z histone variant as these four proteins are also components of SWR1-C, an ATP-dependent chromatin-remodelling complex that deposits H2A.Z into chromatin (Kobor *et al.* 2004; Krogan *et al.* 2003; Mizuguchi *et al.* 2004; Zhang *et al.* 2004). Consistent with a broad requirement of Eaf1 for NuA4 assembly and function, cells lacking *EAF1* have strongly reduced global levels of H4 tetra-acetylation and sensitivity for a wide range of genotoxic agents (Kobor *et al.* 2004; Krogan *et al.* 2004).

Previous work has shown that the catalytic module of NuA4 exists as the functional Piccolo NuA4 (picNuA4) subcomplex composed of Esa1, Yng2, Epl1, and Eaf6 subunits (Auger *et al.* 2008; Boudreault *et al.* 2003; Chittuluru *et al.* 2011). Binding of Esa1 and Yng2 to the EPcA domain of Epl1 is important for the association and function of picNuA4 (Selleck *et al.* 2005). A number of studies have suggested that picNuA4 is anchored to NuA4 through a physical interaction between the Epl1 C-terminus and the Eaf1 scaffolding subunit, as removal of the C-terminal region of Epl1 results in the dissociation of the picNuA4 submodule from NuA4. In contrast to the locus-specific recruitment, acetylation, and activation of NuA4, picNuA4 is thought to catalyze non-targeted global histone acetylation (Boudreault *et al.* 2003). *In vitro,* picNuA4 has a preference in acetylating nucleosomal histones over free histones unlike its larger cousin (Nourani *et al.* 2004; Reid *et al.* 2000; Boudreault *et al.* 2003; Friis *et al.* 2009; Selleck *et al.* 2005). Recent structural analysis identified the Yng2 subunit and the Epl1 N-terminus as the key binding surfaces for picNuA4 association to the nucleosome core particle (Chittuluru *et al.* 2011). Although rooted in the discovery of picNuA4, untargeted histone acetylation is emerging as an important, yet poorly understood, property of HAT complexes.

Here we study the two scenarios represented by loss of the entire Eaf1 protein and the loss of the Epl1 C-terminus to better understand the precise nature of the relationship between NuA4 and picNuA4. Remarkably, removal of the Epl1 C-terminus suppressed the bulk histone acetylation defects and growth defects associated with loss of *EAF1* through the stabilization of the picNuA4 complex. In contrast, NuA4-specific defects, such as decreased promoter H4 acetylation and expression of ribosomal genes, were not rescued by removal of the Epl1 C-

terminus. Large-scale genetic and gene expression analyses revealed commonalities and distinct properties between *eaf1Δ* and *epl1-CΔ* mutants, providing further evidence that these two genetic alterations resulted in distinct perturbations in NuA4 HAT function. Structure-function studies identified the HSA domain as being the key domain for picNuA4 formation, likely by being the docking platform for the Epl1 C-terminus. Lastly, artificially releasing picNuA4 via the removal of the Epl1 C-terminus revealed that picNuA4 was poorly associated to chromatin despite being sufficient to acetylate H4 and H2A.Z. Taken together, the results presented in this chapter suggested that the interface between these two key subunits likely played an important role in maintaining the equilibrium of active NuA4 and picNuA4 in the cell.

4.2 Materials and Methods

4.2.1 Yeast Strains and Plasmids

All strains used in this study are listed in Table 4.1. Yeast strains were generated using standard genetic techniques including homologous recombination and genetic crosses followed by tetrad dissection (Ausubel 1987). Complete deletion of genes, *EPL1* truncations, and 3' end integration of an in frame epitope tag (TAP or 3xFLAG) were achieved using one-step gene integration PCR-amplified modules (Gelbart *et al.* 2001). The *EAF1* gene was PCR-amplified from genomic DNA and cloned into pRS316 (*URA3)* centromeric vector containing a 3x-HA tag. Internal deletions of *EAF1* were performed by adapting the Quick

Change site-directed mutagenesis method (Stratagene) following manufacturer's protocol. All mutations were confirmed by DNA sequencing.

Table 4.1 Yeast strains used in this study

Strain number	Relevant Genotype
MKY6	W303*, MATA, ADE2, can1-100 his3-11 leu2-3,112 trp1-1 ura3-1 lys2Δ*
MKY1762	MKY6, *EPL1-TAP::TRP*
MKY1763	MKY6, *EPL1-TAP::TRP, eaf1::HIS*
MKY1764	MKY6, *epl1-485-TAP::TRP*
MKY1765	MKY6, *epl1-485-TAP::TRP, eaf1::HIS*
MKY1766	MKY6, *epl1-380-TAP::TRP*
MKY1767	MKY6, *epl1-380-TAP::TRP, eaf1::HIS*
MKY583	BY4741, *MATα, his3Δ1 leu2Δ0 LYS2 met15Δ0 ura3Δ0 Δcan1::MATαPr-HIS3 Δlyp1::MATαPr-LEU2*
MKY1419	MKY583, *eaf1 1-982-3XHA::NAT*
MKY1428	MKY583, *eaf1Δ-3XHA::NAT*
MKY1429	MKY583, *EPL1-3xFLAG::KAN*
MKY1430	MKY583, *epl1-485-3xFLAG::KAN*
MKY1431	MKY583, *epl1-380-3xFLAG::KAN*
MKY 1768	MKY6, *pRS316*
MKY1769	MKY6, *EPL1-TAP::TRP, pRS316*
MKY1770	MKY6, *EPL1-TAP::TRP, eaf1::HIS [pRS316]*
MKY1771	MKY6, *EPL1-TAP::TRP, eaf1::HIS [pRS316, EAF1]*
MKY1772	MKY6, *EPL1-TAP:::TRP, eaf1::HIS [pRS316, eaf1-HSAΔ]*
MKY1773	MKY6, *EPL1-TAP::TRP, eaf1::HIS [pRS316, eaf1-SANTΔ]*
MKY1774	MKY6, *EPL1-TAP::TRP, eaf1::HIS [pRS316, eaf1-HSAΔSANTΔ]*
MKY1775	MKY6, *epl1-485-TAP::TRP, eaf1::HIS [pRS316]*
MKY1776	MKY6, *epl1-485-TAP::TRP, eaf1::HIS [pRS316, EAF1]*
MKY1777	MKY6, *epl1-485-TAP::TRP, eaf1::HIS [pRS316, eaf1-HSAΔ]*
MKY1778	MKY6, *epl1-485-TAP::TRP, eaf1::HIS [pRS316, eaf1-SANTΔ]*
MKY1779	MKY6, *epl1-485-TAP ::TRP, eaf1::HIS [pRS316, eaf1-HSAΔSANTΔ]*

4.2.2 Growth and Genotoxic Sensitivity Assays

Overnight cultures grown in YP-dextrose were diluted to OD_{600} 0.5. Cells were 10-fold serially diluted and spotted onto solid YPD plates or plates with 0.005% MMS (Sigma), 50mM hydroxyurea (HU), or 1% formamide (Sigma). For strains containing *URA3* plasmids, the cultures were grown in SC –URA media and serially diluted cells were spotted onto SC –URA plates or plates containing genotoxic agents. The plates were then incubated at the indicated temperature for 36 hours.

4.2.3 Large-Scale Affinity Purification

Purification of native protein complexes were performed using extracts from strains encoding the TAP tag fused in-frame to the 3' end of genes. Purifications were performed from 1L cultures that were harvested at an OD_{600} of 1.00. Large-scale purification was adapted from protocols previous described with minor modifications (Mitchell *et al.* 2008). Briefly, cells were lysed with a coffee grinder with dry ice pellets and resuspended in TAP buffer (20 mM Hepes [pH 8], 350 mM NaCl, 10% glycerol, 0.1% Tween-20, 1x phosphatase inhibitor mix, Complete Protease Inhibitor cocktail [Roche]). NP-40 was added to a final concentration of 1% prior to centrifugation at 3000g for 10 minutes at 4C. Crude extracts were incubated with 200µl of IgG (Millipore) crosslinked M-270 Epoxy beads (Invitrogen) as per manufacturer's protocol for 3 hours at 4C rotating. The beads were then washed with 4ml of TAP buffer three times. The protein complex was eluted in 30µl of 0.1M citrate [pH 3.1] and loaded into 4-20% gradient gel (Bio-rad) for silver stain or western analysis.

4.2.4 RT-qPCR

Overnight cultures were diluted to OD_{600} of 0.15 and grown in YP-dextrose to an OD_{600} of 0.5. Ten OD_{600} units were harvested for RNA extraction and purification using a Qiagen RNeasy minikit as per manufacturer protocol. cDNA was synthesized using QuantiTect Reverse Transcription Kit (Qiagen). cDNA was analyzed using a Rotor-Gene 6000 (Qiagen) and PerfeCTa SYBR green FastMix (Quanta Biosciences). mRNA levels were normalized to *ACT1* mRNA levels. Samples were analyzed in triplicates for three independent RNA preparations. Statistical significance was assessed using Student's *t* test. Primer sequences are listed in Table 4.2.

Table 4.2 Primers used in this study

Name	Method	Primer sequence (5'-3')
EPL1 F	RT	GGACGATCCCTTTAATCCTG
EPL1 R	RT	CTCGAACGGCCATTTGAATC
RPL19B F	RT	TGCAAGCGTTAATTCGATTG
RPL19B R	RT	ACAACAGAAGCGGCAAGTCT
RPS11B F	RT	GAAAAGCAGGACCTCGAATG
RPS11B R	RT	TGGCATTAGTCGGGTGAAAT
RPS3 F	RT	CACTCCAACCAAGACCGAAG
RPS3 R	RT	TCTGACGACACCGTAAGCAG
RPL19B F	ChIP	CTCATCGCTATGGGAATTGG
RPL19B R	ChIP	TGGTGACTTTTTATTCGATTTGG
RPS11B F	ChIP	CATGTTTCCCGCTTTGTTTT
RPS11B R	ChIP	GATTTTCAACAGACGCAGCA
RPS3 F	ChIP	TTTGTTTCCGTAACATCCATACC
RPS3 R	ChIP	AAGAGCTGCATTGATTTGGAA

4.2.5 ChIP-qPCR and ChIP-on-chip

Chromatin immunoprecipitation (ChIP) experiments were performed as described previously (Schulze *et al.* 2009). In brief, 250 ml of cells were grown in YP-dextrose to an OD_{600} of 0.5-0.6 from OD_{600} of 0.15 and were crosslinked with 1% formaldehyde for 20 minutes before chromatin was extracted. The chromatin was sonicated (Bioruptor, Diagenode, Spart, NJ: 10 cycles, 30s on/off, high setting) to yield an average DNA fragment of 500bp. Anti-FLAG antibody (4.2µl, Sigma) was coupled to 60µl of protein A magnetic beads (Invitrogen). After reversal of the crosslinking and DNA purification, the immunoprecipitated and input DNA were analyzed by quantitative real-time PCR (qPCR). Samples were analyzed in triplicate for three independent ChIP experiments. Statistical significance was assessed using Student's *t* test. Primer sequences are listed in Table 4.2. For microarray analysis, after reversal of crosslinking and DNA purification, the DNA was amplified with two rounds of T7 RNA polymerase amplification and hybridized to Affymetrix 1.0R *S. cerevisiae* tiling microarray. A modified version of the model-based analysis of tiling arrays (MAT) algorithm was used to reliably detect Epl1 occupancy across the genome. The data was normalized using both input DNA and a mock IP control.

4.2.6 mRNA Expression Profile

Expression profiling was performed as described previously (van de Peppel *et al.* 2003). Briefly, *EAF1* and *EPL1* alleles were processed four times from two independently inoculated cultures. Dual-channel 70-mer oligonucleotide arrays were used with a common reference wild-type RNA. After RNA isolation, all steps were operated using robotic liquid handlers and scores were calculated as previously described (van Bakel and Holstege 2004;

van de Peppel *et al.* 2003). Differentially expressed genes were determined by p-value of 0.01 and minimum fold change of 1.7 compared to wildtype. Database for Annotation, Visualization, and Integrated Discovery (DAVID) was used for Gene Ontology enrichment analysis (Dennis *et al.* 2003). Multiple testing correction was done using the Benjamini method.

4.2.7 E-MAP

E-MAP assay was performed as described previously (Schuldiner *et al.* 2006). Briefly, using a Singer robot, *EAF1* and *EPL1* alleles were crossed to a library of 1,536 mutants representing a number of processes including transcription, RNA processing and chromatin biology. All strains were screened three to four times and scores were calculated as previously described (Collins *et al.* 2006; Schuldiner *et al.* 2006).

4.2.8 Chromatin Association Assay

Chromatin association assay were performed as previously described (Wang *et al.* 2009). In brief, cells were diluted to OD_{600} 0.15 and collected at logarithmic phase. Following collection, cells were incubated in pre-spheroblast buffer (100 mM PIPES/KOH [pH 9.4], 10 mM DTT, 0.1% sodium azide) for 10 minutes at room temperature rotating, then spheroblasted for 20 minutes at 37C with 20mg/ml Zymoylase-100T (Seikagaku Corporation). Spheroblasts were washed with wash buffer (50 mM HEPES/KOH [pH 7.5], 100mM KCl, 2.5 mM $MgCl_2$, 0.4 M sorbitol) and resuspended in equal volume of EB (50 mM HEPES/KOH [pH 7.5], 100mM KCl, 2.5 mM $MgCl_2$, 1 mM DTT, 1 mM PMSF, and Complete Protease Inhibitor cocktail [Roche]). Cells were lysed with 1% Triton X-100.

Whole cell extracts were saved and the remaining lysate were separated into the chromatin pellet and the supernatant fraction by centrifugation through EBXS (EB + 0.25% Triton X-100 and 30% sucrose). The three fractions were subsequently analyzed by SDS-PAGE and immunoblotted. Immunoblots were scanned with the Odyssey Infrared Imaging System (Licor).

4.3 Results

4.3.1 Epl1 C-terminus Truncation Suppressed the Effects of *EAF1* Deletion by Stabilizing picNuA4 Complex Formation

Many lines of evidence suggested that the physical interaction between the Epl1 C-terminus and Eaf1 anchors the catalytic module to the rest of the NuA4 complex (Auger *et al.* 2008; Boudreault *et al.* 2003). To dissect the functional and structural relationship between Epl1 and Eaf1 more closely, we first examined the genetic interaction between *EAF1* and *EPL1* by combining a complete deletion of the non-essential *EAF1* gene with one of two *EPL1* C-terminal truncation mutants (Boudreault *et al.* 2003). Two variants of *epl1-CΔ* exist, allowing us to comprehensively interrogate its C-terminus. In addition to the N-terminal EPcA domain, the *epl1-485* allele encoded protein contains central stretches of alanine and glutamine repeats whereas the *epl1-380* allele does not (Figure 4.1A). Loss of Eaf1 and the Epl1 C-terminus result in a variety of growth and functional defects typically associated with loss of NuA4 function, such as sensitivity to genotoxic agents such as methyl-methanesulfonate (MMS), hydroxyurea (HU), and formamide, and reduced acetylation of H4

(Figure 4.1B and Figure 4.1C) (Auger *et al.* 2008; Babiarz *et al.* 2006; Boudreault *et al.* 2003; Kobor *et al.* 2004). Surprisingly, upon combining *eaf1Δ* in parallel with *epl1 1-380* or *epl1 1-485* alleles, sensitivity to genotoxic agents of these *eaf1 epl1-CΔ* double mutants was not as severe as the single *eaf1* mutant (Figure 4.1B). The partial suppression was particularly noticeable in the healthier *epl1-485* strain, whereby truncation of its C- terminus in an *eaf1Δ* background was sufficient to partially rescue the growth phenotype to that of an *epl1-485* single mutant (Figure 4.1B). Given that loss of *EAF1* has been shown to reduce the levels of bulk H4 acetylation, we next evaluated the effect of further removing the C-terminus of Epl1 on these core NuA4 activities(Kobor *et al.* 2004; Krogan *et al.* 2004). In contrast to the reduction observed in the *eaf1*Δ mutant, removal of the Epl1 C-terminus had no effect on the level of H4 tetra-acetylation (Figure 4.1C). Interestingly, the H4 acetylation levels in the *eaf1Δ epl1-CΔ* double mutants were similar to that of the *epl1-CΔ* single mutants and wildtype, strongly implying that removal of the Epl1 C-terminus can rescue bulk acetylation defects caused by loss of Eaf1.

Based on the ability of the *EPL1* C-terminal truncation mutants to rescue the defects in H4 acetylation caused by loss of Eaf1, we tested whether this was rooted in changes to NuA4 complex integrity. Proteins associated with a TAP-tagged Epl1 in cells lacking Eaf1 and/or the C-terminus of Epl1 were identified by a small-scale TAP purification followed by silver stain. In agreement with previous reports, loss of *EAF1* resulted in a striking decrease in the levels of NuA4 subunits associated with Epl1-TAP, suggesting that the NuA4 complex was largely disassociated in the absence of Eaf1 (Figure 4.1D) (Mitchell *et al.* 2008). As expected, pull down of *epl1-485-TAP* and *epl1-380-TAP* led to purification of Yng2 and

Esa1, demonstrating release of the picNuA4 complex upon truncation of the Epl1 C-terminus (Figure 4.1D) (Auger *et al.* 2008). Most importantly, by combining the *EPL1* C-terminal truncation mutants with *eaf1Δ,* we found that both Epl1-CΔ proteins were sufficient to reconstitute the picNuA4 complex in the absence of Eaf1 (Figure 4.1D). Consistent with the phenotypic data, the restoration picNuA4 complex integrity in an *eaf1Δ* background suggests that the suppression of *eaf1Δ*-specific defects such as growth and H4 acetylation was mediated through the stabilization of picNuA4 upon Epl1 C-terminus truncation.

The small-scale TAP purification experiments also revealed that the levels of Epl1 varied among the different strains. Further examination on whole cell extracts demonstrated that Epl1 protein levels were dependent on its own C-terminus and Eaf1 (Figure 4.1E). Specifically, loss of *EAF1* led to reduced levels of Epl1 protein while truncation of the Epl1 C-terminus increased Epl1 protein levels. In addition, RT-qPCR data showed that differences in Epl1 protein levels did not occur at the transcriptional level but were rather likely due to protein instability (Figure 4.1F). Taken together, these results suggested that interactions between the Epl1 C-terminus and Eaf1 lie at the core of NuA4 complex stability and function.

A

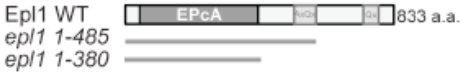
Epl1 WT
EPcA
833 a.a.
epl1 1-485
epl1 1-380

B

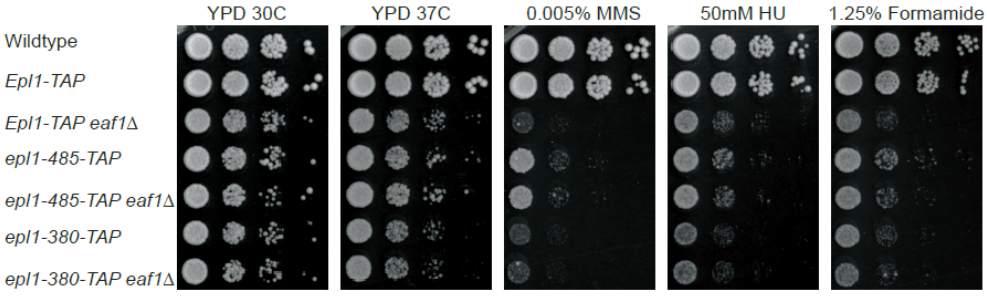
YPD 30C
YPD 37C
0.005% MMS
50mM HU
1.25% Formamide
Wildtype
Epl1-TAP
Epl1-TAP eaf1Δ
epl1-485-TAP
epl1-485-TAP eaf1Δ
epl1-380-TAP
epl1-380-TAP eaf1Δ

C

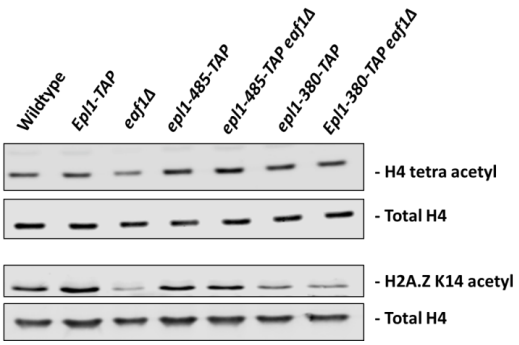
Wildtype
Epl1-TAP
eaf1Δ
epl1-485-TAP
epl1-485-TAP eaf1Δ
epl1-380-TAP
Epl1-380-TAP eaf1Δ
- H4 tetra acetyl
- Total H4
- H2A.Z K14 acetyl
- Total H4

D

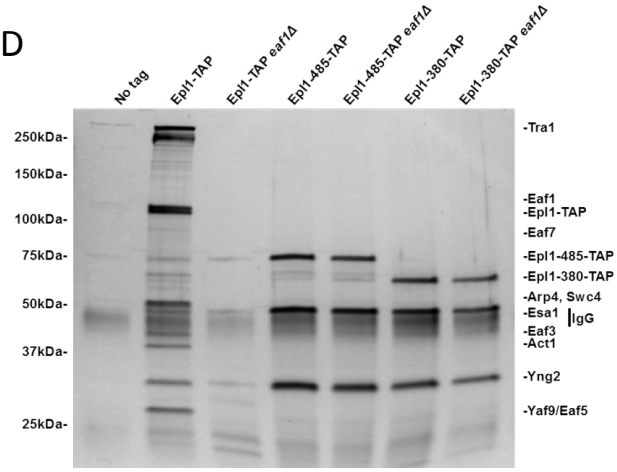
No tag
Epl1-TAP
Epl1-TAP eaf1Δ
Epl1-485-TAP
Epl1-485-TAP eaf1Δ
Epl1-380-TAP
Epl1-380-TAP eaf1Δ
250kDa-
150kDa-
100kDa-
75kDa-
50kDa-
37kDa-
25kDa-
-Tra1
-Eaf1
-Epl1-TAP
-Eaf7
-Epl1-485-TAP
-Epl1-380-TAP
-Arp4, Swc4
-Esa1
IgG
-Eaf3
-Act1
-Yng2
-Yaf9/Eaf5

E

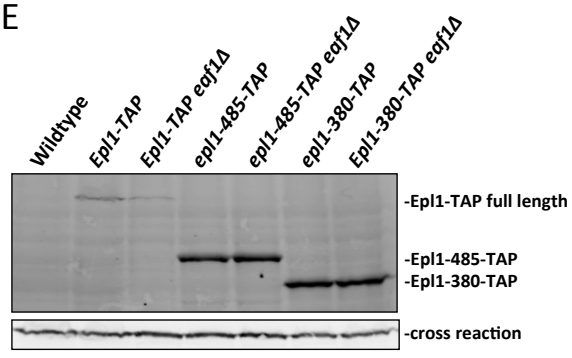
Wildtype
Epl1-TAP
Epl1-TAP eaf1Δ
epl1-485-TAP
epl1-485-TAP eaf1Δ
epl1-380-TAP
Epl1-380-TAP eaf1Δ
-Epl1-TAP full length
-Epl1-485-TAP
-Epl1-380-TAP
-cross reaction

F

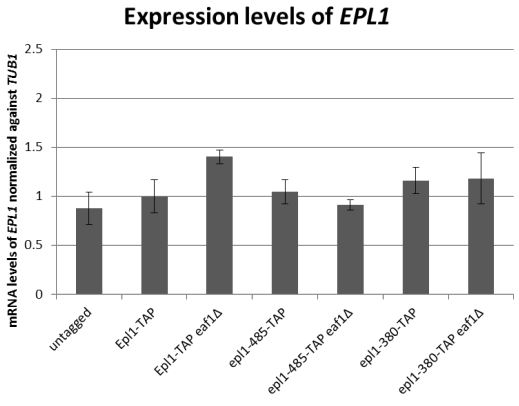
Expression levels of EPL1
mRNA levels of EPL1 normalized against TUB1
2.5
2
1.5
1
0.5
0
untagged
Epl1-TAP
Epl1-TAP eaf1Δ
epl1-485-TAP
epl1-485-TAP eaf1Δ
epl1-380-TAP
epl1-380-TAP eaf1Δ

Figure 4.1 Epl1 C-terminus truncation suppressed the effects of *EAF1* deletion by stabilizing picNuA4 complex formation
(A) Schematic of the *Epl1-CΔ* mutations. (B) Ten-fold serial dilutions of the indicated strains were plated on YPD media, with or without genotoxic agents and incubated for 3 days at the indicated temperature. (C) Whole cell extracts of indicated strains were analyzed by protein blotting with anti-H4 tetra acetylation antibodies. Antibodies against H4 were used as loading control. (D) TAP purification of NuA4 using Epl1-TAP demonstrated dissociation of NuA4 subunits in *eaf1Δ* mutant and stabilization of picNuA4 in *epl1-CΔ* mutants. Purified fractions from indicated strains were loaded onto a 4-20% gradient SDS-PAGE gel and visualized by silver staining. Bands corresponding to NuA4 subunits are indicated on the left. Untagged Epl1 was used as a negative control. Pull down of Epl1-TAP in *EPL1-TAP eaf1Δ* strain was verified by western (data not shown). (E) Whole cell extract were analyzed for total Epl1-TAP level by protein blotting with IgG antibody. IgG unspecific band was used as loading control. (F) mRNA level for *EPL1* were comparable across all strains examined. mRNA level was measured by RT-qPCR and normalized to levels of *TUB1* mRNA.

4.3.2 Loss of Eaf1 and Epl1 C-terminus led to NuA4-Specific Defects at Ribosomal Genes

The loss of NuA4 complex in *eaf1Δ* and *epl1-CΔ* cells suggested abnormalities in NuA4-specific functions in the cell. In yeast, NuA4 is recruited to promoters of ribosomal protein (RP) genes in an activator-dependent manner and H4 acetylation at these specific genomic regions is required for RP gene expression (Reid *et al.* 2000). Utilizing chromatin immunoprecipitation (ChIP) followed by qPCR, we determined that *epl1 1-380* and *eaf1*Δ single mutants both exhibited decreased H4 tetra-acetylation at promoters of *RPL19B*, *RPS11B*, and *RPS3* genes (Figure 4.2A). While both single mutants have substantial H4 acetylation defect, the *eaf1*Δ *epl1 1-380* double mutant also showed a similar decrease in H4 tetra-acetylation at these loci suggesting that they act in the same pathway (Figure 4.2A). This result is in agreement with previous models that indicate picNuA4 does not target H4 acetylation at specific loci such as the RP genes. Consistently, the H4 acetylation pattern closely mirrored the mRNA expression patterns of these genes. As assayed by RT-qPCR, expression of *RPL19B*, *RPS11B*, and *RPS3* was reduced in both single mutants and in the

double mutant (Figure 4.2B). Thus, these results revealed that targeted acetylation by NuA4 at specific loci were lost under both *epl1-CΔ* and *eaf1Δ* conditions. Furthermore, while loss of Epl1 C-terminus was sufficient to suppress global H4 acetylation defects in an *eaf1Δ* background, this inhibition did not extend to loci targeted by NuA4.

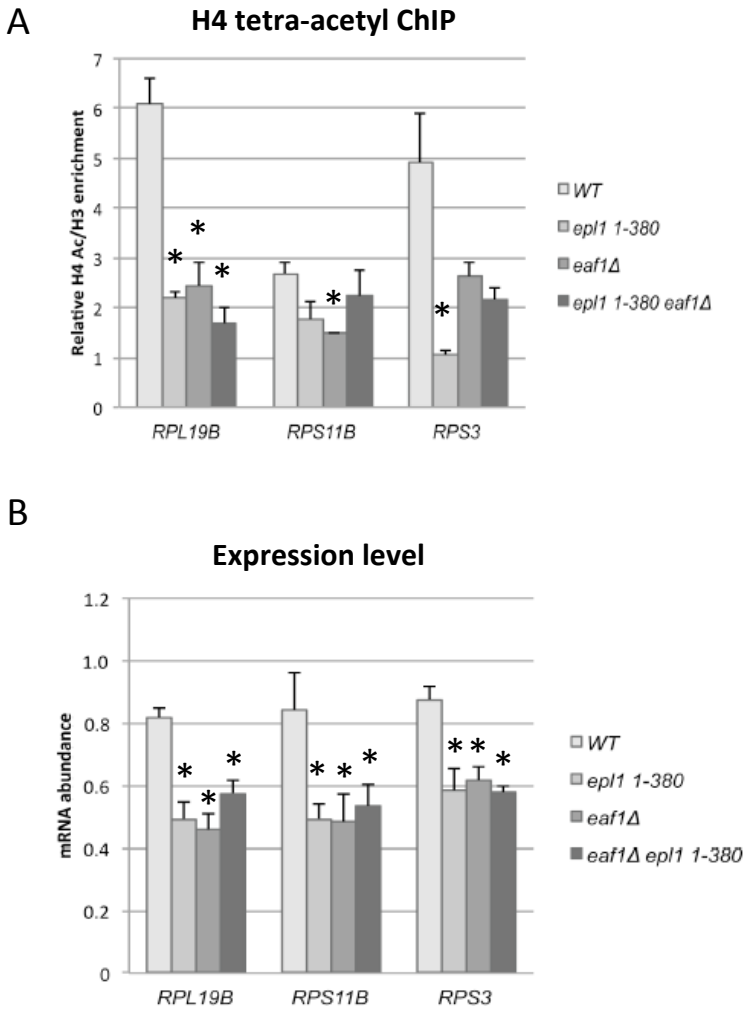

Figure 4.2 Loss of Eaf1 and Epl1 C-terminus led to NuA4-specific defects at ribosomal genes
(A)ChIP of H4 tetra-acetylation at promoters of *RPL19B, RPS11B,* and *RPS3* in wildtype, *epl1 1-380, eaf1Δ,* and *epl1 1-380 eaf1Δ.* Enrichment of H4 tetra-acetylation was normalized to nucleosome density as measured by H3. (B) mRNA levels were measured by RT-qPCR for the indicated transcripts. mRNA levels for all genes were normalized to levels of *ACT1* mRNA. Error bars represent standard errors of the means for three independent experiments.

4.3.3 Distinct and Overlapping Cellular Roles for Eaf1 and the Epl1 C-terminus

Built on our findings that a complete deletion of Eaf1 and truncation of the Epl1 C-terminus led to vastly different consequences on NuA4 complex structure and integrity, we decided to perform genome-wide assays to examine the biological consequences of these two mutations in the cell. A combination of whole genome expression profile and Epistatic Mini-Array Profiling (E-MAP) profiling were used to thoroughly examine *eaf1Δ, epl1-485* and *epl1-380.* As a whole, the yeast transcriptome changed dramatically upon deletion of *EAF1* and truncation of *Epl1,* with an average Spearman correlation of 0.20 against wildtype (Figure 4.3A). However, the gene expression profiles of the three mutants are quite similar with the lowest correlation of 0.799 between *eaf1Δ* and *epl1-485,* and the highest correlation of 0.987 between the two *epl1-CΔ* mutants (Figure 4.3A). This can be attributed to the relatively small number of genes that are differentially expressed in *eaf1Δ, epl1-485* and *epl1-380* compared to wildtype (Figure 4.3B). There were roughly 150 genes whose expression was significantly altered upon either deletion of *EAF1* or truncation of *EPL1* (Figure 4.3B). Altogether, only 18 down-regulated genes and 61 up-regulated were shared between *eaf1Δ, epl1-485* and *epl1-380* (Figure 4.3B). Although NuA4 has been primarily linked to gene activation, our analysis revealed that genes were both up-regulated and down-regulated in the three mutant strains (Figure 4.3B). While *epl1-485* and *epl1-380* share a significant number of differentially expressed genes, it is clear that there are distinct subsets of genes that are differentially expressed between *eaf1Δ* and *epl1-CΔ* (Figure 4.3B and Figure 4.3C).

Functional characterization suggested that genes that required either Eaf1 or Epl1 for proper expression were involved in various metabolic processes such as “carbohydrate catabolic process” (p-value = 7.30E-05), “glycoside metabolic process” (p-value = 1.60E-04) and “protein catabolic process” (p-value = 2.7E-04). Furthermore, both Eaf1 and Epl1 were also required for expression of genes in “response to temperature stimulus” (p-value = 3.00E-19). While expression of ribosomal genes was altered in the expression profile of all three strains, they did not pass our stringent significant threshold (data not shown).

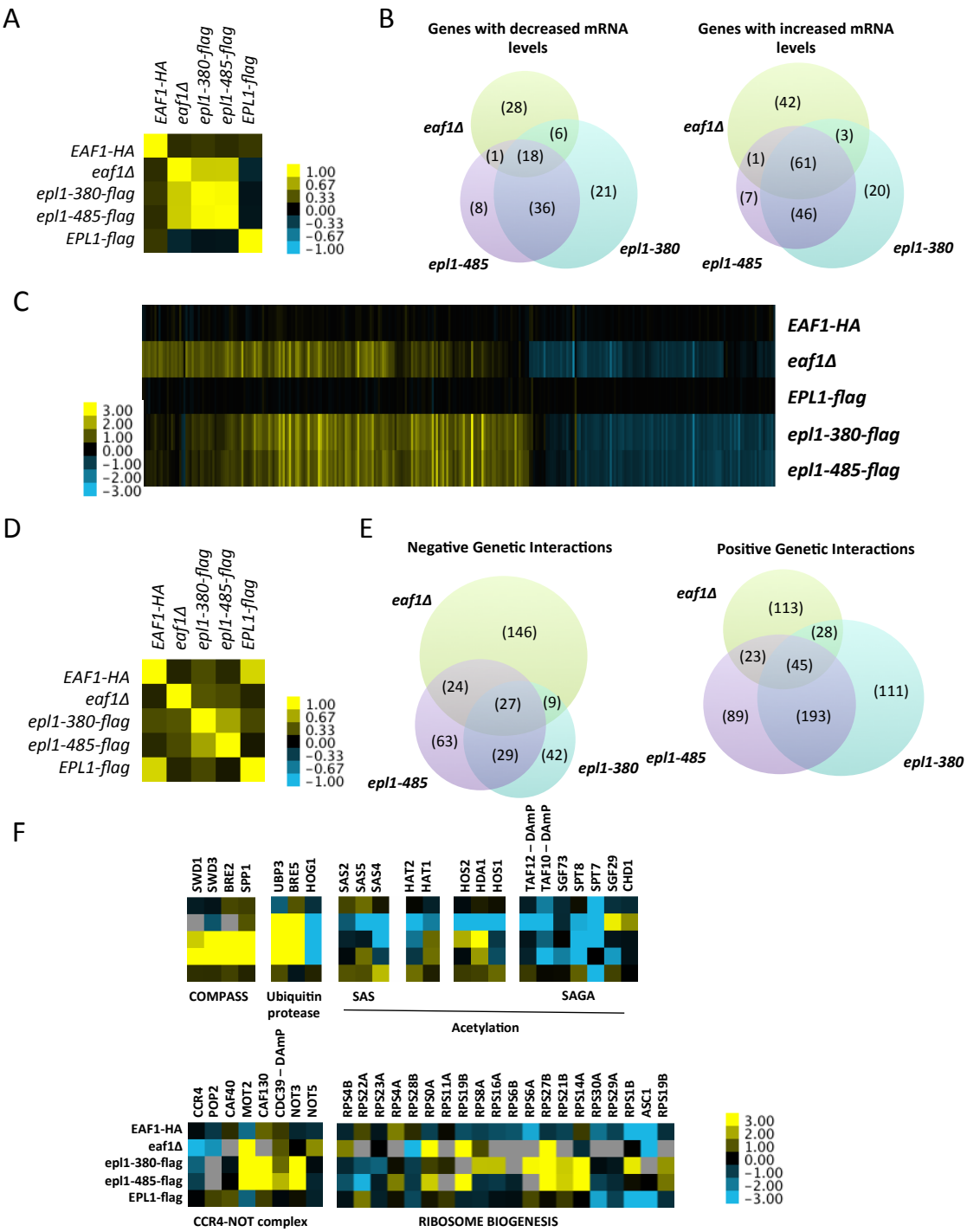
A
EAF1-HA
eaf1Δ
epl1-380-flag
epl1-485-flag
EPL1-flag
1.00
0.67
0.33
0.00
−0.33
−0.67
−1.00
B
Genes with decreased mRNA levels
eaf1Δ
epl1-485
epl1-380
(28)
(6)
(1)
(18)
(21)
(8)
(36)
Genes with increased mRNA levels
(42)
(3)
(1)
(61)
(20)
(7)
(46)
C
EAF1-HA
eaf1Δ
EPL1-flag
epl1-380-flag
epl1-485-flag
3.00
2.00
1.00
0.00
−1.00
−2.00
−3.00
D
E
Negative Genetic Interactions
(146)
(24)
(27)
(9)
(63)
(29)
(42)
Positive Genetic Interactions
(113)
(28)
(23)
(45)
(111)
(89)
(193)
F
SWD1
SWD3
BRE2
SPP1
UBP3
BRE5
HOG1
SAS2
SAS5
SAS4
HAT2
HAT1
HOS2
HDA1
HOS1
TAF12 – DAmP
TAF10 – DAmP
SGF73
SPT8
SPT7
SGF29
CHD1
COMPASS
Ubiquitin protease
SAS
SAGA
Acetylation
CCR4
POP2
CAF40
MOT2
CAF130
CDC39 – DAmP
NOT3
NOT5
RPS4B
RPS22A
RPS23A
RPS4A
RPS28B
RPS0A
RPS11A
RPS19B
RPS8A
RPS16A
RPS6B
RPS6A
RPS27B
RPS21B
RPS14A
RPS30A
RPS29A
RPS1B
ASC1
RPS19B
CCR4-NOT complex
RIBOSOME BIOGENESIS

Figure 4.3 Genetic and gene expression analysis revealed similarities and distinctions between *eaf1* and *epl1* mutants
(A) Spearman correlation of gene expression profile of wildtypes and mutant strains. (B) Venn diagram of overlap in up-regulated and down-regulated genes in *eaf1Δ, epl1-485,* and *epl1-380.* (C) Unsupervised hierarchical cluster matrix of *eaf1Δ* and *epl1 C-Δ* mutants with their respective up- and down- regulated genes. Yellow indicates upregulated genes, and blue represents downregulated genes. (D) Spearman correlation of genetic interaction profiles of wildtypes and mutant strains. Unsupervised hierarchical cluster matrix of *eaf1Δ* and *epl1 C-Δ* mutants with the respective positive and negative genetic interactions. (E) Venn diagram of shared negative genetic interactions and shared positive genetic interactions between *eaf1Δ, epl1-485,* and *epl1-380.* (F) Genetic interaction profiles of *eaf1Δ* and *epl1 C-Δ* with indicated complexes. Blue indicates aggravating interactions, yellow represents alleviating interactions, and gray denotes missing data.

Next, the mutant strains carrying *eaf1*Δ or *epl1-CΔ* derivatives were analyzed by Epistatic Mini Array Profiling (E-MAP), a technique that enables quantitative measurements of aggravating and alleviating genetic interactions against a library of 1,536 mutant genes involved in transcription, RNA processing, and chromatin biology (Schuldiner *et al.* 2006). Similar to the expression data, correlation analysis of the genetic profiles revealed that the two *epl1-CΔ* mutants clustered closer to each other than to the *eaf1*Δ mutant (Figure 4.3D). In line with growth differences between *epl1-485* and *epl1-380,* the two alleles genetically interact with distinct subsets of genes (Negative genetic interactions: p-value = 1.36E-92, Positive genetic interactions: p-value = 2.03E-207) (Figure 4.3E).

E-MAP analysis also revealed similarities and differences between *eaf1*Δ and *epl1-CΔ* mutants. For instance, negative genetic interactions existed for both sets of mutants with genes involved in the SAS, HAT2 and SAGA histone acetyltransferase (Figure 4.3F) (Krogan *et al.* 2004; Mitchell *et al.* 2008). In contrast, *epl1-CΔ* and *eaf1* mutants differed in their interactions with genes encoding for COMPASS, CCR4-NOT complex and subunits of various histone deacetylases (Figure 4.3F). Despite having mostly alleviating interactions with ribosomal subunit encoding genes, both negative and positive interaction existed for

eaf1Δ and *epl1-CΔ* (Figure 4.3F). Interestingly, all three mutants display strong alleviating interaction with *BRE5* and *UBP3,* genes encoding for a ubiquitin protease implicated in degradation of ribosomal proteins and DNA damage response (Figure 4.3F) (Kraft *et al.* 2008; Bilsland *et al.* 2007). Collectively, our large-scale genetic and gene expression analyses demonstrated that *EAF1* and *EPL1* have overlapping yet divergent functions, which is not easily reconciled with these proteins acting similarly in regulating picNuA4 levels and activity.

4.3.4 The Eaf1 HSA Domain was Required for NuA4 Stability and Function

Given the drastic decrease in NuA4 levels in *eaf1Δ* cells, we asked whether specific domains of EAF1 were important for the stability of Epl1 and the NuA4 complex. To this end, internal truncation alleles of *EAF1* lacking the HSA and/or SANT domains were created (Figure 4.4A). While cells lacking the Eaf1 HSA domain had phenotypes similar to deletion of *EAF1,* including defects in both H4 and H2A.Z acetylation and sensitivity to genotoxic stress, cells lacking the Eaf1 SANT domain had histone acetylation levels and growth fitness comparable to those of wildtype cells (Figure 4.4B and Figure 4.4C). Given that dissociation of the NuA4 complex likely was responsible for the drastic phenotype in *eaf1Δ*, it prompted us to examine NuA4 stability in the *EAF1* internal deletion mutants. Consistent with the phenotypic similarity between *eaf1Δ* and *eaf1 HSAΔ,* loss of the HSA domain alone led to the dissociation of the NuA4 complex, indicating that the HSA domain of Eaf1 is important for NuA4 stability (Figure 4.4D). On the other hand, we were able to purify the complete NuA4 complex in the absence of the Eaf1 SANT domain (Figure 4.4D). Samples from the small-scale TAP purification were further analyzed by western blotting to confirm the presence of

Epl1-TAP in all strains. Similar to before, we observed a decrease in Epl1 level in the absence of *EAF1*. Furthermore, strains with the HSA internal deletion also exhibited a similar decrease in Epl1 levels, suggesting that the HSA domain is important for full-length Epl1 stability (Figure 4.4E). In agreement with the results from the silver stain, which demonstrated that the HSA domain was required for NuA4 and picNuA4 stability, we could not detect any Epl1-associated Esa1 in cells lacking the Eaf1 HSA domain (Figure 4.4E). Similar to before, experiments on whole cell extracts confirmed that the stability of the NuA4 catalytic module was dependent on the HSA domain and to a lesser extent on the SANT domain (Figure 4.4F).

Our results placed the Eaf1 HSA domain and the Epl1 C-terminus at the center of NuA4 complex formation and function. As many lines of evidence, including our own, suggest that the Epl1 protein is anchored to Eaf1 through its C-terminus, we would predict that truncation the Epl1 would suppress the *eaf1 HSAΔ* growth (Auger *et al.* 2008; Szerlong *et al.* 2008). Loss of the Eaf1 HSA domain led to a similar growth defect compared to a complete loss of Eaf1 (Figure 4.5A). Truncating the C-terminus of Epl1 in either an *eaf1Δ* background or an *eaf1 HSAΔ* background rescued the growth impediment to levels similar to the *epl1-CΔ* single mutant (Figure 4.5A). Taken together, our observations suggested that the truncation of Epl1 C-terminus partially suppressed *eaf1-HSAΔ* defects.

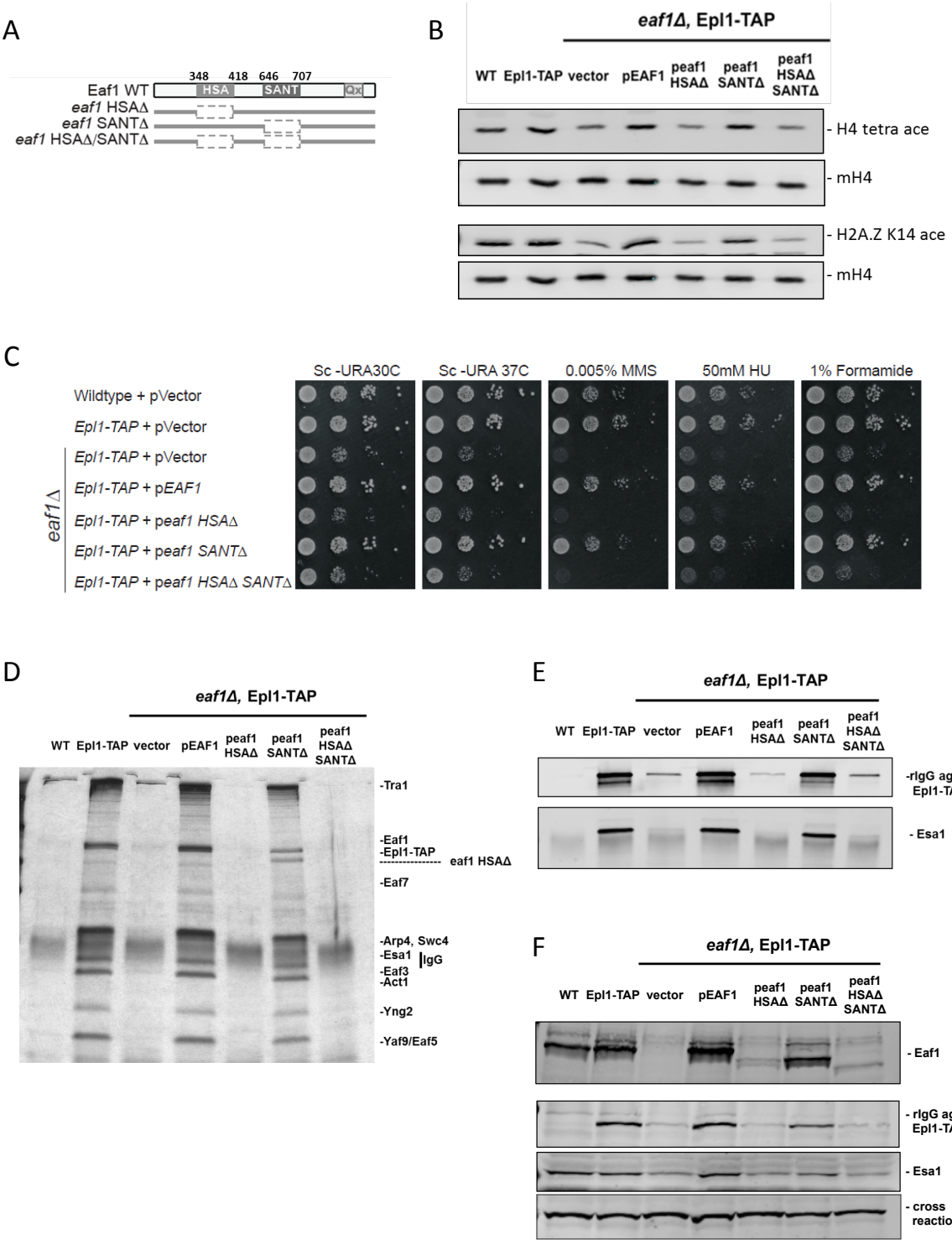
A
348 418 646 707
Eaf1 WT
HSA
SANT
Qx
eaf1 HSAΔ
eaf1 SANTΔ
eaf1 HSAΔ/SANTΔ
B
eaf1Δ, Epl1-TAP
WT Epl1-TAP vector pEAF1 peaf1 HSAΔ peaf1 SANTΔ peaf1 HSAΔ SANTΔ
- H4 tetra ace
- mH4
- H2A.Z K14 ace
- mH4
C
Sc -URA30C
Sc -URA 37C
0.005% MMS
50mM HU
1% Formamide
Wildtype + pVector
Epl1-TAP + pVector
Epl1-TAP + pVector
Epl1-TAP + pEAF1
Epl1-TAP + peaf1 HSAΔ
Epl1-TAP + peaf1 SANTΔ
Epl1-TAP + peaf1 HSAΔ SANTΔ
eaf1Δ
D
eaf1Δ, Epl1-TAP
WT Epl1-TAP vector pEAF1 peaf1 HSAΔ peaf1 SANTΔ peaf1 HSAΔ SANTΔ
-Tra1
-Eaf1
-Epl1-TAP
eaf1 HSAΔ
-Eaf7
-Arp4, Swc4
-Esa1
IgG
-Eaf3
-Act1
-Yng2
-Yaf9/Eaf5
E
eaf1Δ, Epl1-TAP
WT Epl1-TAP vector pEAF1 peaf1 HSAΔ peaf1 SANTΔ peaf1 HSAΔ SANTΔ
-rIgG against Epl1-TAP
- Esa1
F
eaf1Δ, Epl1-TAP
WT Epl1-TAP vector pEAF1 peaf1 HSAΔ peaf1 SANTΔ peaf1 HSAΔ SANTΔ
- Eaf1
- rIgG against Epl1-TAP
- Esa1
- cross reaction

Figure 4.4 The Eaf1 HSA domain was required for NuA4 stability and function
(A) Schematic representation of *EAF1* internal region deletions: HSAΔ, SANTΔ, and HSAΔ/SANTΔ. (B) Whole cell extracts of indicated strains were analyzed by protein blotting with anti-H4 tetra- or anti-H2A.Z K14 acetylation antibodies. Antibodies against H4 were used as a loading control. (C) Ten-fold serial dilutions of the indicated strains were plated onto Sc –URA media containing the indicated genotoxic agents. (D) TAP purification of NuA4 using Epl1-TAP demonstrated disassociation of NuA4 in *eaf1 HSAΔ*. Purified fractions from indicated strains were loaded onto a 4-20% gradient SDS-PAGE gel and visualized by silver staining. Bands corresponding to NuA4 subunits are indicated on the left. Untagged Epl1 was used as a negative control. (E) TAP purifications of indicated strains were loaded on western to verify Epl1-TAP pull down and Esa1 association. IgG and anti-Esa1 antibodies were used to detect Epl1-TAP and Esa1 respectively. (F) Whole cell extract were analyzed for total Epl1-TAP, Eaf1 and Esa1 level by protein blotting. IgG unspecific band was used as loading control.

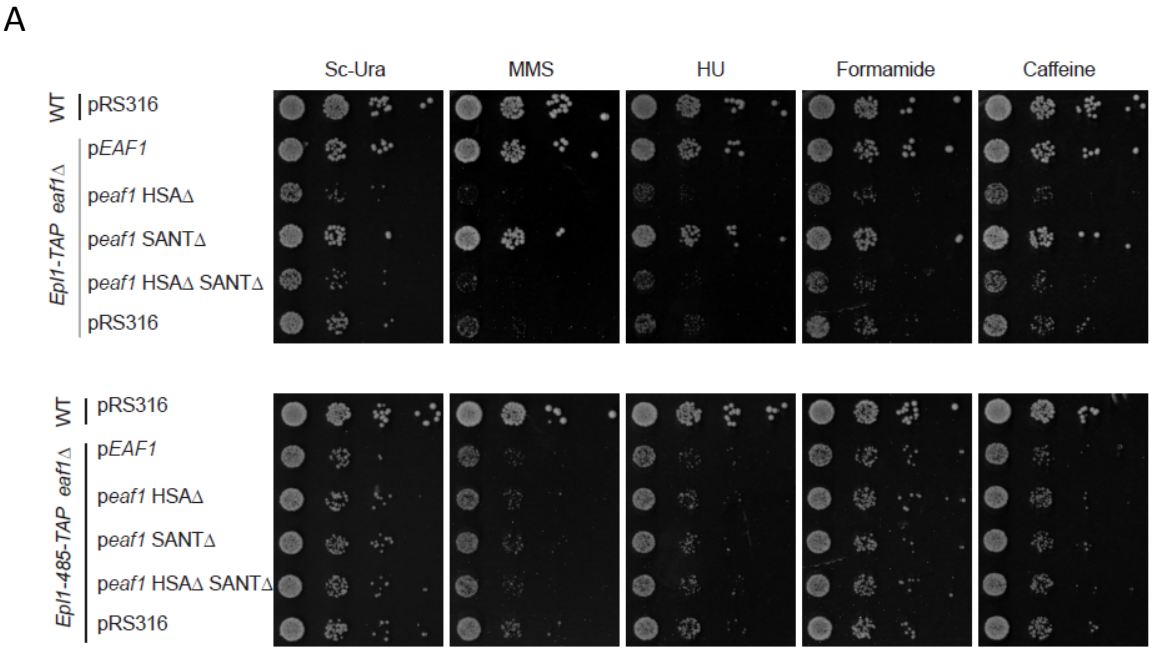

Figure 4.5 e*pl1-CΔ* truncation was epistatic to *eaf1* internal truncation mutants
Ten-fold serial dilutions of the indicated strains were plated onto Sc –URA media containing the indicated genotoxic agents.

4.3.5 Epl1 C-terminus was Required for NuA4 Association with Chromatin

To gain a better understanding of picNuA4 function in the context of the *epl1-CΔ* strain, genome-wide ChIP-on-chip experiments was performed on Epl1-TAP, epl1-485-TAP, and epl1-380-TAP. We expected that the Epl1-TAP occupancy profile would be representative of binding sites for both NuA4 and picNuA4 whereas the occupancy profile of Epl1 lacking the C-terminus (485 and 380) would be representative of sites enriched for picNuA4. Validating our ChIP-on-chip approach, wildtype Epl1 was highly enriched over ribosomal genes as previous reported (Figure 4.6A). In agreement with our H4 acetylation ChIP-qPCR and RT-qPCR data, Epl1 lacking the C-terminus was significantly depleted from the majority of ribosomal genes previously enriched for Epl1-TAP (Figure 4.6B). Furthermore, we found few sites besides ribosomal protein genes to be enriched with NuA4 under our selection criteria. This is similar to previous efforts at mapping NuA4 occupancy sites through HA-Esa1 as a representative subunit of NuA4 (Reid *et al.* 2000). Surprisingly, Epl1 occupancy profiles in epl1-485-TAP and epl1-380-TAP strains yielded few significantly enriched sites across the genome. This result suggested that despite an increase in picNuA4 levels and normal H4 acetylation in the C-terminus truncation mutants, picNuA4 was transiently associated with chromatin under these circumstances.

Subsequently, we used bulk fractionation assay to examined picNuA4 occupancy in *epl1-CΔ* mutants as another measure of picNuA4 association to chromatin. Using centrifugation-based sucrose gradient, chromatin-bound proteins (pellet fraction) were separated from whole cell lysate (supernatant fraction). In the wildtype strain, almost all of the Epl1-TAP in the cell fractioned tightly with the chromatin pellet leaving no detectable amounts of Epl1-TAP in

the supernatant fraction (Figure 4.6C). In addition, despite the decreased levels of Epl1-TAP in an *eaf1Δ* background, Epl1-TAP was enriched in the chromatin fraction with no detectable amounts in the supernatant (Figure 4.6C). Interestingly, upon truncation of the Epl1 C-terminus, a shift in the localization of epl1-485-TAP and epl1-380-TAP was observed. Instead of being highly enriched in the chromatin pellet, the levels of chromatin-bound epl1-CΔ proteins were lower than that of wildtype (Figure 4.6C). Furthermore, there were low levels of epl1-485-TAP and epl1-380-TAP found in the supernatant fraction (Figure 4.6C). Despite a decrease in the levels of chromatin-associated Epl1 in the truncation mutants, the levels of acetylated H4 in chromatin remained the same (Figure 4.6C). Taken together with our genome-wide occupancy profiles, the data suggested that the picNuA4 released in *epl1-CΔ* strains was still sufficient to acetylate H4 in chromatin despite being loosely associated.

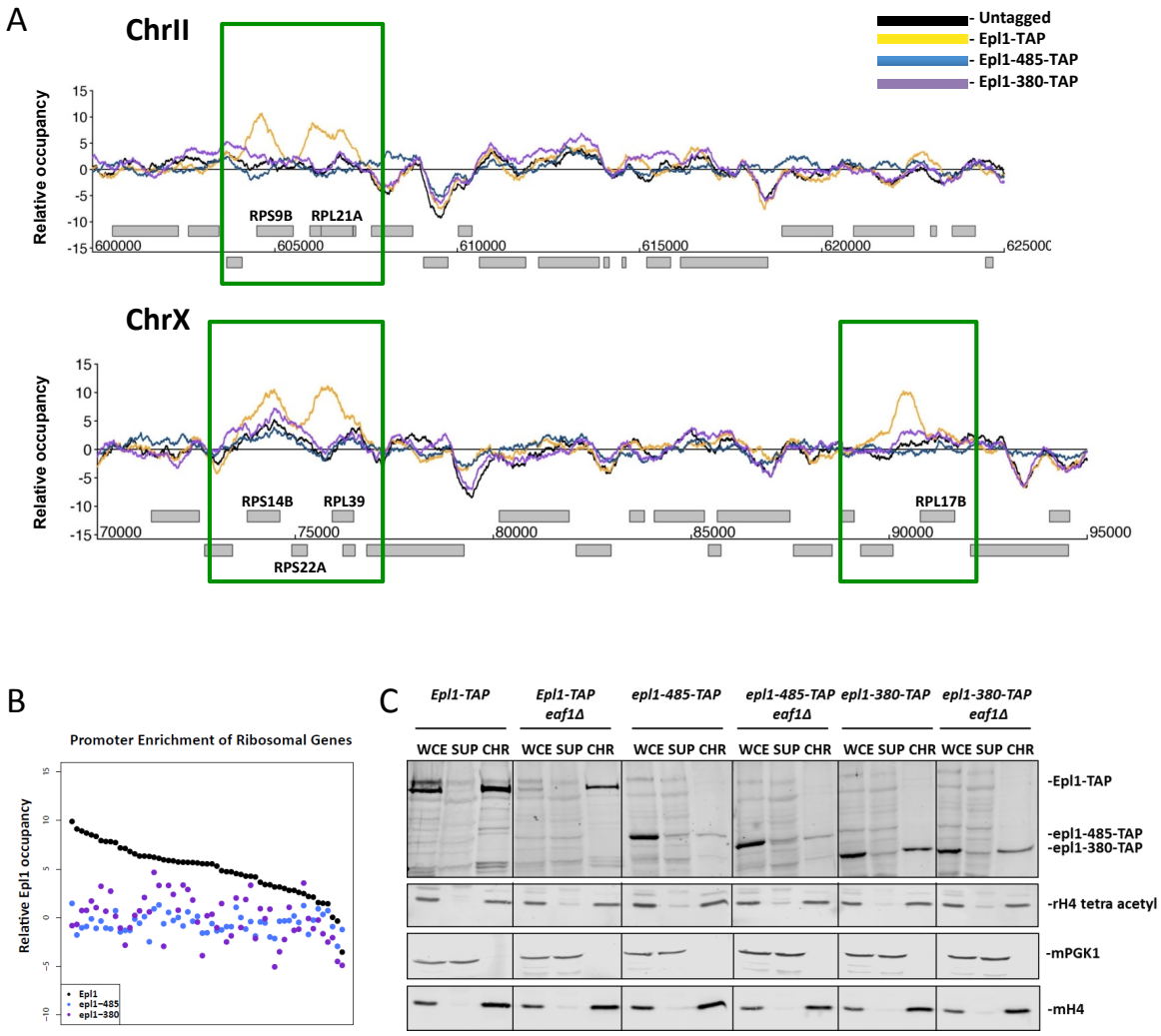

Figure 4.6 Epl1 C-terminus was required for NuA4 association to chromatin
(A) ChIP-chip profile of NuA4 and picNuA4 bound regions in *EPL1-TAP, epl1-485,* and *epl1-380.* Sample genomic regions were plotted for ChrIII and ChrX along the x-axis against the relative occupancy of Epl1 normalized over input. ORFs are indicated as light gray rectangles above the x-axis for Watson genes and below the x-axis for Crick genes. (B) Epl1 C-terminus was required for NuA4 association to ribosomal genes. Relative occupancy of Epl1 over input signal at promoters of ribosomal genes. (C) Loss of Epl1 C-terminus reduced Epl1 association to chromatin. WCE, whole cell extract; SUP, supernatant; CHR, chromatin pellet. The relative amounts of Epl1-TAP and H4 tetra acetylation was determined by immunoblotting. In each case, the fractionation efficiency was judged by the levels of the control proteins, H2A and Pgk1, found in the chromatin fraction and the supernatant fraction, respectively.

4.4 Discussion

This study explored the functional and structural connection between two subunits of the NuA4 HAT complex in *Saccharomyces cerevisiae*. Our experiments focused on dissecting the circuitry between of the Eaf1 protein and the Epl1 C-terminus in regulating NuA4 function and composition. Genome-wide expression and genetic interaction data revealed an expected set of common requirements, but more surprisingly, also remarkably different phenotypic and functional consequences. Detailed biochemical examination revealed that full length Epl1 did not support the formation of a detectable levels picNuA4 complex in the absence of Eaf1. However, deletion of the Epl1 C-terminus restored and stabilized a functional picNuA4 complex in the absence of *EAF1*, suggesting that interaction between the Epl1 C-terminus and Eaf1 may be necessary for complex stability. Furthermore, Eaf1 was important for maintaining the protein level of individual picNuA4 subunits, including Epl1. We subsequently determined that the HSA domain of Eaf1, the proposed interaction domain of Eaf1 with the Epl1 C-terminus, was required for picNuA4 formation and function. Despite being sufficient to restore global H4 acetylation levels in an *eaf1Δ* background, the picNuA4 released in *epl1-CΔ* strains displayed reduced interaction with chromatin. Taken together, our combination of whole-genome investigation and detailed biochemical analysis revealed unexpected differences and similarities of *epl1-CΔ* and *eaf1Δ* in NuA4 complex stability and HAT activity.

The present work shed light on two existing and somewhat conflicting models of NuA4 structural integrity. The first model suggests that upon deletion of the scaffolding Eaf1

protein, the various submodules of the NuA4 complex remain intact, leaving behind a functional and stoichiometric picNuA4 complex sufficient for un-targeted chromatin acetylation (Auger *et al.* 2008). The alternative model suggests that Eaf1 is essential for NuA4 complex integrity and that upon deletion of *EAF1,* there is a significant reduction in the level of NuA4 in the cell (Mitchell *et al.* 2008). Both models place Eaf1 at the center of NuA4 function through a combination of biochemical and genetic means. However, the defining difference between the two models centers on the importance of Eaf1 in regulating the quantitative balance between the various submodules, and in particular picNuA4. In principle, the data presented in this chapter supports the co-existence of both models. The strong decrease of H4 acetylation in the *eaf1Δ* mutant suggests that the released picNuA4 had compromised HAT activity (Krogan *et al.* 2004; Kobor *et al.* 2004). Supported by the NuA4 purification experiments, we observed a significant reduction in the picNuA4 subunits that co-purified with Epl1-TAP when *EAF1* was deleted. However, in contrast to the *eaf1Δ* mutant, the *eaf1Δ epl1-CΔ* mutants have a fully active minimal picNuA4 capable of maintaining basal H4 acetylation levels, suggesting that the catalytic module of NuA4 exists as a functional and independent entity. Consistent with published *in vitro* data, this suggested that the picNuA4 formed under this condition is capable of untargeted chromatin acetylation of the native picNuA4 complex (Boudreault *et al.* 2003).

The work presented in this dissertation consolidates the two prevailing models in the field: we found that while *EAF1* is central for NuA4 stability and function, removal of Epl1 C-terminus was sufficient to restore the growth and H4 acetylation defects of *eaf1Δ*. Furthermore, while both models suggest that loss of Eaf1 or loss of Epl1 C-terminus equally

liberate picNuA4, the data presented in this chapter are difficult to reconcile with such a simple model. Gene expression array analysis identified both overlapping and divergent gene expression clusters between the mutants. Similarly, genetic epistasis analysis uncovered unique genes required to support growth of *eaf1Δ* and *epl1-CΔ*. Taken together with our biochemical examination, our data supports that these two genetic manipulations led to distinct consequences in NuA4 structure and function.

Our combinatorial analysis of cells lacking Eaf1 and the Epl1 C-terminus revealed a novel functional relationship between these two key components of the NuA4 HAT complex. In line with previously reports, cells lacking *EAF1* displayed decreased fitness under genotoxic stress and reduced global H4 acetylation as a result of the dissociation of the HAT complex (Kobor *et al.* 2004; Mitchell *et al.* 2008; Boudreault *et al.* 2003; Auger *et al.* 2008; Babiarz *et al.* 2006). This effect however, was due to the presence of the Epl1 C-terminus, as removal of the C-terminus domain was sufficient to restore the bulk H4 acetylation and growth phenotype of *eaf1Δ*. Specifically, analytical-scale purification experiments identified the stable assembly of picNuA4 upon removal of the Epl1 C-terminus as the likely mechanism underlying the suppression in *eaf1Δ epl1-CΔ* double mutants. Importantly, we demonstrated that Eaf1 is only required for picNuA4 function and stability in the presence of full length Epl1 protein, highlighting a potential regulatory role of the Epl1-C terminus in picNuA4 formation. The inverse relationship between the stability of picNuA4 subunits and the presence of Eaf1 in the cell suggests that Eaf1 may also have an important, yet likely indirect, regulatory role in the stability of the NuA4 catalytic module. In line with this potential role of Eaf1, reduced levels of the Eaf3/5/7 RpdS-associated module have been

reported in the absence of *EAF1* (Rossetto *et al.* 2014). Detailed domain deletion analysis of Eaf1 identified its HSA domain as a key player in the stability of picNuA4 as deletion of the Eaf1 HSA domain led to growth and global H4 acetylation defects. Similarly, *eaf1 HSAΔ* cells also exhibited reduced picNuA4 stability akin to the *eaf1Δ* mutant, while loss of the Eaf1 SANT domain had little effect on cell fitness, NuA4 stability and H4 acetylation. As a whole, the *eaf1 HSAΔ* mutant phenocopied the *eaf1Δ* mutant suggesting that the HSA domain was the key region required for picNuA4 function and stability. Taken together, our data suggested that the interface between the Eaf1 HSA domain and the Epl1 C-terminus is required for maintaining the equilibrium of active NuA4 and picNuA4 in the cell.

Taking advantage of the release of a functional picNuA4 upon Epl1 C-terminal truncation, we examined the genome-wide binding profile of NuA4 and picNuA4. Similar to previous efforts to map NuA4, Epl1 was highly enriched over genes encoding for ribosomal proteins (RP) (Reid *et al.* 2000). In agreement with the current model underlying the functional differences between NuA4 and picNuA4, the peaks associated with RP promoters likely are a result of the targeted recruitment of NuA4 complex by activators such as Rap1 or Abf1 (Reid *et al.* 2000). Adding to our gene-specific analysis of H4 enrichment and mRNA levels at *RPL19b, RPS11B,* and *RPS3,* loss of Epl1 peaks genome-wide at RP promoters in *epl1-CΔ* confirmed that these peaks corresponded to NuA4 binding and not picNuA4. Distinct from NuA4, picNuA4 is proposed to be diffused over the genome and is responsible for basal acetylation (Boudreault *et al.* 2003; Auger *et al.* 2008; Reid *et al.* 2000). Therefore, the lack of distinct peaks other than the RP peaks in the wildtype Epl1 binding profile suggested that picNuA4 was either lowly enriched or transiently associated with the rest of the genome.

Despite the dramatic increase in picNuA4 levels in the cell upon Epl1 C-terminus truncation, there were few novel sites of Epl1-CΔ binding genome-wide.

Interestingly, bulk chromatin association assays provided novel insight into the cellular changes occurring in these mutant strains when the normal equilibrium between NuA4 and picNuA4 levels was disturbed. Upon C-terminal truncation of Epl1, there was a shift from predominantly chromatin-associated Epl1 to equal levels of chromatin-bound and free-floating picNuA4 in these cells. However, the level of acetylated H4 in chromatin remained the same, suggesting that the picNuA4 that remained associated with chromatin is sufficient to maintain basal acetylation. As we observed an increase in picNuA4 levels in *epl1-CΔ* cells, it is tempting to speculate that non-chromatin bound picNuA4 formed under these circumstances might erroneously acetylate non-chromatin specific targets, thus leading to the dramatic growth defects in these mutants. This would not be unexpected as NuA4 is well documented to have numerous non-chromatin acetylation functions (Mitchell *et al.* 2011; Downey *et al.* 2014; Lin *et al.* 2009).

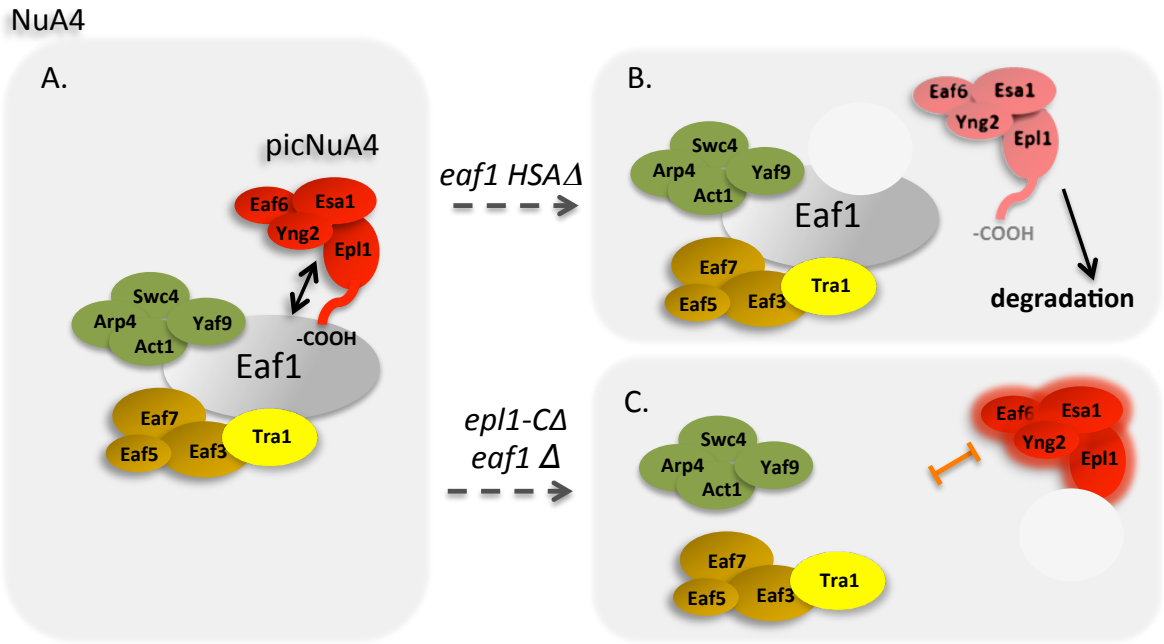

Figure 4.7 Model for the regulatory mechanisms of Eaf1 and Epl1 C-terminus in picNuA4 stability
(A) NuA4 and picNuA4 co-exist in wildtype cells. picNuA4 catalytic module associates with NuA4 through the Epl1 C-terminus and Eaf1 scaffold protein. (B). Deletion of Eaf1 and its HSA domain lead to reduced picNuA4 levels, possibly mediated by a degradation pathway. (C) Removal of the Epl1 C-terminus in an *eaf1Δ* background restores function on chromatin and increases cellular picNuA4 level.

Consolidating this set of multifaceted data, we put forth the following model: adding to previous work suggesting that picNuA4 docks onto Eaf1 through the Epl1 C-terminus, we propose that in addition to this physical interaction, the Eaf1 HSA domain and Epl1 C-terminus are key regulators important for maintaining the cellular balance of NuA4 and picNuA4 (Figure 4.7). We demonstrated that without Eaf1 or its HSA domain, the picNuA4 subunits (Yng2 and Esa1) that dock upon the Epl1 EPcA domain for stability no longer interacts with Epl1. It is tempting to propose that, perhaps, the interaction between Eaf1 (specifically HSA domain) and Epl1 C-terminus is required for Epl1 and picNuA4 stability (Figure 4.7B). It would be interesting to examine whether Eaf1 is indirectly involved in regulating picNuA4 stability through an ubiquitin degradation pathway, especially in light of

the genetic connection with the Ubp3/Bre5 ubiquitin protease highlighted by E-MAP. Secondly, our data also demonstrated that upon truncation of the Epl1 C-terminus, picNuA4 function and stability was restored in an *eaf1Δ* background (Figure 4.7C). Moreover, there was an increase in the cellular levels of picNuA4 in *epl1-CΔ* cells. Our data underscores the regulatory relationship between Eaf1 and Epl1 C-terminus in picNuA4 formation. Taken together, the evidence presented in this chapter supports a model where the stability and levels of picNuA4 is regulated by the Epl1 C-terminus, and that this regulation occurs in concert with the central scaffold protein, Eaf1.

Chapter 5: Conclusion

Since the identification of DNA as the genetic material, immense strides have been made in understanding how DNA stores information and how the information is interpreted. We now recognize that it is not the DNA sequence alone, but also how the DNA is packaged that regulates our cells' ability to read and utilize the genetic information. Realizing that chromatin structure regulates the accessibility of the information contained within DNA was a key breakthrough in the field of chromatin biology. Decades of intense research highlighted the multiple mechanisms that the cell has evolved to package and regulate access to the DNA sequence. Scientists are now embarking on an exciting journey to tease apart how histone modifications, chromatin-remodeling complexes, histone variants, and histone chaperones work together to coordinate the many biological processes that are dependent on DNA.

My dissertation adds to our current understanding of the coordinated activities of the many chromatin-modifying factors in our cells. Spanning multiple chromatin-modifying mechanisms in *S. cerevisiae*, this dissertation examines the functional relationships between histone chaperones, histone variants, post-translational modifications, and chromatin-modifying complexes. More specifically, I explored the mechanistic link between the Asf1 histone chaperone and the SWR1-C chromatin-remodeling complex at subtelomeric regions. I determined that Asf1-dependent H3K56 acetylation was an integral component of H2A.Z nucleosome occupancy. Moreover, I characterized key players in NuA4 histone acetyltransferase biology while at the same time identifying crucial domains that regulate the dynamic equilibrium of its structure and HAT function.

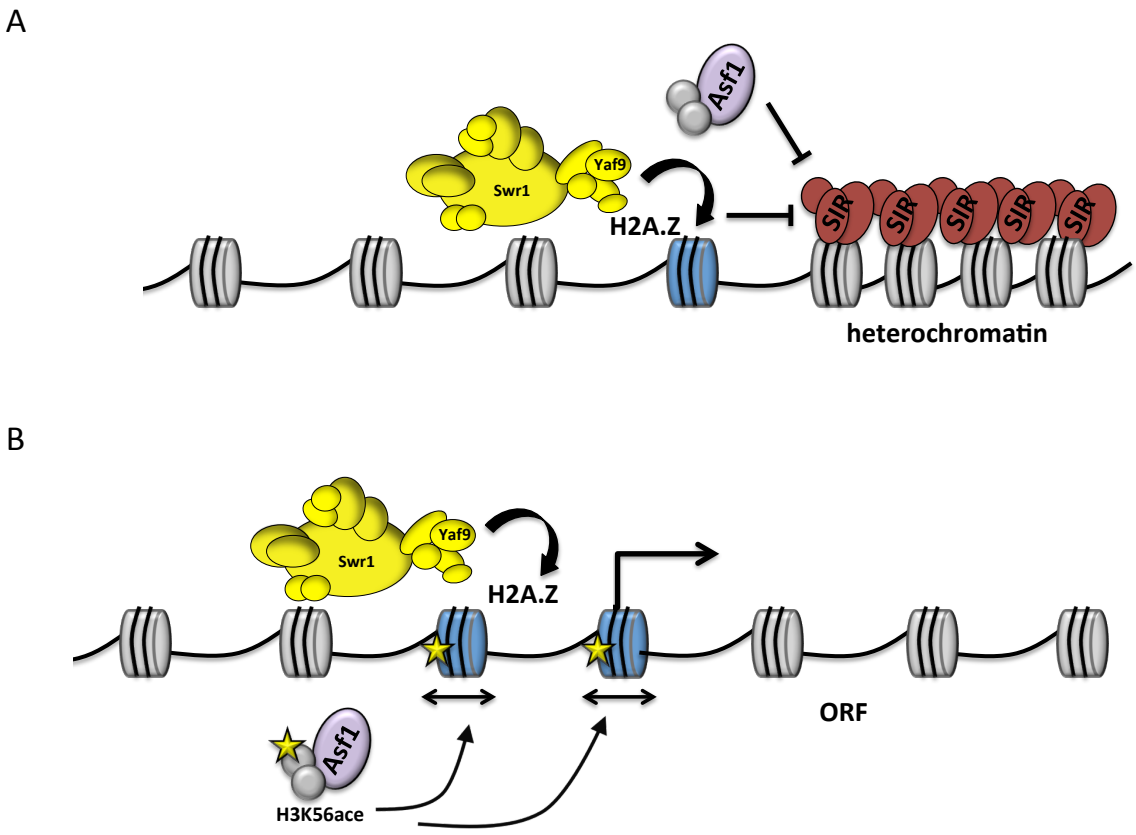

Figure 5.1 Model for Asf1 and SWR1-C interactions in *Saccharomyces cerevisiae*
(A) Asf1 cooperates with SWR1-C to restrict spread of heterochromatin. (B) Asf1-dependent H3K56 acetylation contributes to H2A.Z nucleosome dynamics at gene promoters.

Our understanding of the broad functions of the Asf1 H3/H4 histone chaperone has come a long way since its identification in an anti-silencing screen almost two decades ago (Le *et al.* 1997; Singer *et al.* 1998). In addition to delivering H3/H4 heterodimers to chromatin-remodelers and chaperones for nucleosome assembly, we are now starting to appreciate the functional connections between Asf1 and chromatin-modifying complexes regulating the chromatin landscape. In Chapter 2 of this dissertation, I described one such interaction between Asf1 and the SWR1-C H2A.Z-depositing complex. Using Yaf9 as a representative

subunit of SWR1-C activity at heterochromatin, I found that Asf1 cooperated with the entire SWR1-C to maintain three heterochromatin boundaries on ChrIII R by preventing the spread of SIR complexes onto nearby subtelomeric regions (Figure 5.1). While we know H2A.Z is required for preventing heterochromatin spread at the boundaries of heterochromatin and euchromatin, the exact mechanism of the cooperative activities between Asf1 and SWR1-C at telomeres remains to be determined (Meneghini *et al.* 2003). It is likely that Asf1's role at heterochromatin lies within its key function as a chaperone for H3K56 acetylation, as H3K56 mutants have impaired telomeric silencing in reporter assays and native telomeres (Xu *et al.* 2007; Yang *et al.* 2008; Miller *et al.* 2008). However, while H3K56 mutants exhibit normal telomere occupancy of Sir2, Sir3 and Sir4, I observed increased Sir2 levels at telomeres and spread of Sir2 into subtelomeres in *asf1Δ yaf9Δ* cells (Xu *et al.* 2007). Interestingly in *S. pombe,* Asf1/HIRA cooperates with the Clr6 HDAC complex to maintain heterochromatin silencing and associates with SHREC (Snf2/HDAC repressor complex) to promote nucleosome occupancy at heterochromatic loci (Yamane *et al.* 2011; Kaufman 2011). While these activities in fission yeast are dependent on HP1 and H3K9me3, neither of which exists in *S. cerevisiae*, it alludes to the existence of a similar heterochromatin regulatory pathway involved in the cooperative activities between Asf1 and SWR1-C in *S. cerevisiae.*

In addition to Asf1's role at heterochromatic regions, I found that Asf1 also contributed to maintaining H2A.Z occupancy at euchromatic and subtelomeric gene promoters. This finding is in line with recent publications demonstrating that Asf1 works with chromatin-modifying complexes in a variety of biological contexts. For example, Asf1 cooperates with the SWI/SNF complex to displace nucleosomes at heat shock gene promoters (Erkina and Erkine

2014). Asf1 also recruits chromatin-modifying complexes, such as the SAS complex and the Set2 methyltransferase complex, to promote H4K16 acetylation and H3K36 trimethylation, respectively (Lin *et al.* 2010; Osada *et al.* 2005). Given Asf1's role in the assembly and disassembly of nucleosomes during DNA replication and transcription, it is likely other chromatin-modifying complexes may be active participants in these biological processes.

The genetic relationship between genes encoding for SWR1-C and *ASF1* also alludes to a functional connection that extends beyond heterochromatin maintenance. As I demonstrated in Chapter 2, cells lacking Asf1 and a component of SWR1-C are particularly sensitive to cold temperatures and genotoxic agents. The synergistic growth defect in cells lacking functional components of both chromatin-modifying factors suggested that SWR1-C and Asf1 have additional redundant functions. Indeed, both Asf1 and H2A.Z contribute to chromosome positioning at the nuclear periphery. Asf1 and H3K56 acetylation are crucial for the association of yeast telomeres to the nuclear periphery and long-range interactions between heterochromatic loci (Hiraga *et al.* 2008; Miele *et al.* 2009). H2A.Z's role in transcriptional memory appears to be tightly linked to its role in regulating the nuclear-periphery localization of repressed genes such as *INO1* and *GAL1* (Brickner *et al.* 2007). However, the connection between nuclear anchoring and transcriptional memory remains controversial as other has found that H2A.Z is not required for transcriptional memory of *GAL1* (Halley *et al.* 2010; Kundu and Peterson 2010). Nevertheless, more experiments are needed to address whether H2A.Z and Asf1 are contributing to the three-dimensional organization of chromosomes independently or redundantly.

Taken together, our current understanding of Asf1 would suggest that this histone chaperone has two important functions within the cell. Primarily, Asf1provides free histones for nucleosome assembly and receives H3/H4 heterodimers during nucleosome disassembly. Secondly, it is tempting to speculate that Asf1 is also a key player in establishing distinct chromatin neighbourhoods by recruiting additional chromatin-modifying complexes such as HATs, histone-methyltransferases and chromatin remodelers. It remains to be seen whether the latter function is directly connected to Asf1's primary role as a histone chaperone.

In Chapter 2 and 3 of this dissertation, I identified that H3K56 acetylation by Rtt109 was required for maintaining H2A.Z levels at discreet regions of subtelomeric and euchromatic gene promoters. A histone modification that requires binding of the H3/H4 heterodimer by Asf1histone chaperone, loss of H3K56 acetylation resulted in global changes in H2A.Z occupancy and position. At a subset of gene promoters, H2A.Z was either completely lost or the levels of the histone variant were reduced. At other gene promoters, the position of H2A.Z peaks shifted with respect to the TSS when H3K56 could no longer be acetylated. Our genome-wide approach in Chapter 3 led us to propose that acetylation of H3K56 was crucial in maintaining both H2A.Z levels and specific positioning of H2A.Z at promoters. Several lines of evidence supported a role for H3K56 acetylation in regulating nucleosome positioning. When H3K56 acetylation was first identified in *S. cerevisiae*, it was proposed that this PTM promotes nucleosome instability by loosening the DNA-histone interaction based on its location at the entry and exit point of DNA (Xu *et al.* 2007; Neumann *et al.* 2009). Subsequent structural analyses showed that binding of DNA to the modified tetramer $(H3K56ace/H4)_2$ is much weaker compared to the unmodified tetramer, suggesting that

H3K56 acetylation contributes to nucleosome positioning (Andrews *et al.* 2010). By promoting DNA breathing in tetrameric form and locking in the nucleosome position once the full nucleosome is assembled, H3K56 acetylation has the potential to facilitate nucleosome positioning during nucleosome assembly (Andrews *et al.* 2010; Watanabe *et al.* 2010). In this regard, perhaps it is H3K56's acetylation status during nucleosome assembly that is important for positioning H2A.Z containing nucleosomes at NFRs.

An interesting avenue of research lies within the precise regulatory mechanism between H3K56 acetylation and H2A.Z deposition. One may hypothesize that the relationship between H3K56 acetylation and H2A.Z is characterized by the PTM's role in nucleosome positioning; H3K56 acetylation positions the +1 and -1 nucleosomes, thus creating the distinct NFR required for SWR1-C recruitment and H2A.Z deposition (Ferreira *et al.* 2007; Ranjan *et al.* 2013). Or perhaps a more intriguing idea is the possibility that H3K56 acetylation is directly involved in positioning H2A.Z-containing nucleosomes during SWR1-C catalyzed histone exchange. The latter hypothesis is in line with recently published data suggesting that the Swc2 subunit of SWR1-C interacts with H3K56 on nucleosomes to "lock" in H2A.Z containing nucleosomes (Watanabe *et al.* 2013). Furthermore, constitutively acetylated H3K56 also lead to the reduced nucleosomal H2A.Z, suggesting that perhaps the act of acetylating and deacetylation H3K56 was important for regulating H2A.Z position and occupancy (Watanabe *et al.* 2013)(Phoebe Lu, Data not shown). At this time it is unclear whether the constitutive presence and absence of H3K56ace are affecting H2A.Z occupancy in the same manner; detailed nucleosome position and biochemical analyses are needed to tease apart these intricate mechanisms.

My work in Chapter 4 focused on teasing apart the structural and functional aspects of the NuA4 histone acetyltransferase. By examining the Epl1 and Eaf1 subunits that connect the catalytic sub-module to the rest of the multi-subunit complex, I found that while Eaf1 and its HSA domain were required for NuA4 stability and function, truncation of Epl1 C-terminus in an *eaf1Δ* background was sufficient to rescue picNuA4 formation and H4 acetylation. Furthermore, *epl1-CΔ eaf1Δ* double mutants had notably increased Epl1 levels and higher picNuA4 levels compared to wildtype. Taken together, I proposed that Eaf1 and the Epl1 C-terminus play a regulatory role in the formation of picNuA4 in the cell and likely control the cellular equilibrium of NuA4: picNuA4. This model raises the interesting question of how are Eaf1 and the Epl1 C-terminus regulating NuA4 complex stability. One suggestion is that docking of the Epl1 C-terminus onto the Eaf1 HSA domain stabilizes picNuA4. While an attractive model, if it were true, I would expect Eaf1 to exist as a stable component of picNuA4. Nevertheless, it is clear that Eaf1 appears to be protecting the Epl1 C-terminus from proteolytic degradation; perhaps Eaf1 regulates picNuA4 stability indirectly via NuA4's acetylation activity on non-histone targets. It is tempting to speculate that one such target is the ubiquitin-mediated degradation pathway. Indeed, the mammalian homolog of NuA4 is targeted for degradation by the ubiquitin ligase Mdm2 and a recent screen identified subunits of the proteasome as Esa1 acetylation targets (Legube *et al.* 2002; Mitchell *et al.* 2013). Furthermore, genes encoding for NuA4 subunits genetically interact with genes in ubiquitin-dependent catabolic pathways (Lu *et al.* 2009)(Chapter 4). Thus, it seems likely that NuA4 stability could be regulated through a ubiquitin-mediated degradation pathway. Elucidating the molecular mechanism and functional connection between NuA4 and the degradation

pathway will shed light on how NuA4 activity is regulated in the cell. Identification of ubiquitination targets and sites within the NuA4 complex serves as a crucial first step in teasing apart this potential regulatory pathway. It is likely that the Epl1 C-terminus is a target for ubiquitin-mediated degradation.

We are beginning to appreciate a broader role for HATs in acetylating many non-histone targets through large-scale proteomic screens aimed at identifying acetyl lysine residues in *S. cerevisiae* (Henriksen *et al.* 2012; Lin *et al.* 2009; Mitchell *et al.* 2013). A growing list of literature describing NuA4's role in auto-acetylation provides a potential mechanism for how NuA4 may be regulating its own structure and function. To date, 42 sites of auto-acetylation have been identified on 10 out of the 13 NuA4 subunits (Mitchell *et al.* 2013; Yuan *et al.* 2012; Lin *et al.* 2008). The Epl1 EPcA domain appears to be a key target of NuA4 acetylation and these modifications on Epl1 contribute to the catalytic activity of NuA4 (Mitchell *et al.* 2013). Interestingly, it appears that picNuA4 is sufficient for auto-acetylation of Epl1 *in vitro,* raising the need to examine the contributions of NuA4 and picNuA4 for general lysine acetylation (Berndsen *et al.* 2007). Systematic mutation of sites of NuA4 auto-acetylation would not only uncover acetylation sites needed for NuA4 HAT activity, but also provide novel insight into the regulatory potential of these sites in NuA4 complex stability.

From our findings in Chapter 4, I predicted that severe growth defect in cells lacking the Epl1 C-terminus may have resulted from increased picNuA4 activity as a general lysine acetyltransferase. Indeed, although *epl1-CΔ* resulted in a dramatic increase in picNuA4 levels in the cell, the level of total H4 acetylation did not increase proportionally. Furthermore, a

substantial fraction of picNuA4 in *epl1-CΔ* cells is found in the supernatant instead of being primarily chromatin-bound suggesting that a significant portion of picNuA4 acts on non-chromatin targets. A recent large-scale screen identified over 80 proteins as Esa1 targets, with the majority of proteins containing more than one acetylation site (Mitchell *et al.* 2013). The transfer of an acetyl group onto the lysine residues of proteins can alter their localization, activity, stability and interactions with their target proteins (Spange *et al.* 2009; Yang 2004). Despite a tendency for metabolic enzymes and multi-subunit complexes to be highly acetylated, the biological consequences of the majority of lysine acetylation events identified thus far remain unclear. To fully understand the functional consequence of truncating the Epl1 C-terminus, we also need to examine the acetylation status of non-histone proteins in *epl1-CΔ* cells. Furthermore, this approach will also allow us to differentiate between non-histone targets of picNuA4 and NuA4.

The various domains of Eaf1 are central to its fundamental role as a scaffolding platform for NuA4. The N-terminal region of Eaf1 associates with the Eaf3/5/7 submodule that is linked to the elongating RNA polymerase II to promote DNA accessibility (Auger *et al.* 2008; Rossetto *et al.* 2014). Previous studies show that the SANT domain is required for binding to Tra1, a shared subunit of NuA4 and SAGA that has a regulatory role in targeting the catalytic activity of both HATs (Auger *et al.* 2008; Grant *et al.* 1998; Knutson and Hahn 2011; Helmlinger *et al.* 2011). However, the lack of growth defect in an *eaf1-SANTΔ* is more in line with data I presented in Chapter 4 demonstrating that Tra1 binding does not require the SANT domain (Auger *et al.* 2008). Lastly, while previous studies reported that the shared module docked onto the HSA domain of Eaf1, our more precise excision of the HSA domain

resulted in the complete disassociation of NuA4. While unexpected, our finding highlighted a key role in the Eaf1 HSA domain in NuA4 complex integrity and function. Intriguingly, the mammalian homologue of NuA4, TIP60, contains an Eaf1-like protein as the key scaffolding subunit, p400. Since TIP60 complex is a functional and structural merge of yeast SWR1-C and NuA4, it does not come as a surprise that p400 appears to be an Eaf1-Swr1 fusion protein (Auger *et al.* 2008; Doyon *et al.* 2004; Lu *et al.* 2009). p400 contains SANT, HSA, and ATPase domains, whereas neither of the yeast homologues contain all three domains. The mammalian p400 appears to have the ATPase domain of Swr1 inserted into Eaf1 between the HSA and SANT domain (Auger *et al.* 2008; Lu *et al.* 2009). Indeed, sequence analysis of HSA domain across eukaryotic evolution suggests that the HSA domain of p400 originated from Eaf1, highlighting the functional importance and conservation of the Eaf1 HSA domain (Lu *et al.* 2009).

In closing, the interplay between the various types of chromatin modifications is emerging as a central mechanism by which cells regulate fundamental biological processes. While *S. cerevisiae* has proven to be an effective model organism to tease apart the crosstalk between chromatin-modifying factors, there remains a need to examine similar interactions in higher eukaryotes. Emerging evidence suggests that the human homologues, TIP60 and SRCAP, play critical roles in choreographing intricate developmental steps and cancer progression. Thus, increasing the need to examine the crosstalk between these chromatin-remodelers and the "message" contained within distinct chromatin neighbourhoods by way of post-translational modifications. The work presented in this thesis makes important contributions

towards understanding the interplay between various chromatin-modifying mechanisms in the cell and provides guidance for further investigation in higher eukaryotes.

References

Abbott, D. W., V. S. Ivanova, X. Wang, W. M. Bonner, and J. Ausió, 2001 Characterization of the stability and folding of H2A.Z chromatin particles: implications for transcriptional activation. The Journal of Biological Chemistry 276: 41945–41949.

Adam, M., F. Robert, M. Larochelle, and L. Gaudreau, 2001 H2A.Z is required for global chromatin integrity and for recruitment of RNA polymerase II under specific conditions. Molecular and Cellular Biology 21: 6270–6279.

Adkins, M. W., and J. K. Tyler, 2004 The histone chaperone Asf1p mediates global chromatin disassembly in vivo. The Journal of Biological Chemistry 279: 52069–52074.

Adkins, M. W., J. J. Carson, C. M. English, C. J. Ramey, and J. K. Tyler, 2007 The histone chaperone anti-silencing function 1 stimulates the acetylation of newly synthesized histone H3 in S-phase. The Journal of Biological Chemistry 282: 1334–1340.

Adkins, M. W., S. R. Howar, and J. K. Tyler, 2004 Chromatin disassembly mediated by the histone chaperone Asf1 is essential for transcriptional activation of the yeast PHO5 and PHO8 genes. Molecular Cell 14: 657–666.

Albert, I., T. N. Mavrich, L. P. Tomsho, J. Qi, S. J. Zanton *et al.*, 2007 Translational and rotational settings of H2A.Z nucleosomes across the Saccharomyces cerevisiae genome. Nature 446: 572–576.

Allard, S., R. T. Utley, J. Savard, A. S. Clarke, P. A. Grant *et al.*, 1999 NuA4, an essential transcription adaptor/histone H4 acetyltransferase complex containing Esa1p and the ATM-related cofactor Tra1p. The EMBO journal 18: 5108–5119.

Allfrey, V. G., R. Faulkner, and A. E. Mirsky, 1964 Acetylation and methylation of histones and their possible role in the regulation of RNA synthesis. Proceedings of the National Academy of Sciences of the United States of America 51: 786–794.

Almer, A., and W. Hörz, 1986 Nuclease hypersensitive regions with adjacent positioned nucleosomes mark the gene boundaries of the PHO5/PHO3 locus in yeast. The EMBO journal 5: 2681–2687.

Altaf, M., A. Auger, J. Monnet-Saksouk, J. Brodeur, S. Piquet *et al.*, 2010 NuA4-dependent acetylation of nucleosomal histones H4 and H2A directly stimulates incorporation of H2A.Z by the SWR1 complex. The Journal of Biological Chemistry 285: 15966–15977.

Andrews, A. J., X. Chen, A. Zevin, L. A. Stargell, and K. Luger, 2010 The Histone Chaperone Nap1 Promotes Nucleosome Assembly by Eliminating Nonnucleosomal Histone DNA Interactions. Molecular Cell 37: 834–842.

Auger, A., L. Galarneau, M. Altaf, A. Nourani, Y. Doyon *et al.*, 2008 Eaf1 is the platform for NuA4 molecular assembly that evolutionarily links chromatin acetylation to ATP-dependent exchange of histone H2A variants. Molecular and Cellular Biology 28: 2257–2270.

Ausubel, F. M., 1987 *Current Protocols in Molecular Biology: 1987-1988*.

Babiarz, J. E., J. E. Halley, and J. Rine, 2006 Telomeric heterochromatin boundaries require NuA4-dependent acetylation of histone variant H2A.Z in Saccharomyces cerevisiae. Genes & Development 20: 700–710.

Bannister, A. J., and T. Kouzarides, 2011 Regulation of chromatin by histone modifications. Cell Research 21: 381–395.

Bannister, A. J., P. Zegerman, J. F. Partridge, E. A. Miska, J. O. Thomas *et al.*, 2001 Selective recognition of methylated lysine 9 on histone H3 by the HP1 chromo domain. Nature 410: 120–124.

Barski, A., S. Cuddapah, K. Cui, T.-Y. Roh, D. E. Schones *et al.*, 2007 High-resolution profiling of histone methylations in the human genome. Cell 129: 823–837.

Bennett, G., M. Papamichos-Chronakis, and C. L. Peterson, 2013 DNA repair choice defines a common pathway for recruitment of chromatin regulators. Nature Communications 4: 2084.

Berndsen, C. E., W. Selleck, S. J. McBryant, J. C. Hansen, S. Tan *et al.*, 2007 Nucleosome recognition by the Piccolo NuA4 histone acetyltransferase complex. Biochemistry 46: 2091–2099.

Bilsland, E., M. Hult, S. D. Bell, P. Sunnerhagen, and J. A. Downs, 2007 The Bre5/Ubp3 ubiquitin protease complex from budding yeast contributes to the cellular response to DNA damage. DNA Repair 6: 1471–1484.

Bird, A., 2007 Perceptions of epigenetics. Nature 447: 396–398.

Bird, A. W., D. Y. Yu, M. G. Pray-Grant, Q. Qiu, K. E. Harmon *et al.*, 2002 Acetylation of histone H4 by Esa1 is required for DNA double-strand break repair. Nature 419: 411–415.

Boudreault, A. A., D. Cronier, W. Selleck, N. Lacoste, R. T. Utley *et al.*, 2003 Yeast enhancer of polycomb defines global Esa1-dependent acetylation of chromatin. Genes & Development 17: 1415–1428.

Bönisch, C., and S. B. Hake, 2012 Histone H2A variants in nucleosomes and chromatin: more or less stable? Nucleic Acids Research 40: 10719–10741.

Brickner, D. G., I. Cajigas, Y. Fondufe-Mittendorf, S. Ahmed, P.-C. Lee *et al.*, 2007 H2A.Z-Mediated Localization of Genes at the Nuclear Periphery Confers Epigenetic Memory of Previous Transcriptional State (T. Mistelli, Ed.). PLoS Biology 5: e81.

Brogaard, K., L. Xi, J.-P. Wang, and J. Widom, 2012 A map of nucleosome positions in yeast at base-pair resolution. Nature 486: 496–501.

Brown, C. E., L. Howe, K. Sousa, S. C. Alley, M. J. Carrozza *et al.*, 2001 Recruitment of HAT complexes by direct activator interactions with the ATM-related Tra1 subunit. Science 292: 2333–2337.

Buchanan, L., M. Durand-Dubief, A. Roguev, C. Sakalar, B. Wilhelm *et al.*, 2009 The Schizosaccharomyces pombe JmjC-protein, Msc1, prevents H2A.Z localization in centromeric and subtelomeric chromatin domains. PLOS Genetics 5: e1000726.

Cai, Y., J. Jin, C. Tomomori-Sato, S. Sato, I. Sorokina *et al.*, 2003 Identification of new subunits of the multiprotein mammalian TRRAP/TIP60-containing histone acetyltransferase complex. The Journal of Biological Chemistry 278: 42733–42736.

Cairns, B. R., 2007 Chromatin remodeling: insights and intrigue from single-molecule studies. Nature Structural & Molecular Biology 14: 989–996.

Cairns, B. R., 2009 The logic of chromatin architecture and remodelling at promoters. Nature 461: 193–198.

Celic, I., H. Masumoto, W. P. Griffith, P. Meluh, R. J. Cotter *et al.*, 2006 The sirtuins hst3 and Hst4p preserve genome integrity by controlling histone h3 lysine 56 deacetylation. Current Biology 16: 1280–1289.

Chen, C.-C., J. J. Carson, J. Feser, B. A. Tamburini, S. Zabaronick *et al.*, 2008 Acetylated lysine 56 on histone H3 drives chromatin assembly after repair and signals for the completion of repair. Cell 134: 231–243.

Chittuluru, J. R., Y. Chaban, J. Monnet-Saksouk, M. J. Carrozza, V. Sapountzi *et al.*, 2011 Structure and nucleosome interaction of the yeast NuA4 and Piccolo-NuA4 histone acetyltransferase complexes. Nature Structural & Molecular Biology 18: 1196–1203.

Clapier, C. R., and B. R. Cairns, 2009 The biology of chromatin remodeling complexes. Annual Review of Biochemistry 78: 273–304.

Clarke, A. S., J. E. Lowell, S. J. Jacobson, and L. Pillus, 1999 Esa1p is an essential histone acetyltransferase required for cell cycle progression. Molecular and Cellular Biology 19: 2515–2526.

Collins, S. R., M. Schuldiner, N. J. Krogan, and J. S. Weissman, 2006 A strategy for extracting and analyzing large-scale quantitative epistatic interaction data. Genome Biology 7: R63.

Daganzo, S. M., J. P. Erzberger, W. M. Lam, E. Skordalakes, R. Zhang *et al.*, 2003 Structure and function of the conserved core of histone deposition protein Asf1. Current Biology 13: 2148–2158.

Das, C., J. K. Tyler, and M. E. A. Churchill, 2010 The histone shuffle: histone chaperones in an energetic dance. Trends in Biochemical Sciences 35: 476–489.

De Koning, L., A. Corpet, J. E. Haber, and G. Almouzni, 2007 Histone chaperones: an escort network regulating histone traffic. Nature Structural & Molecular Biology 14: 997–1007.

Dennis, G., B. T. Sherman, D. A. Hosack, J. Yang, W. Gao *et al.*, 2003 DAVID: Database for Annotation, Visualization, and Integrated Discovery. Genome Biology 4: P3.

Dhalluin, C., J. E. Carlson, L. Zeng, C. He, A. K. Aggarwal *et al.*, 1999 Structure and ligand of a histone acetyltransferase bromodomain. Nature 399: 491–496.

Dhillon, N., M. Oki, S. J. Szyjka, O. M. Aparicio, and R. T. Kamakaka, 2006 H2A.Z functions to regulate progression through the cell cycle. Molecular and Cellular Biology 26: 489–501.

Dorigo, B., T. Schalch, K. Bystricky, and T. J. Richmond, 2003 Chromatin Fiber Folding: Requirement for the Histone H4 N-terminal Tail. Journal of Molecular Biology 327: 85–96.

Downey, M., J. R. Johnson, N. E. Davey, B. W. Newton, T. L. Johnson *et al.*, 2014 Acetylome profiling reveals overlap in the regulation of diverse processes by sirtuins, Gcn5 and Esa1. Molecular & Cellular Proteomics mcp.M114.043141.

Downs, J. A., S. Allard, O. Jobin-Robitaille, A. Javaheri, A. Auger *et al.*, 2004 Binding of chromatin-modifying activities to phosphorylated histone H2A at DNA damage sites. Molecular Cell 16: 979–990.

Doyon, Y., and J. Côté, 2004 The highly conserved and multifunctional NuA4 HAT complex. Current Opinion in Genetics & Development 14: 147–154.

Doyon, Y., W. Selleck, W. S. Lane, S. Tan, and J. Côté, 2004 Structural and functional conservation of the NuA4 histone acetyltransferase complex from yeast to humans. Molecular and Cellular Biology 24: 1884–1896.

Driscoll, R., A. Hughes, and S. P. Jackson, 2007 Yeast Rtt109 promotes genome stability by acetylating histone H3 on lysine 56. Science 315: 649–652.

Durant, M., and B. F. Pugh, 2007 NuA4-directed chromatin transactions throughout the Saccharomyces cerevisiae genome. Molecular and Cellular Biology 27: 5327–5335.

Eberharter, A., and P. B. Becker, 2004 ATP-dependent nucleosome remodelling: factors and functions. Journal of Cell Science 117: 3707–3711.

Eberharter, A., S. John, P. A. Grant, R. T. Utley, and J. L. Workman, 1998 Identification and analysis of yeast nucleosomal histone acetyltransferase complexes. Methods (San Diego, Calif.) 15: 315–321.

Ehrenhofer-Murray, A. E., 2004 Chromatin dynamics at DNA replication, transcription and repair. European Journal of Biochemistry / FEBS 271: 2335–2349.

Eissenberg, J. C., and G. Reuter, 2009 Cellular mechanism for targeting heterochromatin formation in Drosophila. International Review of Cell and Molecular Biology 273: 1–47.

Eitoku, M., L. Sato, T. Senda, and M. Horikoshi, 2008 Histone chaperones: 30 years from isolation to elucidation of the mechanisms of nucleosome assembly and disassembly. Cellular and Molecular Life Sciences 65: 414–444.

Ekwall, K., T. Olsson, B. M. Turner, G. Cranston, and R. C. Allshire, 1997 Transient inhibition of histone deacetylation alters the structural and functional imprint at fission yeast centromeres. Cell 91: 1021–1032.

Emili, A., D. M. Schieltz, J. R. Yates, and L. H. Hartwell, 2001 Dynamic interaction of DNA damage checkpoint protein Rad53 with chromatin assembly factor Asf1. Molecular Cell 7: 13–20.

Erkina, T. Y., and A. Erkine, 2014 ASF1 and the SWI/SNF complex interact functionally during nucleosome displacement, while FACT is required for nucleosome reassembly at yeast heat shock gene promoters during sustained stress. Cell Stress & Chaperones.

Faast, R., V. Thonglairoam, T. C. Schulz, J. Beall, J. R. Wells *et al.*, 2001 Histone variant H2A.Z is required for early mammalian development. Current Biology 11: 1183–1187.

Fan, J. Y., F. Gordon, K. Luger, J. C. Hansen, and D. J. Tremethick, 2002 The essential histone variant H2A.Z regulates the equilibrium between different chromatin conformational states. Nature Structural Biology 9: 172–176.

Fan, J. Y., D. Rangasamy, K. Luger, and D. J. Tremethick, 2004 H2A.Z alters the nucleosome surface to promote HP1alpha-mediated chromatin fiber folding. Molecular Cell 16: 655–661.

Fedor, M. J., and R. D. Kornberg, 1989 Upstream activation sequence-dependent alteration of chromatin structure and transcription activation of the yeast GAL1-GAL10 genes. Molecular and Cellular Biology 9: 1721–1732.

Ferreira, H., J. Somers, R. Webster, A. Flaus, and T. Owen-Hughes, 2007 Histone tails and the H3 alphaN helix regulate nucleosome mobility and stability. Molecular and Cellular Biology 27: 4037–4048.

Fillingham, J., J. Recht, A. C. Silva, B. Suter, A. Emili *et al.*, 2008 Chaperone control of the activity and specificity of the histone H3 acetyltransferase Rtt109. Molecular and Cellular Biology 28: 4342–4353.

Flemming, W., 1882 *Zellsubstanz, Kern und Zelltheilung*. F. C. W. Vogel, Leipzig.

Franco, A. A., and P. D. Kaufman, 2005 Histone deposition protein Asf1 maintains DNA replisome integrity and interacts with replication factor C. Genes & Development 19: 1365–1375.

Friis, R. M. N., B. P. Wu, S. N. Reinke, D. J. Hockman, B. D. Sykes *et al.*, 2009 A glycolytic burst drives glucose induction of global histone acetylation by picNuA4 and SAGA. Nucleic Acids Research 37: 3969–3980.

Gelbart, M. E., T. J. Rechsteiner, T. J. Richmond, and T. Tsukiyama, 2001 Interactions of Isw2 chromatin remodeling complex with nucleosomal arrays: analyses using recombinant yeast histones and immobilized templates. Molecular and Cellular Biology 21: 2098–2106.

Gévry, N., H. M. Chan, L. Laflamme, D. M. Livingston, and L. Gaudreau, 2007 p21 transcription is regulated by differential localization of histone H2A.Z. Genes & Development 21: 1869–1881.

Girton, J. R., and K. M. Johansen, 2008 Chromatin structure and the regulation of gene expression: the lessons of PEV in Drosophila. Advances in Genetics 61: 1–43.

Gkikopoulos, T., K. M. Havas, H. Dewar, and T. Owen-Hughes, 2009 SWI/SNF and Asf1p cooperate to displace histones during induction of the saccharomyces cerevisiae HO promoter. Molecular and Cellular Biology 29: 4057–4066.

Gordon, F., K. Luger, and J. C. Hansen, 2005 The core histone N-terminal tail domains function independently and additively during salt-dependent oligomerization of nucleosomal arrays. The Journal of Biological Chemistry 280: 33701–33706.

Grant, P. A., D. M. Schieltz, M. G. Pray-Grant, J. R. Yates, and J. L. Workman, 1998 The ATM-related cofactor Tra1 is a component of the purified SAGA complex. Molecular Cell 2: 863–867.

Grunstein, M., 1997 Histone acetylation in chromatin structure and transcription. Nature 389: 349–352.

Guillemette, B., A. R. Bataille, N. Gévry, M. Adam, M. Blanchette *et al.*, 2005 Variant histone H2A.Z is globally localized to the promoters of inactive yeast genes and regulates nucleosome positioning. PLoS Biology 3: e384.

Halley, J. E., T. Kaplan, A. Y. Wang, M. S. Kobor, and J. Rine, 2010 Roles for H2A.Z and its acetylation in GAL1 transcription and gene induction, but not GAL1-transcriptional memory. PLoS Biology 8: e1000401.

Han, J., and Z. Zhang, 2007 Rtt109 acetylates histone H3 lysine 56 and functions in DNA replication. Science 315: 653–655.

Hardy, S., P.-E. Jacques, N. Gévry, A. Forest, M.-E. Fortin *et al.*, 2009 The euchromatic and heterochromatic landscapes are shaped by antagonizing effects of transcription on H2A.Z deposition. PLOS Genetics 5: e1000687.

Hartley, P. D., and H. D. Madhani, 2009 Mechanisms that specify promoter nucleosome location and identity. Cell 137: 445–458.

Helmlinger, D., S. Marguerat, J. Villén, D. L. Swaney, S. P. Gygi *et al.*, 2011 Tra1 has specific regulatory roles, rather than global functions, within the SAGA co-activator complex. The EMBO Journal 30: 2843–2852.

Henriksen, P., S. A. Wagner, B. T. Weinert, S. Sharma, G. Bačinskaja *et al.*, 2012 Proteome-wide analysis of lysine acetylation suggests its broad regulatory scope in Saccharomyces cerevisiae. Molecular & Cellular Proteomics : MCP 11: 1510–1522.

Hentrich, T., J. M. Schulze, E. Emberly, and M. S. Kobor, 2012 CHROMATRA: a Galaxy tool for visualizing genome-wide chromatin signatures. Bioinformatics (Oxford, England) 28: 717–718.

Hiraga, S.-I., S. Botsios, and A. D. Donaldson, 2008 Histone H3 lysine 56 acetylation by Rtt109 is crucial for chromosome positioning. The Journal of Cell Biology 183: 641–651.

Huh, J.-W., J. Wu, C.-H. Lee, M. Yun, D. Gilada *et al.*, 2012 Multivalent di-nucleosome recognition enables the Rpd3S histone deacetylase complex to tolerate decreased H3K36 methylation levels. The EMBO Journal 31: 3564–3574.

Hyland, E. M., M. S. Cosgrove, H. Molina, D. Wang, A. Pandey *et al.*, 2005 Insights into the role of histone H3 and histone H4 core modifiable residues in Saccharomyces cerevisiae. Molecular and Cellular Biology 25: 10060–10070.

Ikura, T., V. V. Ogryzko, M. Grigoriev, R. Groisman, J. Wang *et al.*, 2000 Involvement of the TIP60 histone acetylase complex in DNA repair and apoptosis. Cell 102: 463–473.

Imai, S., C. M. Armstrong, M. Kaeberlein, and L. Guarente, 2000 Transcriptional silencing and longevity protein Sir2 is an NAD-dependent histone deacetylase. Nature 403: 795–800.

Iouzalen, N., J. Moreau, and M. Méchali, 1996 H2A.ZI, a new variant histone expressed during Xenopus early development exhibits several distinct features from the core histone H2A. Nucleic Acids Research 24: 3947–3952.

Ishibashi, T., D. Dryhurst, K. L. Rose, J. Shabanowitz, D. F. Hunt *et al.*, 2009 Acetylation of vertebrate H2A.Z and its effect on the structure of the nucleosome. Biochemistry 48: 5007–5017.

Iyer, V. R., and K. Struhl, 1995 Poly(dA:dT), a ubiquitous promoter element that stimulates transcription via its intrinsic DNA structure. The EMBO Journal 14: 2570–2579.

Jeong, J. S., H.-S. Rho, and H. Zhu, 2011 A functional protein microarray approach to characterizing posttranslational modifications on lysine residues. Methods in Molecular Biology (Clifton, N.J.) 723: 213–223.

Jiang, C., and B. F. Pugh, 2009 Nucleosome positioning and gene regulation: advances through genomics. Nature Reviews Genetics 10: 161–172.

Jin, C., C. Zang, G. Wei, K. Cui, W. Peng *et al.*, 2009 H3.3/H2A.Z double variant-containing nucleosomes mark "nucleosome-free regions" of active promoters and other regulatory regions. Nature Genetics 41: 941–945.

Kalocsay, M., N. J. Hiller, and S. Jentsch, 2009 Chromosome-wide Rad51 spreading and SUMO-H2A.Z-dependent chromosome fixation in response to a persistent DNA double-strand break. Molecular Cell 33: 335–343.

Kaplan, T., C. L. Liu, J. A. Erkmann, J. Holik, M. Grunstein *et al.*, 2008 Cell Cycle– and Chaperone-Mediated Regulation of H3K56ac Incorporation in Yeast. PLOS Genetics 4: e1000270.

Kaufman, P. D., 2011 New Partners for HP1 in Transcriptional Gene Silencing. Molecular Cell 41: 1–2.

Keogh, M.-C., T. A. Mennella, C. Sawa, S. Berthelet, N. J. Krogan *et al.*, 2006 The Saccharomyces cerevisiae histone H2A variant Htz1 is acetylated by NuA4. Genes & Development 20: 660–665.

Kimura, A., T. Umehara, and M. Horikoshi, 2002 Chromosomal gradient of histone acetylation established by Sas2p and Sir2p functions as a shield against gene silencing. Nature Genetics 32: 370–377.

Knutson, B. A., and S. Hahn, 2011 Domains of Tra1 important for activator recruitment and transcription coactivator functions of SAGA and NuA4 complexes. Molecular and Cellular Biology 31: 818–831.

Kobor, M. S., S. Venkatasubrahmanyam, M. D. Meneghini, J. W. Gin, J. L. Jennings *et al.*, 2004 A protein complex containing the conserved Swi2/Snf2-related ATPase Swr1p deposits histone variant H2A.Z into euchromatin. PLoS Biology 2: E131.

Kolonko, E. M., B. N. Albaugh, S. E. Lindner, Y. Chen, K. A. Satyshur *et al.*, 2010 Catalytic activation of histone acetyltransferase Rtt109 by a histone chaperone. Proceedings of the National Academy of Sciences of the United States of America 107: 20275–20280.

Korber, P., S. Barbaric, T. Luckenbach, A. Schmid, U. J. Schermer *et al.*, 2006 The histone chaperone Asf1 increases the rate of histone eviction at the yeast PHO5 and PHO8 promoters. The Journal of Biological Chemistry 281: 5539–5545.

Kornberg, R. D., 1974 Chromatin structure: a repeating unit of histones and DNA. Science 184: 868–871.

Kouzarides, T., 2007 SnapShot: Histone-modifying enzymes. Cell 131: 822–822.e1.

Kraft, C., A. Deplazes, M. Sohrmann, and M. Peter, 2008 Mature ribosomes are selectively degraded upon starvation by an autophagy pathway requiring the Ubp3p/Bre5p ubiquitin protease. Nature Cell Biology 10: 602–610.

Krogan, N. J., K. Baetz, M.-C. Keogh, N. Datta, C. Sawa *et al.*, 2004 Regulation of chromosome stability by the histone H2A variant Htz1, the Swr1 chromatin remodeling complex, and the histone acetyltransferase NuA4. Proceedings of the National Academy of Sciences of the United States of America 101: 13513–13518.

Krogan, N. J., M.-C. Keogh, N. Datta, C. Sawa, O. W. Ryan *et al.*, 2003 A Snf2 Family ATPase Complex Required for Recruitment of the Histone H2A Variant Htz1. Molecular Cell 12: 1565–1576.

Kundu, S., and C. L. Peterson, 2010 Dominant role for signal transduction in the transcriptional memory of yeast GAL genes. Molecular and Cellular Biology 30: 2330–2340.

Lam, F. H., D. J. Steger, and E. K. O'Shea, 2008 Chromatin decouples promoter threshold from dynamic range. Nature 453: 246–250.

Larochelle, M., and L. Gaudreau, 2003 H2A.Z has a function reminiscent of an activator required for preferential binding to intergenic DNA. The EMBO Journal 22: 4512–4522.

Le, S., C. Davis, J. B. Konopka, and R. Sternglanz, 1997 Two new S-phase-specific genes from Saccharomyces cerevisiae. Yeast (Chichester, England) 13: 1029–1042.

Lee, C.-K., Y. Shibata, B. Rao, B. D. Strahl, and J. D. Lieb, 2004 Evidence for nucleosome depletion at active regulatory regions genome-wide. Nature Genetics 36: 900–905.

Lee, W., D. Tillo, N. Bray, R. H. Morse, R. W. Davis *et al.*, 2007 A high-resolution atlas of nucleosome occupancy in yeast. Nature Genetics 39: 1235–1244.

Legube, G., L. K. Linares, C. Lemercier, M. Scheffner, S. Khochbin *et al.*, 2002 Tip60 is targeted to proteasome-mediated degradation by Mdm2 and accumulates after UV irradiation. The EMBO Journal 21: 1704–1712.

Lemieux, K., M. Larochelle, and L. Gaudreau, 2008 Variant histone H2A.Z, but not the HMG proteins Nhp6a/b, is essential for the recruitment of Swi/Snf, Mediator, and SAGA to the yeast GAL1 UAS(G). Biochemical and Biophysical Research Communications 369: 1103–1107.

Li, B., J. Jackson, M. D. Simon, B. Fleharty, M. M. Gogol *et al.*, 2009 Histone H3 lysine 36 dimethylation (H3K36me2) is sufficient to recruit the Rpd3s histone deacetylase complex and to repress spurious transcription. The Journal of Biological Chemistry 284: 7970–7976.

Li, B., S. G. Pattenden, D. Lee, J. Gutiérrez, J. Chen *et al.*, 2005 Preferential occupancy of histone variant H2AZ at inactive promoters influences local histone modifications and chromatin remodeling. Proceedings of the National Academy of Sciences of the United States of America 102: 18385–18390.

Li, G., and D. Reinberg, 2011 Chromatin higher-order structures and gene regulation. Current Opinion in Genetics & Development 21: 175–186.

Lin, L.-J., and M. C. Schultz, 2011 Promoter regulation by distinct mechanisms of functional interplay between lysine acetylase Rtt109 and histone chaperone Asf1. Proceedings of the National Academy of Sciences of the United States of America 108: 19599–19604.

Lin, L.-J., L. V. Minard, G. C. Johnston, R. A. Singer, and M. C. Schultz, 2010 Asf1 can promote trimethylation of H3 K36 by Set2. Molecular and Cellular Biology 30: 1116–1129.

Lin, Y.-Y., J.-Y. Lu, J. Zhang, W. Walter, W. Dang *et al.*, 2009 Protein acetylation microarray reveals that NuA4 controls key metabolic target regulating gluconeogenesis. Cell 136: 1073–1084.

Lin, Y.-Y., Y. Qi, J.-Y. Lu, X. Pan, D. S. Yuan *et al.*, 2008 A comprehensive synthetic genetic interaction network governing yeast histone acetylation and deacetylation. Genes & Development 22: 2062–2074.

Lu, J.-Y., Y.-Y. Lin, H. Zhu, L.-M. Chuang, and J. D. Boeke, 2011 Protein acetylation and aging. Aging 3: 911–912.

Lu, P. Y. T., and M. S. Kobor, 2014 Maintenance of heterochromatin boundary and nucleosome composition at promoters by the Asf1 histone chaperone and SWR1-C chromatin remodeler in Saccharomyces cerevisiae. Genetics 197: 133–145.

Lu, P. Y. T., N. Lévesque, and M. S. Kobor, 2009 NuA4 and SWR1-C: two chromatin-modifying complexes with overlapping functions and components. Biochemistry and Cell Biology = Biochimie et Biologie Cellulaire 87: 799–815.

Luger, K., A. W. Mäder, R. K. Richmond, D. F. Sargent, and T. J. Richmond, 1997 Crystal structure of the nucleosome core particle at 2.8 A resolution. Nature 389: 251–260.

Luk, E., A. Ranjan, P. C. FitzGerald, G. Mizuguchi, Y. Huang *et al.*, 2010 Stepwise histone replacement by SWR1 requires dual activation with histone H2A.Z and canonical nucleosome. Cell 143: 725–736.

Luk, E., N.-D. Vu, K. Patteson, G. Mizuguchi, W.-H. Wu *et al.*, 2007 Chz1, a nuclear chaperone for histone H2AZ. Molecular Cell 25: 357–368.

Lusser, A., and J. T. Kadonaga, 2003 Chromatin remodeling by ATP-dependent molecular machines. BioEssays : news and reviews in molecular, cellular and developmental biology 25: 1192–1200.

Maas, N. L., K. M. Miller, L. G. DeFazio, and D. P. Toczyski, 2006 Cell Cycle and Checkpoint Regulation of Histone H3 K56 Acetylation by Hst3 and Hst4. Molecular Cell 23: 109–119.

Malik, H. S., and S. Henikoff, 2003 Phylogenomics of the nucleosome. Nature Structural & Molecular Biology 10: 882–891.

Martinato, F., M. Cesaroni, B. Amati, and E. Guccione, 2008 Analysis of Myc-induced histone modifications on target chromatin. (E. Abraham, Ed.). PloS One 3: e3650.

Masumoto, H., D. Hawke, R. Kobayashi, and A. Verreault, 2005 A role for cell-cycle-regulated histone H3 lysine 56 acetylation in the DNA damage response. Nature 436: 294–298.

Mavrich, T. N., I. P. Ioshikhes, B. J. Venters, C. Jiang, L. P. Tomsho *et al.*, 2008 A barrier nucleosome model for statistical positioning of nucleosomes throughout the yeast genome. Genome Research 18: 1073–1083.

Meijsing, S. H., and A. E. Ehrenhofer-Murray, 2001 The silencing complex SAS-I links histone acetylation to the assembly of repressed chromatin by CAF-I and Asf1 in Saccharomyces cerevisiae. Genes & Development 15: 3169–3182.

Meneghini, M. D., M. Wu, and H. D. Madhani, 2003 Conserved histone variant H2A.Z protects euchromatin from the ectopic spread of silent heterochromatin. Cell 112: 725–736.

Miele, A., K. Bystricky, and J. Dekker, 2009 Yeast silent mating type loci form heterochromatic clusters through silencer protein-dependent long-range interactions. PLOS Genetics 5: e1000478.

Millar, C. B., F. Xu, K. Zhang, and M. Grunstein, 2006 Acetylation of H2AZ Lys 14 is associated with genome-wide gene activity in yeast. Genes & Development 20: 711–722.

Miller, A., J. Chen, T. E. Takasuka, J. L. Jacobi, P. D. Kaufman *et al.*, 2010 Proliferating cell nuclear antigen (PCNA) is required for cell cycle-regulated silent chromatin on replicated and nonreplicated genes. The Journal of Biological Chemistry 285: 35142–35154.

Miller, A., B. Yang, T. Foster, and A. L. Kirchmaier, 2008 Proliferating cell nuclear antigen and ASF1 modulate silent chromatin in Saccharomyces cerevisiae via lysine 56 on histone H3. Genetics 179: 793–809.

Mitchell, L., S. Huard, M. Cotrut, R. Pourhanifeh-Lemeri, A.-L. Steunou *et al.*, 2013 mChIP-KAT-MS, a method to map protein interactions and acetylation sites for lysine acetyltransferases. Proceedings of the National Academy of Sciences of the United States of America 110: E1641–50.

Mitchell, L., J.-P. Lambert, M. Gerdes, A. S. Al-Madhoun, I. S. Skerjanc *et al.*, 2008 Functional dissection of the NuA4 histone acetyltransferase reveals its role as a genetic hub and that Eaf1 is essential for complex integrity. Molecular and Cellular Biology 28: 2244–2256.

Mitchell, L., A. Lau, J.-P. Lambert, H. Zhou, Y. Fong *et al.*, 2011 Regulation of Septin Dynamics by the Saccharomyces cerevisiae Lysine Acetyltransferase NuA4. PloS One 6: e25336.

Mizuguchi, G., X. Shen, J. Landry, W.-H. Wu, S. Sen *et al.*, 2004 ATP-driven exchange of histone H2AZ variant catalyzed by SWR1 chromatin remodeling complex. Science 303: 343–348.

Morrison, A. J., and X. Shen, 2009 Chromatin remodelling beyond transcription: the INO80 and SWR1 complexes. Nature Reviews Molecular Cell Biology 10: 373–384.

Morrison, A. J., J. Highland, N. J. Krogan, A. Arbel-Eden, J. F. Greenblatt *et al.*, 2004 INO80 and gamma-H2AX interaction links ATP-dependent chromatin remodeling to DNA damage repair. Cell 119: 767–775.

Mousson, F., A. Lautrette, J.-Y. Thuret, M. Agez, R. Courbeyrette *et al.*, 2005 Structural basis for the interaction of Asf1 with histone H3 and its functional implications. Proceedings of the National Academy of Sciences of the United States of America 102: 5975–5980.

Mousson, F., F. Ochsenbein, and C. Mann, 2007 The histone chaperone Asf1 at the crossroads of chromatin and DNA checkpoint pathways. Chromosoma 116: 79–93.

Muthurajan, U. M., Y. Bao, L. J. Forsberg, R. S. Edayathumangalam, P. N. Dyer *et al.*, 2004 Crystal structures of histone Sin mutant nucleosomes reveal altered protein-DNA interactions. The EMBO Journal 23: 260–271.

Neumann, H., S. M. Hancock, R. Buning, A. Routh, L. Chapman *et al.*, 2009 A method for genetically installing site-specific acetylation in recombinant histones defines the effects of H3 K56 acetylation. Molecular Cell 36: 153–163.

Nguyen, V. Q., A. Ranjan, F. Stengel, D. Wei, R. Aebersold *et al.*, 2013 Molecular architecture of the ATP-dependent chromatin-remodeling complex SWR1. Cell 154: 1220–1231.

Nourani, A., R. T. Utley, S. Allard, and J. Côté, 2004 Recruitment of the NuA4 complex poises the PHO5 promoter for chromatin remodeling and activation. The EMBO Journal 23: 2597–2607.

Oki, M., and R. T. Kamakaka, 2004 Barrier proteins remodel and modify chromatin to restrict silenced domains. Molecular and Cellular Biology 24: 1956–1967.

Olins, A. L., and D. E. Olins, 1974 Spheroid chromatin units (v bodies). Science 183: 330–332.

Osada, S., M. Kurita, J.-I. Nishikawa, and T. Nishihara, 2005 Chromatin assembly factor Asf1p-dependent occupancy of the SAS histone acetyltransferase complex at the silent mating-type locus HMLalpha. Nucleic Acids Research 33: 2742–2750.

Osada, S., A. Sutton, N. Muster, C. E. Brown, J. R. Yates *et al.*, 2001 The yeast SAS (something about silencing) protein complex contains a MYST-type putative acetyltransferase and functions with chromatin assembly factor ASF1. Genes & Development 15: 3155–3168.

Osborne, E. A., S. Dudoit, and J. Rine, 2009 The establishment of gene silencing at single-cell resolution. Nature Genetics 41: 800–806.

Ozdemir, A., H. Masumoto, P. Fitzhjohn, A. Verreault, and C. Logie, 2006 Histone H3 Lysine 56 Acetylation: A New Twist in the Chromosome Cycle. Cell Cycle 5: 2602–2608.

Papamichos-Chronakis, M., and C. L. Peterson, 2013 Chromatin and the genome integrity network. Nature Reviews Genetics 14: 62–75.

Papamichos-Chronakis, M., J. E. Krebs, and C. L. Peterson, 2006 Interplay between Ino80 and Swr1 chromatin remodeling enzymes regulates cell cycle checkpoint adaptation in response to DNA damage. Genes & Development 20: 2437–2449.

Papamichos-Chronakis, M., S. Watanabe, O. J. Rando, and C. L. Peterson, 2011 Global regulation of H2A.Z localization by the INO80 chromatin-remodeling enzyme is essential for genome integrity. Cell 144: 200–213.

Park, Y.-J., and K. Luger, 2008 Histone chaperones in nucleosome eviction and histone exchange. Current Opinion in Structural Biology 18: 282–289.

Peterson, C. L., and M.-A. Laniel, 2004 Histones and histone modifications. Current Biology 14: R546–51.

Raisner, R. M., and H. D. Madhani, 2008 Genomewide screen for negative regulators of sirtuin activity in Saccharomyces cerevisiae reveals 40 loci and links to metabolism. Genetics 179: 1933–1944.

Raisner, R. M., P. D. Hartley, M. D. Meneghini, M. Z. Bao, C. L. Liu *et al.*, 2005 Histone variant H2A.Z marks the 5' ends of both active and inactive genes in euchromatin. Cell 123: 233–248.

Ramey, C. J., S. R. Howar, M. W. Adkins, J. Linger, J. Spicer *et al.*, 2004 Activation of the DNA damage checkpoint in yeast lacking the histone chaperone anti-silencing function 1. Molecular and Cellular Biology 24: 10313–10327.

Rando, O. J., and H. Y. Chang, 2009 Genome-wide views of chromatin structure. Annual Review of Biochemistry 78: 245–271.

Rangasamy, D., I. Greaves, and D. J. Tremethick, 2004 RNA interference demonstrates a novel role for H2A.Z in chromosome segregation. Nature Structural & Molecular Biology 11: 650–655.

Ranjan, A., G. Mizuguchi, P. C. FitzGerald, D. Wei, F. Wang *et al.*, 2013 Nucleosome-free region dominates histone acetylation in targeting SWR1 to promoters for H2A.Z replacement. Cell 154: 1232–1245.

Ransom, M., B. K. Dennehey, and J. K. Tyler, 2010 Chaperoning histones during DNA replication and repair. Cell 140: 183–195.

Raveh-Sadka, T., M. Levo, U. Shabi, B. Shany, L. Keren *et al.*, 2012 Manipulating nucleosome disfavoring sequences allows fine-tune regulation of gene expression in yeast. Nature Genetics 44: 743–750.

Recht, J., T. Tsubota, J. C. Tanny, R. L. Diaz, J. M. Berger *et al.*, 2006 Histone chaperone Asf1 is required for histone H3 lysine 56 acetylation, a modification associated with S phase in mitosis and meiosis. Proceedings of the National Academy of Sciences of the United States of America 103: 6988–6993.

Reid, J. L., P. O. Brown, K. Struhl, and V. R. Iyer, 2000 Coordinate regulation of yeast ribosomal protein genes is associated with targeted recruitment of Esa1 histone acetylase. Molecular Cell 6: 1297–1307.

Robinson, P. J. J., and D. Rhodes, 2006 Structure of the “30 nm” chromatin fibre: a key role for the linker histone. Current Opinion in Structural Biology 16: 336–343.

Robinson, P. J. J., L. Fairall, V. A. T. Huynh, and D. Rhodes, 2006 EM measurements define the dimensions of the “30-nm” chromatin fiber: evidence for a compact, interdigitated structure. Proceedings of the National Academy of Sciences of the United States of America 103: 6506–6511.

Rogakou, E. P., C. Boon, C. Redon, and W. M. Bonner, 1999 Megabase chromatin domains involved in DNA double-strand breaks in vivo. The Journal of Cell Biology 146: 905–916.

Rossetto, D., M. Cramet, A. Y. Wang, A.-L. Steunou, N. Lacoste *et al.*, 2014 Eaf5/7/3 form a functionally independent NuA4 submodule linked to RNA polymerase II-coupled nucleosome recycling. The EMBO Journal 33: 1397–1415.

Rufiange, A., P.-E. Jacques, W. Bhat, F. Robert, and A. Nourani, 2007 Genome-wide replication-independent histone H3 exchange occurs predominantly at promoters and implicates H3 K56 acetylation and Asf1. Molecular Cell 27: 393–405.

Rusche, L. N., A. L. Kirchmaier, and J. Rine, 2003 The establishment, inheritance, and function of silenced chromatin in Saccharomyces cerevisiae. Annual Review of Biochemistry 72: 481–516.

Santisteban, M. S., T. Kalashnikova, and M. M. Smith, 2000 Histone H2A.Z regulats transcription and is partially redundant with nucleosome remodeling complexes. Cell 103: 411–422.

Sarma, K., and D. Reinberg, 2005 Histone variants meet their match. Nature Reviews Molecular Cell Biology 6: 139–149.

Schneider, J., P. Bajwa, F. C. Johnson, S. R. Bhaumik, and A. Shilatifard, 2006 Rtt109 Is required for proper H3K56 acetylation a chromatin mark associated with the elongating RNA polymerase II. The Journal of Biological Chemistry 281: 37270–37274.

Schuldiner, M., S. COLLINS, J. S. Weissman, and N. KROGAN, 2006 Quantitative genetic analysis in Saccharomyces cerevisiae using epistatic miniarray profiles (E-MAPs) and its application to chromatin functions. Methods (San Diego, Calif.) 40: 344–352.

Schulze, J. M., J. Jackson, S. Nakanishi, J. M. Gardner, T. Hentrich *et al.*, 2009 Linking cell cycle to histone modifications: SBF and H2B monoubiquitination machinery and cell-cycle regulation of H3K79 dimethylation. Molecular Cell 35: 626–641.

Schwabish, M. A., and K. Struhl, 2006 Asf1 mediates histone eviction and deposition during elongation by RNA polymerase II. Molecular Cell 22: 415–422.

Segal, E., and J. Widom, 2009 Poly(dA:dT) tracts: major determinants of nucleosome organization. Current Opinion in Structural Biology 19: 65–71.

Segal, E., Y. Fondufe-Mittendorf, L. Chen, A. Thåström, Y. Field *et al.*, 2006 A genomic code for nucleosome positioning. Nature 442: 772–778.

Selleck, W., I. Fortin, D. Sermwittayawong, J. Côté, and S. Tan, 2005 The Saccharomyces cerevisiae Piccolo NuA4 histone acetyltransferase complex requires the Enhancer of Polycomb A domain and chromodomain to acetylate nucleosomes. Molecular and Cellular Biology 25: 5535–5542.

Shahbazian, M. D., and M. Grunstein, 2007 Functions of site-specific histone acetylation and deacetylation. Annual Review of Biochemistry 76: 75–100.

Sharma, U., D. Stefanova, and S. G. Holmes, 2013 Histone variant H2A.Z functions in sister chromatid cohesion in Saccharomyces cerevisiae. Molecular and Cellular Biology 33: 3473–3481.

Sharp, J. A., E. T. Fouts, D. C. Krawitz, and P. D. Kaufman, 2001 Yeast histone deposition protein Asf1p requires Hir proteins and PCNA for heterochromatic silencing. Current Biology 11: 463–473.

Shia, W.-J., B. Li, and J. L. Workman, 2006 SAS-mediated acetylation of histone H4 Lys 16 is required for H2A.Z incorporation at subtelomeric regions in Saccharomyces cerevisiae. Genes & Development 20: 2507–2512.

Shivaswamy, S., A. Bhinge, Y. Zhao, S. Jones, M. Hirst *et al.*, 2008 Dynamic remodeling of individual nucleosomes across a eukaryotic genome in response to transcriptional perturbation. PLoS Biology 6: e65.

Shroff, R., A. Arbel-Eden, D. Pilch, G. Ira, W. M. Bonner *et al.*, 2004 Distribution and Dynamics of Chromatin Modification Induced by a Defined DNA Double-Strand Break. Current Biology 14: 1703–1711.

Singer, M. S., A. Kahana, A. J. Wolf, L. L. Meisinger, S. E. Peterson *et al.*, 1998 Identification of high-copy disruptors of telomeric silencing in Saccharomyces cerevisiae. Genetics 150: 613–632.

Sinha, M., and C. L. Peterson, 2009 Chromatin dynamics during repair of chromosomal DNA double-strand breaks. Epigenomics 1: 371–385.

Smith, E. R., A. Eisen, W. Gu, M. Sattah, A. Pannuti *et al.*, 1998 ESA1 is a histone acetyltransferase that is essential for growth in yeast. Proceedings of the National Academy of Sciences of the United States of America 95: 3561–3565.

Spange, S., T. Wagner, T. Heinzel, and O. H. Krämer, 2009 Acetylation of non-histone proteins modulates cellular signalling at multiple levels. The International Journal of Biochemistry & Cell Biology 41: 185–198.

Strahl, B. D., and C. D. Allis, 2000 The language of covalent histone modifications. Nature 403: 41–45.

Strahl-Bolsinger, S., A. Hecht, K. Luo, and M. Grunstein, 1997 SIR2 and SIR4 interactions differ in core and extended telomeric heterochromatin in yeast. Genes & Development 11: 83–93.

Struhl, K., and E. Segal, 2013 Determinants of nucleosome positioning. Nature Structural & Molecular Biology 20: 267–273.

Subramanian, V., A. Mazumder, L. E. Surface, V. L. Butty, P. A. Fields *et al.*, 2013 H2A.Z acidic patch couples chromatin dynamics to regulation of gene expression programs during ESC differentiation. PLoS Genetics 9: e1003725.

Suka, N., K. Luo, and M. Grunstein, 2002 Sir2p and Sas2p opposingly regulate acetylation of yeast histone H4 lysine16 and spreading of heterochromatin. Nature Genetics 32: 378–383.

Suka, N., Y. Suka, A. A. Carmen, J. Wu, and M. Grunstein, 2001 Highly specific antibodies determine histone acetylation site usage in yeast heterochromatin and euchromatin. Molecular Cell 8(2):473–479.

Suto, R. K., M. J. Clarkson, D. J. Tremethick, and K. Luger, 2000 Crystal structure of a nucleosome core particle containing the variant histone H2A.Z. Nature Structural Biology 7: 1121–1124.

Sutton, A., J. Bucaria, M. A. Osley, and R. Sternglanz, 2001 Yeast ASF1 protein is required for cell cycle regulation of histone gene transcription. Genetics 158: 587–596.

Svotelis, A., N. Gévry, and L. Gaudreau, 2009 Regulation of gene expression and cellular proliferation by histone H2A.Z. Biochemistry and Cell Biology = Biochimie et Biologie Cellulaire 87: 179–188.

Szenker, E., D. Ray-Gallet, and G. Almouzni, 2011 The double face of the histone variant H3.3. Cell research 21: 421–434.

Szerlong, H., K. Hinata, R. Viswanathan, H. Erdjument-Bromage, P. Tempst *et al.*, 2008 The HSA domain binds nuclear actin-related proteins to regulate chromatin-remodeling ATPases. Nature Structural & Molecular Biology 15: 469–476.

Tagami, H., D. Ray-Gallet, G. Almouzni, and Y. Nakatani, 2004 Histone H3.1 and H3.3 complexes mediate nucleosome assembly pathways dependent or independent of DNA synthesis. Cell 116: 51–61.

Takahashi, Y.-H., J. M. Schulze, J. Jackson, T. Hentrich, C. Seidel *et al.*, 2011 Dot1 and histone H3K79 methylation in natural telomeric and HM silencing. Molecular Cell 42: 118–126.

Takahata, S., Y. Yu, and D. J. Stillman, 2009 FACT and Asf1 regulate nucleosome dynamics and coactivator binding at the HO promoter. Molecular Cell 34: 405–415.

Talbert, P. B., and S. Henikoff, 2010 Histone variants - ancient wrap artists of the epigenome. Nature Reviews Molecular Cell Biology 11: 264–275.

Tamburini, B. A., and J. K. Tyler, 2005 Localized histone acetylation and deacetylation triggered by the homologous recombination pathway of double-strand DNA repair. Molecular and Cellular Biology 25: 4903–4913.

Tjeertes, J. V., K. M. Miller, and S. P. Jackson, 2009 Screen for DNA-damage-responsive histone modifications identifies H3K9Ac and H3K56Ac in human cells. The EMBO Journal 28: 1878–1889.

Tolkunov, D., K. A. Zawadzki, C. Singer, N. Elfving, A. V. Morozov *et al.*, 2011 Chromatin remodelers clear nucleosomes from intrinsically unfavorable sites to establish nucleosome-depleted regions at promoters. Molecular Biology of the Cell 22: 2106–2118.

Trotter, K. W., H.-Y. Fan, M. L. Ivey, R. E. Kingston, and T. K. Archer, 2008 The HSA domain of BRG1 mediates critical interactions required for glucocorticoid receptor-dependent transcriptional activation in vivo. Molecular and Cellular Biology 28: 1413–1426.

Tsubota, T., C. E. Berndsen, J. A. Erkmann, C. L. Smith, L. Yang *et al.*, 2007 Histone H3-K56 acetylation is catalyzed by histone chaperone-dependent complexes. Molecular Cell 25: 703–712.

Turner, B. M., 2005 Reading signals on the nucleosome with a new nomenclature for modified histones. Nature structural & molecular biology 12: 110–112.

Tyler, J. K., C. R. Adams, S. R. Chen, R. Kobayashi, R. T. Kamakaka *et al.*, 1999 The RCAF complex mediates chromatin assembly during DNA replication and repair. Nature 402: 555–560.

van Attikum, H., and S. M. Gasser, 2009 Crosstalk between histone modifications during the DNA damage response. Trends in Cell Biology 19: 207–217.

van Attikum, H., O. Fritsch, and S. M. Gasser, 2007 Distinct roles for SWR1 and INO80 chromatin remodeling complexes at chromosomal double-strand breaks. The EMBO Journal 26: 4113–4125.

van Bakel, H., and F. C. P. Holstege, 2004 In control: systematic assessment of microarray performance. EMBO Reports 5: 964–969.

van Daal, A., and S. C. Elgin, 1992 A histone variant, H2AvD, is essential in Drosophila melanogaster. Molecular Biology of the Cell 3: 593–602.

van de Peppel, J., P. Kemmeren, H. van Bakel, M. Radonjic, D. van Leenen *et al.*, 2003 Monitoring global messenger RNA changes in externally controlled microarray experiments. EMBO Reports 4: 387–393.

Van, C., J. S. Williams, T. A. Kunkel, and C. L. Peterson, 2015 Deposition of histone H2A.Z by the SWR-C remodeling enzyme prevents genome instability. DNA Repair 25: 9–14.

Värv, S., K. Kristjuhan, K. Peil, M. Lõoke, T. Mahlakõiv *et al.*, 2010 Acetylation of H3 K56 is required for RNA polymerase II transcript elongation through heterochromatin in yeast. Molecular and Cellular Biology 30: 1467–1477.

Venkatesh, S., M. Smolle, H. Li, M. M. Gogol, M. Saint *et al.*, 2012 Set2 methylation of histone H3 lysine 36 suppresses histone exchange on transcribed genes. Nature 489: 452–455.

Verzijlbergen, K. F., A. W. Faber, I. J. Stulemeijer, and F. van Leeuwen, 2009 Multiple histone modifications in euchromatin promote heterochromatin formation by redundant mechanisms in Saccharomyces cerevisiae. BMC Molecular Biology 10: 76.

Vogelauer, M., J. Wu, N. Suka, and M. Grunstein, 2000 Global histone acetylation and deacetylation in yeast. Nature 408: 495–498.

Wang, A. Y., J. M. Schulze, E. Skordalakes, J. W. Gin, J. M. Berger *et al.*, 2009 Asf1-like structure of the conserved Yaf9 YEATS domain and role in H2A.Z deposition and acetylation. Proceedings of the National Academy of Sciences of the United States of America 106: 21573–21578.

Watanabe, S., M. Radman-Livaja, O. J. Rando, and C. L. Peterson, 2013 A histone acetylation switch regulates H2A.Z deposition by the SWR-C remodeling enzyme. Science 340: 195–199.

Watanabe, S., M. Resch, W. Lilyestrom, N. Clark, J. C. Hansen *et al.*, 2010 Structural characterization of H3K56Q nucleosomes and nucleosomal arrays. Biochimica et Biophysica Acta 1799: 480–486.

Weiner, A., A. Hughes, M. Yassour, O. J. Rando, and N. Friedman, 2010 High-resolution nucleosome mapping reveals transcription-dependent promoter packaging. Genome Research 20: 90–100.

Whitehouse, I., and T. Tsukiyama, 2006 Antagonistic forces that position nucleosomes in vivo. Nature Structural & Molecular Biology 13: 633–640.

Whitehouse, I., O. J. Rando, J. Delrow, and T. Tsukiyama, 2007 Chromatin remodelling at promoters suppresses antisense transcription. Nature 450: 1031–1035.

Williams, S. K., D. Truong, and J. K. Tyler, 2008 Acetylation in the globular core of histone H3 on lysine-56 promotes chromatin disassembly during transcriptional activation. Proceedings of the National Academy of Sciences of the United States of America 105: 9000–9005.

Wippo, C. J., L. Israel, S. Watanabe, A. Hochheimer, C. L. Peterson *et al.*, 2011 The RSC chromatin remodelling enzyme has a unique role in directing the accurate positioning of nucleosomes. The EMBO Journal 30: 1277–1288.

Wong, M. M., L. K. Cox, and J. C. Chrivia, 2007 The chromatin remodeling protein, SRCAP, is critical for deposition of the histone variant H2A.Z at promoters. The Journal of Biological Chemistry 282: 26132–26139.

Wu, W.-H., S. Alami, E. Luk, C.-H. Wu, S. Sen *et al.*, 2005 Swc2 is a widely conserved H2AZ-binding module essential for ATP-dependent histone exchange. Nature Structural & Molecular Biology 12: 1064–1071.

Wu, W.-H., C.-H. Wu, A. G. Ladurner, G. Mizuguchi, D. Wei *et al.*, 2009 N terminus of Swr1 binds to histone H2AZ and provides a platform for subunit assembly in the chromatin remodeling complex. The Journal of Biological Chemistry 284: 6200–6207.

Wurtele, H., G. S. Kaiser, J. Bacal, E. St-Hilaire, E.-H. Lee *et al.*, 2012 Histone H3 lysine 56 acetylation and the response to DNA replication fork damage. Molecular and Cellular Biology 32: 154–172.

Xu, F., Q. Zhang, K. Zhang, W. Xie, and M. Grunstein, 2007 Sir2 deacetylates histone H3 lysine 56 to regulate telomeric heterochromatin structure in yeast. Molecular Cell 27: 890–900.

Yamane, K., T. Mizuguchi, B. Cui, M. Zofall, K.-I. Noma *et al.*, 2011 Asf1/HIRA facilitate global histone deacetylation and associate with HP1 to promote nucleosome occupancy at heterochromatic loci. Molecular Cell 41: 56–66.

Yang, B., A. Miller, and A. L. Kirchmaier, 2008 HST3/HST4-dependent deacetylation of lysine 56 of histone H3 in silent chromatin. Molecular Biology of the Cell 19: 4993–5005.

Yang, X. J., 2004 The diverse superfamily of lysine acetyltransferases and their roles in leukemia and other diseases. Nucleic Acids Research.

Yen, K., V. Vinayachandran, and B. F. Pugh, 2013 SWR-C and INO80 Chromatin Remodelers Recognize Nucleosome-free Regions Near +1 Nucleosomes. Cell 154: 1246–1256.

Yi, C., M. Ma, L. Ran, J. Zheng, J. Tong *et al.*, 2012 Function and molecular mechanism of acetylation in autophagy regulation. Science.

Yuan, H., D. Rossetto, H. Mellert, W. Dang, M. Srinivasan *et al.*, 2012 MYST protein acetyltransferase activity requires active site lysine autoacetylation. The EMBO Journal 31: 58–70.

Zhang, H., D. O. Richardson, D. N. Roberts, R. T. Utley, H. Erdjument-Bromage *et al.*, 2004 The Yaf9 component of the SWR1 and NuA4 complexes is required for proper gene expression, histone H4 acetylation, and Htz1 replacement near telomeres. Molecular and Cellular Biology 24: 9424–9436.

Zhang, H., D. N. Roberts, and B. R. Cairns, 2005 Genome-wide dynamics of Htz1, a histone H2A variant that poises repressed/basal promoters for activation through histone loss. Cell 123: 219–231.

Zhou, B. O., S.-S. Wang, L.-X. Xu, F.-L. Meng, Y.-J. Xuan *et al.*, 2010 SWR1 complex poises heterochromatin boundaries for antisilencing activity propagation. Molecular and Cellular Biology 30: 2391–2400.

Zlatanova, J., and A. Thakar, 2008 H2A.Z: view from the top. Structure 16: 166–179.